Title

Characterization of Medication Related Osteonecrosis of the Jaws Pathophysiology and Local RANKL Delivery as an Experimental Intervention

Permalink

https://escholarship.org/uc/item/1w67p813

Author

Soundia, Akrivoula

Publication Date

2020

Peer reviewed|Thesis/dissertation

UNIVERSITY OF CALIFORNIA

Los Angeles

Characterization of Medication Related Osteonecrosis of the Jaws Pathophysiology and Local

RANKL Delivery as an Experimental Intervention

A dissertation submitted in partial satisfaction of the

requirements of the degree Doctor of Philosophy

in Oral Biology

by

Akrivoula Soundia

2020

ABSTRACT OF THE DISSERTATION

Characterization of Medication Related Osteonecrosis of the Jaws Pathophysiology and Local

RANKL Delivery as an Experimental Intervention

by

Akrivoula Soundia

Doctor of Philosophy in Oral Biology

University of California, Los Angeles, 2020

Professor Sotirios Tetradis, Chair

Medication related osteonecrosis of the jaws (MRONJ) is a severe adverse effect of antiresorptive and angiogenic medication prescribed to patients with osteoporosis or bone malignancies. Our laboratory has been working on the elucidation of the mechanisms of this disease for the past decade. In this dissertation, we further characterized pathogenesis in rodents and humans and explored the delivery of RANKL as a therapeutic approach.

Tooth extraction was performed on diseased or healthy teeth in mice treated with saline, OPG-Fc (the equivalent of denosumab in rodents) or bisphosphonates. Extraction of healthy teeth

did not suffice to induce MRONJ in mice treated with antiresorptives. In contrast, extraction of diseased teeth induced mucosal defects, absence of radiographic healing, periosteal reaction, significant osteonecrosis and bone exposure in mice treated with antiresorptives. Extraction of periodontally diseased teeth in zoledronate (ZA) treated rats resulted in altered socket healing with a significant amount of osteonecrosis. An increased signal of collagen type III, MMP-9, MMP-13 and α-SMA was seen in the sockets of these rats compared to saline treated rats or zoledronate treated rats with extraction of healthy teeth.

We also took advantage of our patient database to investigate the radiographic appearance of stage 0 MRONJ patients. We concluded that sclerosis, cortical erosion, periosteal reaction, sequestration and crater-like defect are more commonly present in stage 0 MRONJ patients as opposed to dental disease patients. Additionally, if a stage 0 MRONJ patient presents with radiographic sequestration at initial visit, they are at a higher risk to progress to frank bone exposure in less than a year.

Next, we explored local RANKL delivery as a potential therapy for MRONJ. RANKL was delivered in the sockets of ZA or saline treated rats in a collagen tape. In the extraction sockets of ZA treated rats with RANKL treatment, there was an improvement in mucosal and radiographic healing, a decrease in osteonecrosis and bone exposure and a simultaneous increase in osteoclast numbers compared to the ZA treated rats that had not received local RANKL treatment.

We also investigated the role of macrophages in MRONJ development. In a model of periodontitis, zoledronate treated mice demonstrated a predominance of M1 macrophages (macs) and an absence of M2 macs compared to the saline treated mice. The above M1 macrophages also expressed MMP-13. Rosiglitazone treatment reversed the M1/M2 ratio in ZA treated mice 2 weeks after periodontal disease was induced and reduced epithelium to crest distance in ZA mice.

However, a difference was not detected in the bone exposure incidence, the epithelium to crest distance or the osteonecrotic areas between ZA mice with or without rosiglitazone treatment. Our data provide insight to the pathogenesis of MRONJ, describe the radiographic profile of stage 0 MRONJ patients and suggest that local RANKL delivery may be efficient in minimizing MRONJ incidence and improving socket healing.

The dissertation of Akrivoula Soundia is approved.

Sanjay Mallya

Flavia Pirih

Tara Aghaloo

Sotirios Tetradis, Committee Chair

University of California, Los Angeles

2020

DEDICATION

I dedicate this work to

Misho,

my family, Timotheo, Theodora and Maria,

and my two puppies

TABLE OF CONTENTS

LIST OF FIGURES

LIST OF TABLES

LIST OF ACRONYMS

ANOVA: One-way analysis of variance

Arg1: Arginase 1

BP: Bisphosphonates

CEJ: Cementoenamel junction

Col: Collagen

EDTA: Ethylenediaminetetraacetic acid

iNOS: inducible nitric oxide synthase

ip: intraperitoneally

LPS: Lipopolysaccharide

MMP-9: Matrix Metalloproteinase 9

MMP-13: Matrix Metalloproteinase 13

MRONJ: Medication related osteonecrosis of the jaws

ONJ: Osteonecrosis of the jaws

Pc red: Picrosirius red

RANKL: Receptor of activator of NFκB ligand

ROI: Region of interest

Rosi: Rosiglitazone

TRAP: Tartrate resistant acid phosphatase

ZA: Zoledronic acid

α-SMA: α smooth muscle actin

μCT: Micro Computed Tomography

ACKNOWLEDGEMENTS

Chapter 4 is published as 'Radiographic predictors of bone exposure in stage 0 Medication Related Osteonecrosis of the Jaws (MRONJ)'. A Soundia, D Hadaya, S Mallya, T Aghaloo, S Tetradis. Oral Surgery, Oral Medicine, Oral Pathology, Oral Radiology 2018 Dec;126(6):537-544. Permission to reproduce the above studies was granted by Elsevier and Sage journals. Chapter 5 is in preparation for publication.

VITA

Publications

1. Mixed density mandibular mass in a patient with pain and paresthesia. **A Soundia**, T Aghaloo, S Tetradis, YL Lin, M Husain. Journal of American Dental Association (JADA). 2019 May 30, Epub ahead of print

2. Vasculature submucosal changes at early stages of osteonecrosis of the jaw (ONJ). I Gkouveris, D Hadaya, **A Soundia**, O Bezouglaia, Y Chau, S Dry, F Pirih, T Aghaloo, S Tetradis- *Bone.* 2019 Jun;123:234-245

3. Development of Osteonecrosis of the Jaw after extracting teeth with experimental periapical disease. D Hadaya, **A Soundia,** S Dry, T Aghaloo, S Tetradis, *Journal of Oral and Maxillofacial Surgery.* 2019 Jan;77(1):71-86

4. Clinically Relevant Doses of Sclerostin Antibody Do Not Induce Osteonecrosis of the Jaw (ONJ) in Rats with Experimental Periodontitis. D Hadaya, I Gkouveris, **A Soundia**, O Bezouglaia, R Boyce, M Stolina, S Dry, F Pirih, T Aghaloo, S Tetradis- *Journal of Bone and Mineral Research.* 2019 Jan;34(1):171-181

5. Radiographic predictors of bone exposure in stage 0 Medication Related Osteonecrosis of the Jaws (MRONJ). **A Soundia**, D Hadaya, S Mallya, T Aghaloo, S Tetradis. Oral Surgery, Oral Medicine, Oral Pathology, Oral Radiology 2018 Dec, **highlighted** by the Journal of the American Dental Association Specialty scan-Radiology, Fall 2018, appeared on the **cover** of OOOO Journal, 2018 Dec;126(6):537-544

6. Non-surgical management of MRONJ utilizing local wound care. D Hadaya, **A Soundia**, E Freymiller, S Tetradis, T Aghaloo- *Journal of Oral and Maxillofacial Surgery.* 2018 Nov;76(11):2332-2339

7. Zoledronate Impairs Socket Healing after Extraction of Teeth with Experimental Periodontitis. **A Soundia**, D Hadaya, N Esfandi, I Gkouveris, R Christensen, SM Dry, O Bezouglaia, F Pirih, N Nikitakis, T Aghaloo, S Tetradis- *Journal of Dental Research,* 2018 Mar;97(3):312-320

8. Osteonecrosis of the jaws (ONJ) in mice after extraction of teeth with periradicular disease. **A Soundia**, D Hadaya, N Esfandi, RS de Molon, O Bezouglaia, SM Dry, FQ Pirih, Aghaloo T, Tetradis S.- *Bone,* 2016 Sep;90:133-41

9. Rheumatoid arthritis exacerbates the development and severity of osteonecrosis of the jaws (ONJ) in mice. RS de Molon, C Hsu, O Bezouglaia, SM Dry, F Q. Pirih, **A Soundia**, F Cunha, J Cirelli, TL Aghaloo, S Tetradis – *Journal of Bone and Mineral Research,* 2016 Aug;31(8):1596-607

10. Nanodiamond-Gutta Percha Composite Biomaterials For Multi-Functional Root Canal Therapy. D Lee, S Kim, A Limansubroto, A Yen, **A Soundia**, CY Wang, W Shi, C Hong, S Tetradis, Y Kim, No-Hee Park, M. Kang, and D Ho-*American Chemical Society nano* 2015 24:11490-501

Service

Reviewer   Oral Diseases (2018 – Present)

Awards

2019	**Arthur H. Wuehrmann Prize for Best Radiology paper in OOOO**, American Association of Oral and Maxillofacial Radiology, Oral Surg Oral Med Oral Pathol Oral Radiol 2018 December
2019	**AADR Hatton Award, 1ˢᵗ place (senior category)**, American Association for Dental Research (AADR), June 2019, Vancouver, BC
2019	**Third place in PhD/post-doctoral category,** UCLA Research Day 2019, Los Angeles, CA
2018-2019	**Dissertation Year Fellowship**, UCLA Graduate School, Los Angeles, CA
2018	**Howard Raper award** for a graduate student with academic career potential, American Association of Oral and Maxillofacial Radiology, San Antonio, TX
2017-2018	**Gerondelis Fellowship** for outstanding Greek graduate students in the US
2018	**First place in Resident/Master's category**, UCLA Research Day, Los Angeles, CA
2016	**Nominated as a competitor for the Hatton Award (senior category),** American Association for Dental Research (AADR), Los Angeles, CA

CHAPTER 1

INTRODUCTION

MRONJ definition

Medication related osteonecrosis of the jaws (MRONJ) is a severe complication of antiresorptive and antiangiogenic medications. These medications are prescribed to patients to combat osteoporosis, bone malignancies, Paget's disease, hypercalcemia of malignancy among other conditions. MRONJ is defined as exposed bone or bone that can be probed through a fistula that persists for more than eight weeks in a patient with history of antiresorptive or antiangiogenic medications and no history of radiation in the head and neck area[1, 2].

Staging and treatment

The American Association of Oral and Maxillofacial Surgeons (AAOMS) identifies four stages of MRONJ (stage 0-3). Stage 0 describes patients that do not demonstrate frank bone exposure but present with abnormal symptoms and/or clinical and radiographic findings. These radiographic findings may include sclerosis or unhealed extraction sockets. However, the radiographic appearance is not taken into account when staging is defined according to the latest position papers of AAOMS and the American Society of Bone and Mineral Research (ASBMR) task force. Moreover, stage 0 is not recognized by the ASBMR Task Force altogether mainly due to a danger of MRONJ overdiagnosis. According to the Task Force, if patients with common dental disease get diagnosed with stage 0 MRONJ detrimental effects to their skeletal health may occur if their physicians elect the discontinuation of their antiresorptive treatment[2]. On the other hand, several studies in the literature validate the existence of a non-exposed variant of MRONJ. In fact,

a multicenter study from Fedele et al reports that approximately 50% of stage 0 patients will develop frank bone exposure within 4-5 months.[3] [4]

Stage 1 patients are the patients that show clinically exposed bone without pain or evidence of inflammation/infection. Additionally, these patients may present with a variety of radiographic findings including sclerosis, sequestration, periosteal reaction, lytic changes. Interestingly, a study by Walton et al showed that patients receiving oncologic doses of antiresorptive medications present more often with stage 1 MRONJ[5]. The reason for this is not clear. However, the authors hypothesize that oncologic patients are possibly under more meticulous dental care and perform more active oral hygiene. Treatment methods include antibacterial mouth rinse, clinical follow-up on a quarterly basis and patient education and review of indications for continued bisphosphonate therapy[1].

Stage 2 patients present with bone exposure and have pain and/or clinical findings of infection/inflammation. In the above study by Walton et al, patients receiving antiresorptives for osteoporosis presented more often with stage 2 MRONJ[5]. Treatment is overall more aggressive for these patients including pain control medications, oral antibiotics, oral antibacterial solutions and debridement to relive soft tissue infection[1].

Lastly, stage 3 patients demonstrate pain and/or infection and may present with oronasal communication, extraoral fistula or even a pathologic fracture. Additionally, the affected area of the jaws extends beyond the confines of the alveolar bone to the maxillary sinus, zygoma, inferior border of the mandible or the mandibular ramus. Patients with stage 3 MRONJ show radiographic features like periosteal reaction more often than stage 1 or 2 patients. Additionally, their cumulative frequency of radiographic markers such as sclerosis, lytic changes, sequestration and periosteal reaction is more severe and extensive compared to stage 1 or 2 patients. These patients

are often surgically treated with debridement. Antibacterial oral rinses and antibiotics are also employed[5].

Prevention of the disease is crucial and endodontic treatments, atraumatic surgical procedures and periodontal treatment are recommended dental practices before the onset and during antiresorptive therapy. In fact, preventive dental measures such as adjustment of ill-fitting dentures, identification and treatment of existing dental infections and referral to oral surgeons for necessary extractions before antiresorptive treatment onset was found to decrease MRONJ incidence in patients with multiple myeloma treated with zoledronic acid [6]. Adjuvant techniques including laser treatment, platelet rich plasma and hyperbaric oxygen have shown encouraging results in patients with established MRONJ. [7]. Other alternatives include the discontinuation or modification of the antiresorptive/antiangiogenic treatment regimen. However, at the moment, there is lack of conclusive evidence to support that discontinuation of the systemic medications has a beneficial effect on MRONJ lesions. In fact, animal studies show that discontinuation of bisphosphonates does not improve MRONJ incidence and severity[8]. Case reports also show a beneficial effect of teriparatide in patients undergoing surgical treatment of MRONJ possibly due to its anabolic effect and its favorable effects on osseous healing[9].

Recently, a thorough study by Hadaya et al has described a conservative way of managing MRONJ patients utilizing vigorous local wound care with a chlorhexidine solution. 71% of patients following this protocol showed resolution of the mucosal wound and another 22% showed improvement of wound healing[10]. This is an encouraging alternative method of treating MRONJ which requires no surgical treatment.

Medications associated with MRONJ

The main classes of antiresorptive medications implicated in MRONJ pathophysiology are bisphosphonates and denosumab. Bisphosphonates have a high binding affinity to hydroxyapatite and become endocytosed by osteoclasts after bone resorption occurs. Aledronate, ibandronate and pamidronate have been widely used for the treatment of post-menopausal osteoporosis. Zoledronate is a very potent bisphosphonate which is used mainly to treat bone malignancies. Bisphosphonate intestinal retention is low and the side effects of oral bisphosphonates include gastric ulcers, nausea, heartburn, esophagus irritation and MRONJ. Intravenous bisphosphonates present with rare side effects such as atrial fibrillation, renal insufficiency, atypical femoral fractures and MRONJ. Acute phase reaction has been observed and manifests with fever, myalgia and arthralgia. Hypocalcemia has also been described and may cause secondary hyperparathyroidism and is more commonly seen in patients with renal malfunction and limited calcium intake. [11]

Bisphosphonates alter the mevalonate pathway by inhibiting the enzyme farnesyl pyrophosphate synthase. The mevalonate pathway is a biosynthetic pathway which leads to production of cholesterol, other sterols and isoprenoid lipids. Farnesyl pyrophosphate and geranyl-pyrophosphosphate are necessary for the prenylation and activation of small GTPases such as Ras and Rho. The above small GTPases are essential in maintaining osteoclast morphology, cytoskeleton arrangement, membrane ruffling, trafficking, and cell survival. After osteoclasts endocytose bisphosphonates, their resorptive ability is compromised and they are led to apoptosis [12] [13].

Denosumab, on the other hand, is a monoclonal antibody to RANKL that is used to treat osteoporosis, multiple myeloma and bone metastases from solid tumors. Denosumab binds to RANKL and does not allow it to bind to RANK-Fc, a receptor that is found on the surface of pre-

osteoclastic populations. Therefore, it eliminates osteoclastogenesis and results in apoptosis of existing osteoclasts. Denosumab has been shown to be superior in increasing bone mineral density of the hip and lumbar spine compared to bisphosphonates. Its side effects include back pain, joint pain, common cold, hypocalcemia. [14]. Clinical and animal studies have shown that osteoclastic activity is restored after denosumab discontinuation. In fact, spontaneous vertebral fractures have been reported in patients after discontinuing denosumab within 8-20 months. [8] [15] [16]

MRONJ has been reported with a similar incidence and severity in patients treated with bisphosphonates and denosumab. The risk of patients receiving osteoporotic doses is estimated to be approximately 1 in 10,000 whereas the risk increases to approximately 1-6% in patients receiving oncologic doses. Some studies reveal higher incidence of MRONJ which may reach up to 15%.[17].

Antiangiogenic medications, such as VEGF inhibitors and tyrosine kinase inhibitors, have also been associated with MRONJ. The most common drugs implicated in MRONJ pathogenesis are bevacizumab and sunitinib. The risk of MRONJ incidence is approximately 0.2% in patients receiving antiangiogenic medications and it increases to approximately 0.9% in patients receiving the above medications concomitantly with bisphosphonates, according to clinical studies[1]. However, animal studies have not been able to reproduce clinical MRONJ with exposed bone in rats treated only with VEGF inhibitors. [18]

Recently, case reports have linked new classes of medications, such as anti-rheumatic drugs (etanercept, adalimumab), chemotherapeutics (methotrexate), steroids (prednisone) to MRONJ development. As MRONJ becomes more and more documented, it is possible that new pharmacologic agents will become implicated in its pathogenesis[19],[20, 21]

Pathophysiology

Significant progress has been made in an effort to understand the underlying mechanism of MRONJ development. Numerous animal studies replicating clinical, radiographic and histologic features of MRONJ in small or larger animals have been contributed to the literature [22-26]. Additionally, thorough reports of clinical data have helped describe the disease and elucidate its pathophysiologic cues[4, 27, 28].

Bone remodeling inhibition

Bisphosphonates have been proven very effective in reducing bone resorption and thus reducing risk fracture in post-menopausal osteoporotic patients. Bone remodeling is, therefore, altered due to the lack of osteoclastic activity. Osteoblastic activity is not directly affected by bisphosphonate treatment resulting in uniformly mineralized bone. [29].

Bisphosphonates have been shown to deposit in higher quantities in areas of active bone turnover. Studies in dogs have shown that the rate of bone remodeling in the mandible is approximately double compared to the maxilla and six times faster than the femur [30]. Additionally, intracortical remodeling was more significantly impaired in the alveolar bone of the maxilla and mandible compared to the ribs or the long bones in dogs treated with oncologic doses of bisphosphonates[31]. Another study by Cheong et al showed an increased uptake of fluorescent bisphosphonates around areas of tooth extraction or dental disease compared to healthy sites of the maxillary alveolar bone[32]. The above data point to a predisposition of uptake of bisphosphonates in the highly active bone of the maxillary and mandibular alveoli, particularly around areas of trauma or inflammation, which may explain the specificity of the disease to the jaws.

Importantly, denosumab and bisphosphonates act on osteoclasts through completely different pharmacologic mechanisms. In fact, denosumab completely eliminates osteoclasts and prevents osteoclastogenesis [33]. Bisphosphonates, contrary, render osteoclasts unable to carry out bone resorption and eventually induce apoptosis [13]. However, both these pharmacologic agents cause MRONJ in similar incidence and severity both in animal studies and in humans [34] [1, 26]. It appears, therefore, that osteoclast impairment and, thus, bone remodeling inhibition is central in MRONJ pathogenesis regardless of the pharmacologic agent in use.

Angiogenesis inhibition

Zoledronic acid has been shown to decrease circulating levels of VEGF and decreases angiogenesis in vitro. Additionally, zoledronic acid is thought to prevent tumor invasion and metastases by inhibiting endothelial cell adhesion and migration in humans. [35] [36] [37]. However, no similar findings have been reported in patients treated with denosumab.

Anti-angiogenic medications, such as bevacizumab and sunitinib, have been linked with MRONJ development. Moreover, a study by Gkouveris et al showed that immunohistochemical markers of vasculature such as α-SMA (an arterial marker) were decreased around osteonecrotic lesions in ZA and OPG-Fc treated mice compared to veh-treated animals. Additionally, VEGF-a and V-CAM (a marker of activated endothelial cells) were found increased the first 1 week but plummeted by week 4 in mice treated with ZA and OPG-Fc compared to veh-treated mice. [38].

Infection and inflammation

Tooth extraction is the most common risk factor for the initiation of MRONJ. However, in adults, almost all extractions occur due to periapical or periodontal inflammation/infection. Many animal models have been developed and have shown that a combination of antiresorptive treatment

and induction of dental disease are sufficient to cause MRONJ even in the absence of tooth extraction[24-26, 39]. Moreover, preventive dental measures reduce MRONJ incidence in patients treated with oncologic doses of bisphosphonates and aggressive local wound care with an antibacterial solution was reported to result in wound resolution[6, 10]. Lastly, animal studies have shown that removal of periodontal disease before tooth extraction improves MRONJ lesions in mice treated with bisphosphonates[40].

Soft tissue toxicity

Early, mostly in vitro studies showed that nitrogen-containing bisphosphonates may induce apoptosis not only in osteoclasts but also other cell populations, such as oral, cervical and prostate epithelial cells. Moreover, oral bisphosphonates have been reported to cause esophageal damage and irritation[1, 41]. Similar findings have not been reported for denosumab, thus disfavoring this hypothesis[42].

Immunity dysfunction

Many MRONJ patients report receiving steroids and chemotherapeutic agents known for their immunosuppressant role in combination with antiresorptive medications[43]. In animal models, infusion of mesenchymal stem cells or T-reg cells improved MRONJ severity[44]. Additionally, an altered phenotype of macrophages has been reported with an M1 predilection around osteonecrotic lesions[45, 46]. The above data point to a significant role of immunity impairment/alteration in MRONJ development.

Risk factors

It has been well established that MRONJ risk increases with antiresorptive/antiangiogenic treatment duration and dose. Studies have shown that a significant increase of MRONJ incidence

is noted 3-4 years after onset of bisphosphonate treatment [47]. Denosumab patients showed a plateau of MRONJ incidence in years 2-3 after treatment onset [48].

Dentoalveolar trauma, usually in the form of tooth extraction, is the most common instigating factor and increases MRONJ risk by a 16-fold margin[49-53]. Other local factors may include trauma from dentures and concomitant periapical/periodontal inflammation[54, 55]. Moreover, the fact that dental inflammation is the leading cause of tooth extraction in adults may be a confounding factor causing additive risk to the already established risk from tooth extraction.

Treatment with agents such as corticosteroids and antiangiogenic medications have been reported to contribute to MRONJ risk[56, 57]. Additionally, other conditions, such as anemia, diabetes have been shown to increase MRONJ incidence[48].

A genetic predisposition related to single nucleotide polymorphisms in genes related to collagen formation and bone metabolism has been reported in clinical studies. These genes include the RBMS3 gene, a gene associated with bone density and collagen formation and the gene responsible for farnesyl diphosphate synthase activity (the enzyme specifically inhibited by BPs) [58] [59]. A recent study form Yang et al identified SNPs in the locus SIRT/HERC (a gene related to cellular regulation, response to stress and longevity) to be associated with iv BP induced MRONJ [60].

RATIONALE

Medication related osteonecrosis of the jaws is a rare but severe adverse effect of antiresorptive and antiangiogenic medications, prescribed to patients with osteoporosis and bone malignancies [1, 2, 61]. Although MRONJ was described in the literature in 2003 [27, 62] its pathogenetic mechanism is still elusive. Dental inflammation/infection and bone remodeling inhibition are predominant hypotheses in MRONJ development.

Dental inflammation/infection appears to play a crucial role in MRONJ development and severity. Tooth extraction is the most common instigating factor of MRONJ [1]. However, most teeth in adults are extracted due to pre-existing dental infection [63, 64]. Additionally, pre-existing dental inflammation triggers an immune response around teeth which may be altered in the presence of antiresorptive treatment [45, 46]. Therefore, we elected to investigate the radiographic and histologic phenotype of the jaws of antiresorptive treated rodents with extraction of teeth with pre-existing dental inflammation.

During our studies, the radiographic appearance of the jaws has been proven important in better evaluating the extent of the underlying bony changes in animals and humans [5 65 66, 67]. In stage 0 MRONJ, where the mucosal appearance is non-specific, radiographic assessment can be an informative indicator for the future behavior of the disease. We hypothesized that the radiographic appearance of stage 0 MRONJ patients can be a predictor of future bone exposure.

The disease has been reported in patients receiving different types of medications, such as bisphosphonates or denosumab (a RANKL inhibitor) [27,68,69]. The risk for MRONJ among cancer patients exposed to denosumab or bisphosphonates is comparable and usually ranges from 0.7-1.9% [1]. Bisphosphonates act by altering the mevalonate pathway via inhibiting farnesyl

pyrophosphate synthase and cause disruption of resorption activity [70]. In contrast, denosumab binds RANKL and inhibits the bond between RANK and RANKL, preventing osteoclastogenesis and osteoclast survival [33]. Despite the distinct pharmacologic mechanisms of these medications, both BPs and denosumab are associated with MRONJ. This implies a central role of osteoclast inhibition and imbalanced bone remodeling in MRONJ pathogenesis. RANKL is a molecule which plays an instrumental role in osteoclastic activity [71],[72]. Although inhibition of bone resorption appears to play a central role in MRONJ development, RANKL therapy has not yet been explored as a possible treatment of MRONJ. We hypothesize that local RANKL delivery can ameliorate MRONJ lesions in an antiresorptive setting by increasing bone resorption and removal of necrotic bone.

We also, specifically, investigated the role of macrophages in MRONJ pathogenesis given their significant role in bone homeostasis and their monocytic lineage from which osteoclasts originate. Given the ability of rosiglitazone to reverse the M1/M2 macrophages ratio which has been implicated in MRONJ pathogenesis we hypothesized that rosiglitazone treatment may improve MRONJ[73, 74].

The following aims were tested:

SPECIFIC AIMS

1. **To evaluate MRONJ development after extraction of teeth with severe periradicular disease in mice treated with OPG-Fc or bisphosphonates.** MRONJ features were assessed by visual inspection of the extraction sockets, μCT and histological analysis.

2. **To investigate wound healing in extraction sockets of periodontally inflamed teeth in rats treated with bisphosphonates.** Assessment was performed utilizing μCT, histological and immunohistochemical analysis

3. **To characterize the radiographic appearance of stage 0 MRONJ patients and explore possible radiographic markers which may serve as predictors for disease advancement.** A retrospective analysis of the radiographic appearance of stage 0 MRONJ patients was performed and a correlation between initial radiographic appearance and progression to bone exposure was made.

4. **To investigate the local delivery of RANKL as therapeutic approach in extraction sockets of bisphosphonate treated rats.** RANKL delivery was performed with a collagen sponge sutured in the rat extraction sockets and bone exposure, osteonecrosis extent and osteoclast numbers were measured in two different timepoints.

5. **To investigate the role of macrophage polarization in MRONJ development.** Macrophages polarization (M1/M2) was studied via immunohistochemistry and the enhancement of the M2 phenotype in MRONJ lesions was investigated through rosiglitazone treatment.

CHAPTER 2

OSTEONECROSIS OF THE JAWS (ONJ) IN MICE AFTER EXTRACTION OF TEETH WITH PERIRADICULAR DISEASE

Abstract

Osteonecrosis of the jaws (ONJ) is a complication of antiresorptive medications, such as denosumab or bisphosphonates, prescribed to patients with bone malignancy or osteoporosis. The most common instigating local factor in ONJ pathogenesis is tooth extraction. However, in adults the great majority of teeth are extracted due to dental disease. Here, we have investigated alveolar bone healing after extraction of healthy teeth or teeth with naturally occurring periradicular disease in mice treated with high dose zoledronic acid (ZA), a potent bisphosphonate, or OPG-Fc, a RANKL inhibitor. C57BL/6 mice were treated for eight weeks and in vivo micro-CT was performed to identify spontaneously occurring periradicular lesions around the roots of maxillary molars. Then, extractions of molars with and without dental disease were performed in all groups. Four weeks later, animals were euthanized and maxillae were dissected and analyzed. Clinically, all veh animals with extraction of healthy or diseased teeth, and most OPG-Fc or ZA animals with extraction of healthy teeth showed normal mucosal healing. On the contrary, most animals with OPG-Fc or ZA treatment and extraction of diseased teeth demonstrated impaired healing with visible mucosal defects. Radiographically, bone socket healing was significantly compromised in OPG-Fc and ZA-treated mice with periradicular disease in comparison to other groups. Histologically, all veh animals showed normal mucosal healing and socket remodeling. OPG-Fc and ZA animals with extraction of healthy teeth showed normal mucosal healing, woven bone formation in the socket, and decreased remodeling of the original socket confines. OPG-Fc and ZA animals with extraction of diseased teeth showed mucosal defects, persistent prominent

inflammatory infiltrate, bone exposure and areas of osteonecrosis. These findings support a central role of dental disease in the pathogenesis of ONJ, not only as the instigating cause for tooth extraction, but also as a compounding factor in ONJ development and pathophysiology.

Introduction

Medication related osteonecrosis of the jaws (ONJ) is defined as necrotic, exposed bone in the maxillofacial region for at least 8 weeks, in patients on antiresorptive treatment [2] or antiangiogenic medications [2], but without a history of head and neck radiation. Patients with primary bone cancer or metastatic disease on high dose bisphosphonates (BPs), notably zoledronic acid (ZA), or denosumab most commonly suffer from this condition. Patients with osteoporosis or Paget's disease receiving either oral or parenteral antiresorptive medications are at much lower risk [1, 2].

Dentoalveolar surgery is a major local risk factor associated with ONJ incidence, with 52-61% of patients reporting tooth extraction as the precipitating event for clinical manifestation of the disease [48, 50, 55]. Based on these clinical observations, ONJ animal models have been developed that combine antiresorptive treatment and extraction of maxillary or mandibular teeth in order to recapitulate clinical, radiographic, and histologic features of the disease [22, 23, 75-79].

The vast majority of teeth in adult patients are extracted due to dental disease [63, 80], which is also true for patients with ONJ. Periodontal or periapical disease, even in the absence of tooth extraction is associated with ONJ occurrence [81] and is considered a local risk factor for the disease [1, 2]. Moreover, improved oral hygiene measures significantly reduce ONJ incidence in patients with multiple myeloma and metastatic cancer [6, 82]. Indeed, we and others have described ONJ models

14

in rodents treated with antiresorptive medications and induced experimental dental disease, without extractions, that capture several attributes of ONJ in patients [8, 24-26, 34, 83, 84]

During these studies, we identified an unexpected model of ONJ in animals with naturally occurring periradicular lesions around the maxillary molar teeth, when they were treated with high doses of ZA or with the RANKL inhibitors RANK-Fc or OPG-Fc. It is noteworthy that no experimental intervention was performed in these animals and the ONJ-like lesions, characterized by periosteal bone apposition, osteonecrosis, severe inflammation and bone exposure, developed spontaneously [26]. Here, taking advantage of this ONJ model, we have combined the two methodologies of local risk factors (extraction and dental disease), in association with systemic treatment with two different types of antiresorptives, a BP or a RANKL inhibitor, to more closely replicate the clinical setting and investigate ONJ pathogenesis. We have extracted healthy teeth or teeth with natural periradicular lesions in animals treated with vehicle (veh), ZA, or OPG-Fc and have assessed the animals clinically, radiographically, and histologically. Our data indicate that extraction of diseased, but not healthy, teeth is associated with high incidence of ONJ in this mouse model.

Materials and Methods

Animal care

Animals were kept and treated according to guidelines of the UCLA Chancellor's Animal Research Committee. Throughout the experimental period, mice were housed in corn-bedding plastic cages (4 mice per cage) in pathogen-free conditions with a light/ dark cycle of 12 hours, fed a standard laboratory diet, and given water ad libitum. Fifty seven nine-week-old C57BL/6J

male mice (Jackson Laboratory, Bar Harbor, ME, USA), weighing 25g on average(range from 23-28g), were randomly assigned to receive intraperitoneal injections of endotoxin free saline (veh), 10 mg/kg OPG-Fc (composed of the RANKL-binding domain of osteoprotegerin linked to the Fc portion of IgG, kindly provided by Amgen Inc, Thousand Oaks, CA), or 200 µg/kg zoledronic acid (ZA) twice a week in morning hours. There were 19 veh, 18 OPG-Fc, and 20 ZA treated animals. The antiresorptive doses were chosen in order to induce ONJ in the presence of dental disease, based on our previous studies [8, 25, 26, 34]. The protocol followed all recommendations of the ARRIVE (Animal Research: Reporting in Vivo Experiments) guidelines for execution and submission of studies in animals.

Animals were treated for eight weeks with veh, OPG-Fc or ZA, and then in vivo µCT was performed to assess the presence of spontaneous periradicular disease. The study included 6 experimental groups: veh, OPG-Fc and ZA treated animals with either extraction of healthy or diseased teeth. Two days after imaging, mice were anesthetized utilizing isoflurane, maxillary molars from both sides were extracted. For all groups, sites with a fractured buccal cortical plate or fractured teeth during extraction were excluded from subsequent analysis. Four weeks after extractions animals were sacrificed, maxillae were dissected and photographs of the specimens were obtained utilizing a digital optical microscope (Keyence VHX-1000, Osaka, Japan). Then specimens underwent radiographic and histologic assessment, as described below. During ex vivo radiographic evaluation, sites with remaining roots were also excluded from subsequent analysis. The final study groups consisted of 28, 24 and 25 maxillary sites for veh, OPG-Fc or ZA animals respectively.

In vivo µCT scanning

16

In vivo imaging was performed utilizing the Skyscan 1176 in vivo μCT scanner (Bruker Corporation, Belgium) at 18 μm resolution, 50 kVp and 500 μA. Volumetric image data were converted to DICOM format and imported in the Dolphin Imaging software (Chatsworth, CA, USA) to generate 3D and multiplanar reconstructed images. Altered alveolar bone morphology with widening of the periodontal space around the maxillary molar roots and/or presence of periosteal bone apposition at the alveolar ridge outline were a priori considered an indication of periradicular disease.

All scans were de-identified. The presence of periradicular disease was recorded. The distance from the cemento-enamel junction (CEJ) to the alveolar crest (AC) was measured at the distal surface of the second molar, as previously described [8, 26]. Buccal cortical thickness was measured on axial slices oriented parallel to the occlusal plane, in the area of the 2nd molar at the level of the apical third of the roots [8, 26].

ex vivo μCT scanning

Dissected maxillae were imaged by high-resolution ex vivo μCT utilizing the SkyScan 1172 μCT scanner (SkyScan, Kontich, Belgium), as described [8, 26]. Volumetric image data were converted to DICOM format and imported in the Dolphin Imaging software to generate 3D and multiplanar reconstructed images, as above.

All scans were de-identified. Healing of extraction sockets was rated as complete (healing of more than 75% of the socket), partial (healing of 25% - 75% of the socket) or absent (healing of less than 25% of the socket). Also, the bone volume (BV), tissue volume (TV), and BV/TV of the alveolar bone excluding the extraction socket were measured, as described [8, 26].

Histology and TRAP staining

Maxillae were fixed for 48 h in 4% paraformaldehyde and then decalcified in 14% EDTA for 3 weeks. Samples were paraffin embedded and 5 μm-thick cross sections were made perpendicular to the long axis of the alveolar ridge at the area of maximum radiographic and clinical changes, as assessed by μCT analysis and clinical photographs. H&E stained slides were digitally scanned utilizing the Aperio AT automated slide scanner and automated image analysis was performed using the Aperio Image Scope software (Aperio Technologies, Inc., Vista, CA, USA). The area of the alveolar bone, from the alveolar crest to the floor of the nasal cavity was defined as the region of interest (ROI). The total number of osteocytic lacunae, the number of empty lacunae, and the surface of osteonecrotic area(s) were quantified. An area of osteonecrosis was defined as a loss of more than five osteocytes with confluent areas of empty lacunae [8, 24, 26]. Lacunae housing necrotic, karyolitic osteocytes, indicated by eosinophilic stained nuclei, were counted as empty osteocytes. The shortest distance from the inferior part of the epithelium to the alveolar crest was measured. If the bone was extruding above the epithelium the distance was recorded as negative. The Aperio Image Scope software was used to quantify the total bone area, the surface area of osteonecrosis and to make all linear measurements. All histology and digital imaging was performed at the Translational Pathology Core Laboratory (TPCL) at the David Geffen School of Medicine at UCLA.

For enumeration of osteoclasts, tartrate-resistant acid phosphatase (TRAP) staining was performed utilizing the leukocyte acid phosphatase kit (387A-IKT Sigma Aldrich, St. Louis, MO, USA). Positive cells were identified as multinucleated (≥2) TRAP-positive cells in contact with or very close proximity to the bone surface, in the ROI and were counted manually (AS).

Statistics

Raw data were analyzed using the GraphPad Prism Software (GraphPad Software, Inc. La Jolla, CA). Descriptive statistics were used to calculate the mean and the standard error of the mean (SEM). Data were analyzed by a two-way ANOVA and post-hoc Tukey's test for multiple comparisons among the various groups, with a statistical significance of $p<0.05$. The presence or absence of mucosal defect after tooth extraction and the degree of socket healing (complete, partial or absent) were analyzed using the Fisher's exact test.

Results

Radiographic assessment of spontaneous periradicular bone loss around maxillary molars

In vivo microCT revealed the presence of periradicular bone loss in 12/28, 10/24 and 8/25 maxillary sites of all vehicle, OPG-Fc or ZA animals respectively, with no statistical difference among vehicle, OPG-Fc and ZA groups ($p>0.05$). µCT imaging showed a normal PDL space and alveolar bone in vehicle, OPG-Fc and ZA animals with healthy teeth (Fig 1A, A1, B, B1, C and C1). In contrast, significant alveolar bone loss (white arrows) and increased bone thickness (white arrowheads) were seen around the molar roots of animals with periradicular disease (Fig 1D, D1, E, E1, F, F1). Quantification of radiographic features showed statistically increased bone loss in diseased vs. healthy teeth in all groups (Fig 1G). A common radiographic finding in patients with ONJ is periosteal bone deposition causing alveolar expansion [85]. To quantify potential bone deposition along the buccal maxillary cortex, we measured the thickness of the buccal bone in all six groups. Indeed, buccal cortical thickness increased in the diseased vs. healthy site of ZA and OPG-Fc groups, as well as in the diseased site of the ZA and OPG-Fc groups vs. the diseased site of the vehicle group (Fig 1H).

Clinical assessment of mucosal healing after tooth extraction

Visual inspection showed that four weeks after extraction, the alveolar mucosa healed normally in all vehicle treated animals (Fig 2A and D). Normal soft tissue healing was also present in the majority of mice treated with antiresorptives with extraction of healthy teeth, with only 1 of 14 (7.1%) and 2 of 17 (11.7%) OPG-Fc or ZA animals, respectively, demonstrating soft tissue defects (Fig 2B, C, G). In contrast, 7 of 10 (70 %) of OPG-Fc and 6 of 8 (75%) of ZA animals that had undergone extraction of teeth with periradicular disease showed mucosal defects and the presence of exposed bone in the area of the extraction (Fig 2E and F, blue arrows and 2G).

Radiographic assessment of socket healing after tooth extraction

High-resolution *ex vivo* micro-CT was performed to assess bone architecture of the alveolar ridge after tooth extraction. Vehicle animals, irrespective of extraction of healthy or diseased teeth, demonstrated remodeling of the socket outline and, in the great majority of cases, near complete healing of the extraction socket (Fig 3 A, A1, D, D1, D2, G). OPG-Fc and ZA animals that had undergone extraction of healthy teeth, also displayed some extraction socket healing in nearly all sites (12/13 and 14/15 respectively), with the majority of sockets (9/14 and 14/15 respectively) showing complete healing (Fig 3 B, B1, C, C1, G). Interestingly, in the antiresorptive but not vehicle treated animals, the original outline of the extraction socket was easily identifiable and the socket healed with a granular, woven-like bone that lacked normal trabecular architecture. In contrast, in OPG-Fc and ZA animals, extraction sockets of diseased teeth showed overall decreased healing compared to socket of extracted healthy teeth (Fig 3 G), with several animals showing absence (5/10 and 5/8 respectively) of intra-socket bone formation as seen by multiplanar views (Fig 3 E, E2, F, F2) and 3D rendering (Fig 3 E1, F1, black arrows). Occasional bony spicules were

20

also noted within the empty extraction sockets (Fig 3 F, F2, white arrows). As expected, OPG-Fc and ZA animals demonstrated increased BV/TV values of the alveolar ridge, compared to vehicle animals, without any difference between sites of healthy vs. diseased teeth (Fig 3H).

Histologic assessment of socket healing after tooth extraction

After μCT assessment, histologic evaluation of the maxillae was performed (Fig 4). Vehicle animals with extraction of healthy teeth showed normal healed epithelium (Fig 4A, white arrow) with presence of rete pegs, fibrous connective tissue with no significant inflammatory infiltrate, and remodeled extraction sockets (Fig 4A, A1). Animals treated with either OPG-Fc or ZA and with extraction of healthy teeth also showed normal soft tissue healing, including a regular epithelial lining with the presence of rete pegs (Fig 4B, C, white arrows) and fibrous connective tissue without a significant inflammatory infiltrate. Dense woven bone occupied most of the extraction socket, while the boundaries of the original extraction socket could be easily recognized (Fig 4, B, B1, C, C1).

Vehicle animals with extraction of diseased teeth also showed mostly normal epithelial lining (Fig 4D, white arrow). The underlying connective tissue contained a mild inflammatory infiltrate. In the healing extraction socket, woven bone with multiple reversal lines, and marrow fibrosis were noted (Fig 4D, D1, D2, D3). In OPG-Fc or ZA animals with extraction of diseased teeth (Fig 4E, E1, E2, E3, F, F1, F2, F3), epithelial migration (black arrows) and abundant inflammatory infiltrate (green arrows) in both the epithelial and connective tissue compartments were noted. In several specimens, the extraction socket had not healed with any bone and was not

21

covered by epithelium or connective tissue, but was exposed to the oral cavity (blue arrows). In other specimens, an epithelial defect was present, and thin fragmented connective tissue, and foreign material debris covered the extraction sockets (orange arrows). Osteonecrosis (Fig 4 E, E1, E2, E3, F, F1, F2, F3 yellow arrows) of the alveolar bone and occasional small sequestra (light blue arrows) were noted.

Quantification of the histologic findings revealed a statistically significant increase in the number of empty osteocytic lacunae and in the osteonecrotic area in OPG-Fc and ZA animals with extraction of diseased teeth compared to extraction of healthy teeth in the same treatment group or compared to extraction of diseased teeth in vehicle animals (Fig 5 A and B). Also, OPG-Fc vs. ZA animals with extraction of diseased teeth showed a higher number of empty osteocytic lacunae and osteonecrotic area (Fig 5 A and B).

Epithelium to alveolar bone crest distance was similar in vehicle animals with extraction of healthy or diseased teeth and in OPG-Fc and ZA animals with extraction of healthy teeth. However, in some OPG-Fc and ZA animals with extraction of diseased teeth, the epithelial to alveolar bone crest distance decreased and in animals with bone exposure it assumed a negative value. This was presumably due to the epithelial migration in combination with inhibition of alveolar bone crest resorption (Fig 5C).

TRAP staining was performed to evaluate osteoclast numbers (Fig 5D). As expected, high numbers of osteoclasts were present in vehicle animals with extraction of healthy teeth, and statistically higher numbers in vehicle animals with extraction of diseased teeth. OPG-Fc treatment

inhibited formation of osteoclasts in all animals. As previously observed [8, 26, 34], TRAP+ cells in

ZA treated animals were atypical, with a round shape and pyknotic nuclear morphology that were

detached from the bone surface (not shown). Significantly increased numbers of these atypical

TRAP+ cells were seen in animals with extraction of diseased vs. healthy teeth.

Discussion

Major progress has been made in the understanding of ONJ pathophysiologic mechanisms

since the disease was first reported more than a decade ago [27, 62]. However, significant gaps in our

knowledge still exist [2]. A strategy towards bridging these gaps is the concerted effort of research

groups in developing animal models that closely mimic ONJ presentation in humans [61]. For these

models, animals are treated systemically with high-dose antiresorptives in combination with a local

intervention.

Two approaches to induce changes to the local oral environment and precipitate ONJ

development have been utilized [2, 42, 61]. One approach involves tooth extraction [22, 23, 75-79], prompted

by well-established observations in clinical studies that clearly associate ONJ with tooth

extractions [48, 50, 55]. These models employ extraction of healthy teeth in combination with

antiresorptives. However, in adult patients, more than 90% of teeth are extracted due to severe

dental disease, including periodontitis, extensive caries, periapical disease, root fracture, or failed

endodontic treatment [63, 80]. Severe dental disease, as the precipitating factor leading to extraction,

also occurs in patients on antiresorptives who eventually develop ONJ. Patients with bone cancer

or osteoporosis would not be candidates for elective extraction of healthy teeth. This raises the

concern that animal models of ONJ with extraction of healthy teeth might not fully capture the

clinical setting of patients with extraction of teeth so severely affected by dental disease that they cannot be managed through conservative interventions.

A second approach in introducing local risk factors for ONJ development in animals utilizes induction of severe dental disease [8, 24-26, 34, 84]. This approach was prompted by the association of periodontal or periapical disease with ONJ in patients in the absence of tooth extraction [1, 2, 81, 86]. An additional revealing observation was the 1981 publication by Gotcher and Jee, reporting the presence of exposed alveolar bone trabeculae protruding into the oral cavity or well into the oral epithelium of rice rats with periodontitis treated with dichloromethylene diphosphonate (Cl2MDP) [83]. Thus, the authors effectively reported the development of experimental ONJ nearly 22 years before the disease was reported in patients [27, 62]. However, these dental disease models do not reflect the most common presentation of ONJ in patients, which is a non-healing socket after tooth extraction [1, 2]

The need to more accurately reflect the clinical reality has led researchers to continue developing and improving animal models [2, 42, 61]. In this effort, here we have combined the two approaches of altering the local oral environment to favor ONJ development along with extraction of both healthy and diseased teeth. Furthermore, animals were treated with two different classes of antiresorptives: ZA, a potent BP, or OPG-Fc, a RANKL inhibitor. We confirmed the presence of dental disease prior to tooth extractions by performing in vivo microCT and radiographically assessing the architecture of the periodontal bone and the alveolar ridge. As expected, the incidence of dental disease was similar in all groups.

Mucosa healed normally after extraction of healthy or diseased teeth in veh animals, and following extraction of healthy teeth in animals treated with antiresorptives. In contrast, extraction of diseased teeth in animals treated with antiresorptives resulted in mucosal defects resembling

24

clinical ONJ in 70-75% of the sites. Radiographic assessment of the extraction socket revealed normal healing of all the sockets in veh animals with extraction of healthy or diseased teeth. In OPG-Fc or ZA animals with extraction of healthy teeth, the extraction sockets healed mostly with woven bone that was distinct from the remaining alveolar bone. However, in the same animal groups, but with extraction of diseased teeth, 50-60% of the animals showed defective socket healing. Histologic assessment confirmed the clinical and radiographic findings revealing increased osteonecrosis, mucosal defects, bone exposure, and occasional sequestration in animals with extraction of diseased teeth that were treated with antiresorptives.

Our findings closely parallel the clinical, radiographic, and histologic features of ONJ in patients with exposed and necrotic bone, without (Stage 1) or with (Stage 2) evidence of infection [1, 2]. Interestingly, we did not observe any animals with extensive changes of the alveolar bone structure, pathologic fractures, extraoral fistulae, or oronasal communication that would be classified as Stage 3 ONJ. The absence of such severely affected animals is possibly due to the short duration of our experiments, the lower incidence of Stage 3 ONJ compared to other stages [43, 87, 88], or the lack of a concomitant systemic factor that would compound healing of the oral tissues [1, 2].

Surprisingly, very few animals with extraction of healthy teeth and treated with antiresorptives presented with mucosal defects or radiographic and histologic features resembling ONJ. This finding appears in agreement with some, but not all, published studies that have utilized extraction of healthy teeth in animals on BP or other antiresorptive treatment. Indeed, the reported outcomes of disease incidence and severity in ONJ rodent extraction models vary considerably [61]. This variability has been hypothesized to be due to the type, route of administration, and dose regimen of BP delivery, in combination with the lack of well-defined outcome measures that define

the presence of ONJ in rodents [61]. It is noteworthy, that studies consistently reporting ONJ-like features in mice or rat extraction models include in their experimental design systemic risk factors such as steroid or chemotherapy treatment, vitamin D deficiency, or diabetes all of which alter soft tissue and/or bone homeostasis and compound wound healing [22, 23, 44, 75, 76, 78].

Our results here point to an additional factor contributing to the variability of ONJ incidence and severity in animal model studies that lack a concomitant systemic risk factor [77, 79, 89-94]. In our experience, occurrence of spontaneous periradicular lesions around maxillary teeth in C57Bl/6J or DBA1/J male mice ranges from 35-50% [26], varies among vendor shipment of animals, and is unavoidable. The only way to predictably affirm the presence or absence of changes in alveolar bone is to perform in vivo microCT prior to tooth extraction, as performed in our present studies. Thus, it is plausible that in some studies, extractions could have involved diseased teeth that might have inadvertently escaped detection. Based on our data presented herein, such extractions in animals under antiresorptive treatment would likely present with clinical, radiographic, and histologic features of ONJ-like lesions.

In our studies, OPG-Fc vs. ZA animals showed a significantly larger number of empty osteocytic lacunae and osteonecrotic area, suggesting that the extent of osteonecrosis might be slightly greater after OPG-Fc treatment. We had made a similar observation of higher number of empty osteocytic lacunae with OPG-Fc vs. ZA treatment previously [26]. This finding could be within expected experimental variation. However, it could also reflect diverse residual osteoclastic activity after treatment with the two antiresorptives. Indeed, OPG-Fc abolished formation of osteoclastic cells, suggesting complete inhibition of bone resorption. On the other hand, TRAP positive cells were present in the ZA animals, but demonstrated an altered morphology. Thus, some degree of bone resorption must have occurred that caused ZA release from the bone matrix

and subsequent intracellular translocation to induced alterations in osteoclast function and morphology. Nevertheless, it is important to note that both OPG-Fc and ZA animals presented similar incidence of mucosal defects and extraction socket healing deficits.

From a clinical point of view, our studies demonstrate the importance of detailed radiographic assessment of bone changes prior to tooth extraction in patients on antiresorptive treatment. Indeed, the most recent International Consensus paper [2] recommends that in patients for whom ONJ is a clinical concern and teeth extractions are considered, small field of view (FOV), high resolution Cone Beam Computed Tomography (CBCT) or multi-detector CT scans are recommended, if available. These imaging modalities provide valuable information on changes in cortical and trabecular architecture, periosteal reaction, osteolysis, or sequestration.

In conclusion, we have created an approach that refines existing ONJ mouse models to more closely parallel the clinical setting. We report that extraction of diseased, but not of healthy teeth in mice treated with high-dose antiresorptives led to mucosal defects, and radiographic and histologic features of ONJ. Our data, in association with previous published reports, strongly suggest a central role for dental disease in pathogenesis of ONJ, not only as the instigating cause for tooth extraction, but also as a compounding factor in ONJ development.

Figure 1. In-vivo µCT assessment of the maxillary molars prior to tooth extraction
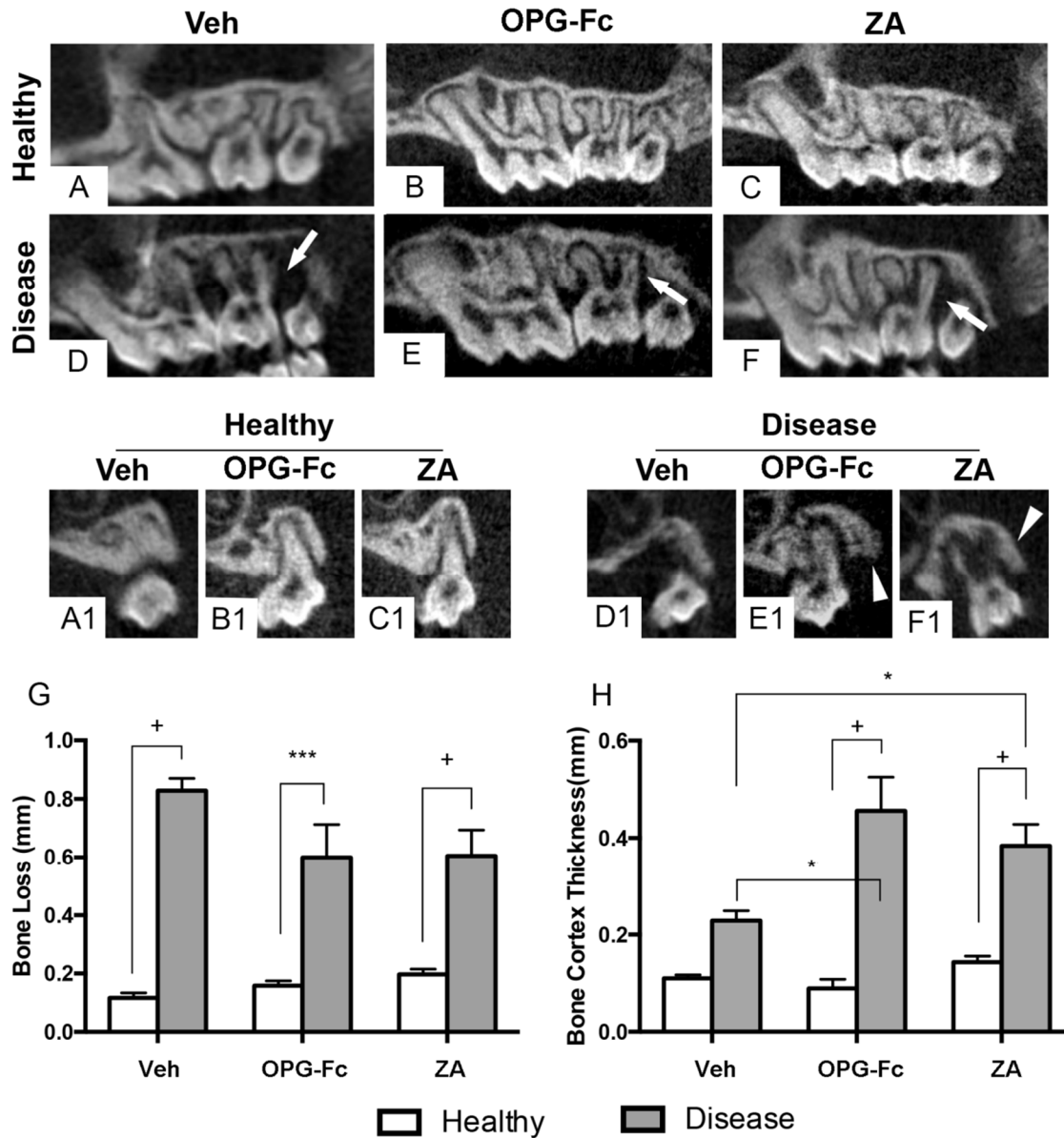
Figure 1: In-vivo µCT assessment of the maxillary molars prior to tooth extraction. (A, B, C) Sagittal and (A1, B1, C1) coronal sections of sites with healthy molars in vehicle, OPG-Fc, and ZA groups, respectively. (D-F) Sagittal and (D1-F1) coronal sections of sites with diseased molars in vehicle, OPG-Fc, and ZA groups, respectively. Quantification of (G) interproximal bone loss and (H) buccal cortex thickness. + Statistically significantly different, p < 0.0001. *Statistically

significant difference among compared groups, p < 0.05. Differences among groups were calculated by two-way ANOVA and post-hoc Tukey's test for multiple comparisons. Data represent the mean ± SEM.

Figure 2. Visual assessment of mucosal healing of maxillary alveolar ridge after tooth extraction.
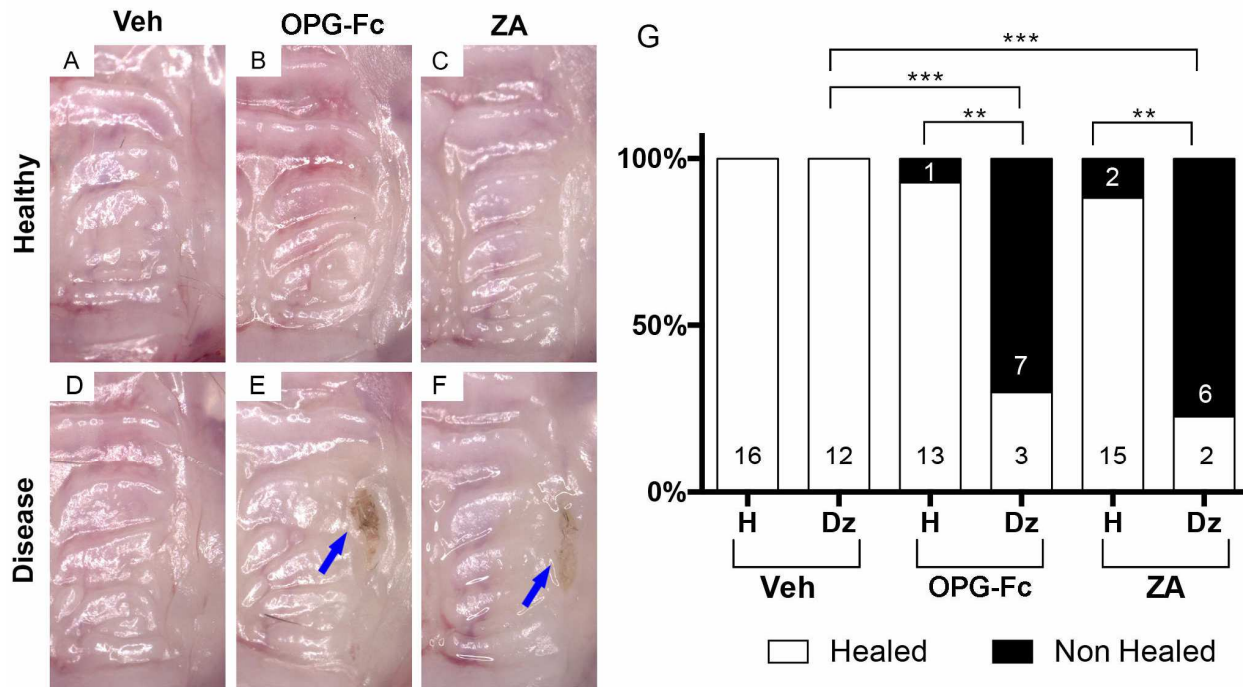
Figure 2: Visual assessment of mucosal healing of maxillary alveolar ridge after tooth extraction. (A-C) Maxillae in veh, OPG-Fc, and ZA groups after extraction of healthy teeth, respectively. (D-F) Maxillae in veh, OPG-Fc, and ZA groups after extraction of diseased teeth, respectively. Blue arrows point to areas of exposed bone. (G) Qualitative assessment of mucosal healing after healthy or diseased teeth in various treatment groups. *** Statistically significantly different, p < 0.001. ** Statistically significantly different, p < 0.01. Differences between groups were calculated by Fisher exact probability test.

Figure 3. μCT assessment of the edentulous maxillary alveolar ridge and quantification of μCT findings.
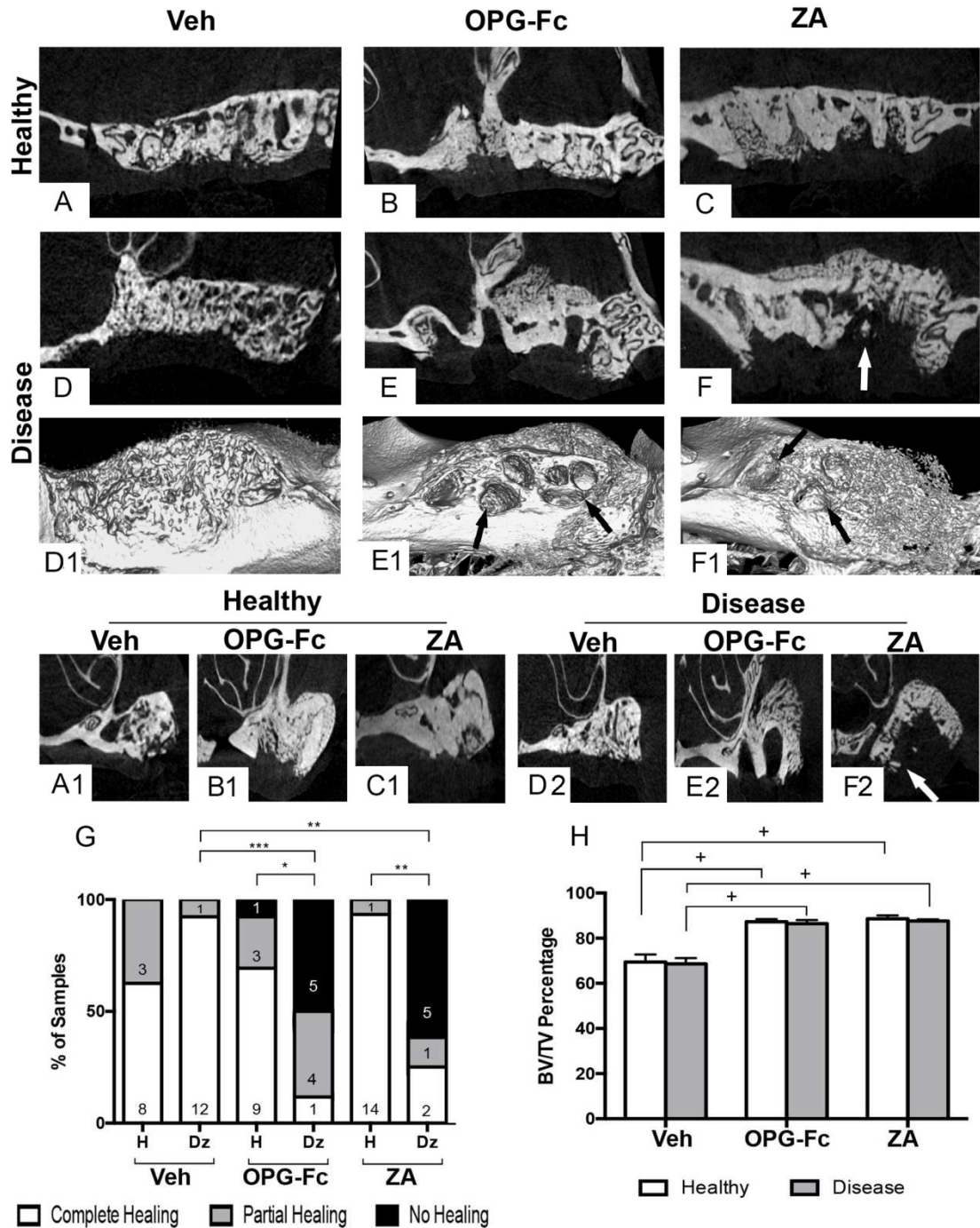
Figure 3: µCT assessment of the edentulous maxillary alveolar ridge and quantification of µCT findings. (A-F) Sagittal, (A1, B1, C1, D2, E2, F2) coronal views and (D1, E1, F1) 3D renderings of edentulous alveoli after extraction of healthy (A, B, C, and A1, B1, C1) or diseased (D, E, F, D1, E1, F1, D2, E2, F2) teeth in vehicle, OPG-Fc, or ZA groups. (G) Qualitative assessment of socket healing after extraction of healthy or diseased teeth in various treatment groups (H). Quantification of bone volume / tissue volume. + Statistically significantly different, $p < 0.0001$. ***Statistically significantly difference, $p < 0.001$. **Statistically significantly different, $p < 0.01$. *Statistically significantly different, $p < 0.05$. Differences between groups for (G) were calculated by Fisher exact probability test. Differences among groups for (H) were calculated by two-way ANOVA and post-hoc Tukey's test for multiple comparisons. Data represent the mean ± SEM.

Figure 4. Representative H&E-stained images from maxillae of all groups
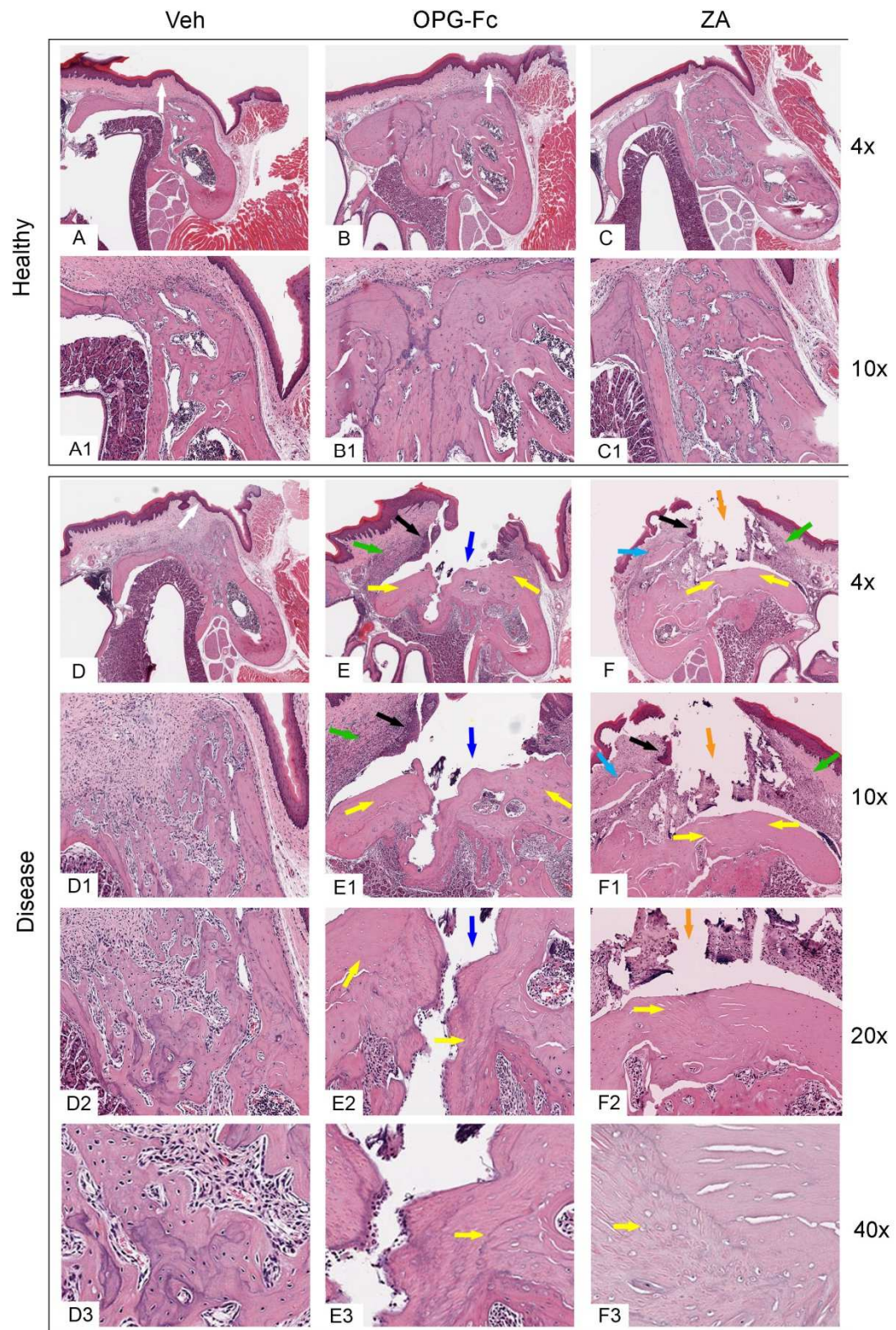
Figure 4. Representative H&E-stained images from maxillae of all groups. Alveolar ridge after extraction of (A, A1, B, B1, C, C1) healthy or (D, D1, D2, D3, E, E1, E2, E3, F, F1, F2, F3) diseased teeth of vehicle, OPG-Fc, and ZA groups, respectively, viewed at 4 x (A, B, C, D, E, F), 10 x (A1, B1, C1, D1, E1, F1), 20 x (D2, E2, F2), or 40x (D3, E3, F3) magnification. White arrows point to normal epithelia lining, green arrows to inflammatory infiltrate, black arrows to epithelial migration, blue arrows to bone exposure, orange arrows to fragmented connective tissue, yellow arrows to areas of osteonecrosis, light blue arrows to sequestra.

Figure 5. Quantification of the histologic findings
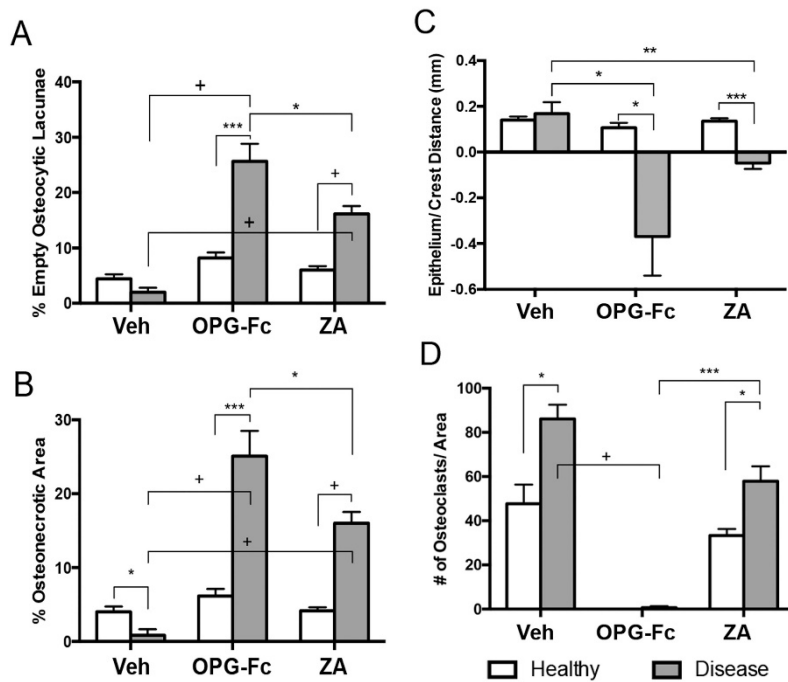
Figure 5: Quantification of the histologic findings. (A) percent empty osteolytic lacunae, (B) percentage of osteonecrotic area, (C) distance from lower point of epithelium to alveolar bone crest (D) number of TRAP+ cells per area + Statistically significantly different, $p < 0.0001$. ***Statistically significantly different, $p < 0.001$. **Statistically significantly different, $p < 0.01$. *Statistically significant different, $p < 0.05$. Differences among groups were calculated by two-

way ANOVA and post-hoc Tukey's test for multiple comparisons. Data represent the mean ±

SEM.

CHAPTER 3

ZOLEDRONATE IMPAIRS SOCKET HEALING AFTER EXTRACTION OF TEETH WITH EXPERIMENTAL PERIODONTITIS

Abstract

Osteonecrosis of the jaws (ONJ) is a rare but severe complication of antiresorptive medications, such as bisphosphonates, used in the treatment of bone malignancy or osteoporosis. Tooth extraction and dental disease have been strongly associated with ONJ development. Here, we have investigated molecular and cellular markers of socket healing after extraction of healthy or teeth with experimental periodontitis in Wistar-Han rats treated with zoledronic acid (ZA). We included four experimental groups: Groups 1 and 2 with extraction of healthy or teeth with ligature-induced experimental periodontitis (EP) in vehicle treated animals, and Groups 3 and 4 with extraction of healthy or teeth with EP in ZA treated animals, respectively. Animals were pretreated with vehicle or ZA for a week and EP was induced. Four weeks later, the second maxillary molars were extracted, sockets were allowed to heal for four weeks, animals were euthanized and maxillae were isolated. Radiographically, extraction sockets in Groups 1, 2 and 3 demonstrated normal healing. Contrary, incomplete socket healing was noted after extraction of teeth with EP in ZA-treated rats of Group 4. Histologically, persistent inflammation and extensive osteonecrosis were seen in Group 4. Disorganization of the collagen network, collagen type III predominance and lack of collagen fiber insertion in the necrotic bone were associated with impaired socket healing. Cells positive for MMP-9, MMP-13 and α-SMA expression were present at the areas of epithelial invagination and adjacent to osteonecrotic bone. Importantly, human biopsies from ONJ patients showed similar findings. Our data emphasize the importance

of dental disease and tooth extraction in ONJ pathogenesis and help delineate an altered profile in wound healing markers during ONJ development.

Introduction

Osteonecrosis of the jaws (ONJ) is a rare but severe complication of antiresorptive medications, specifically bisphosphonates (BPs) and RANKL inhibitors, or antiangiogenic medications [1, 61]. Duration, dose and potency of antiresorptives, concomitant diseases or additional medications are known to increase incidence and severity of ONJ. However, the ONJ detailed pathophysiologic mechanisms remain poorly understood, largely due to the low ONJ incidence, and the proposed conservative treatment protocols that do not allow extensive sampling. Animal models, provide significant insight but need to be critically considered, since bone homeostasis of experimental animals and interventional approaches do not always parallel clinical scenarios [2]. Altered inflammatory response, infection, defective angiogenesis, bisphosphonate toxicity to soft tissues, increased turnover of alveolar bone, oversuppression of bone remodeling and genetic predisposition might contribute to ONJ pathophysiology [95].

ONJ may occur spontaneously, underneath a denture or at areas with periodontal or periapical infection. However, the most common local instigating factor for ONJ development, is trauma and particularly, tooth extraction [27, 96]. Teeth in adults are mainly extracted due to periodontal or pulpal disease [63]. Clinical studies support an association between dental disease with ONJ occurrence [97], while dental preventive measures reduce ONJ incidence [6].

Extraction socket healing involves several cellular processes and the interplay of soft and osseous tissue healing. The wound/socket-healing process is divided into inflammatory; proliferative; and modeling/remodeling phases [98, 99]. Early events include hemostasis, formation

of a provisional wound matrix, and neutrophil and monocyte infiltration. In the proliferation phase, granulation tissue forms and the vascular network is restored. Layers of woven bone are deposited adjacent to the socket borders. Finally, in the modeling/remodeling phase changes occur in the connective tissue and bone architecture, including replacement of woven with lamellar bone and bone marrow [100].

Animal models reproduce clinical, radiographic and histologic features of ONJ [25, 79, 84]. Zoledronic acid (ZA), a potent BP, or RANKL inhibitors and periapical or periodontal disease cause osteonecrosis of alveolar bone in rats and mice [24, 26, 34]. These findings led us to hypothesize that in antiresorptives treated animals, extraction of teeth with experimental periodontitis (EP), and thus with pre-existing osteonecrosis, would result in compromised socket healing and progression of ONJ like findings. Indeed, extraction of teeth with spontaneous periradicular disease, but not healthy teeth, in mice treated with ZA or a RANKL inhibitor induced clinical bone exposure and osteonecrosis. [101].

Though socket healing is delayed in tooth extraction sites of most human patients receiving strong anti-resorptives, ONJ occurs in only a small fraction of such tooth extractions [1]. An improved understanding of this topic, especially concerning preexisting circumstances that increase the risk that a specific tooth extraction will lead to ONJ is of great clinical importance. The focus of our studies herein is to investigate changes in socket and wound healing markers (type III collagen, matrix metalloproteinases MMP-9, MMP-13 and presence of α–SMA positive cells) after extraction of healthy teeth or of teeth with preexisting EP in rats treated with vehicle or ZA.

Materials and Methods

Animal care

Forty-five rats were randomly assigned to receive saline (vehicle) or 200μg/kg ZA (LKT Laboratories, St Paul, MN) intraperitoneally, 2x/week in am. At time of injection body weight was recorded for all animals.

Rats received veh or ZA for a week, and 4.0 silk ligatures were placed around the left maxillary second molar to induce experimental periodontitis (EP). Ten (10/22) veh-treated rats received molar ligation and 12 (12/22) did not. 11 (11/23) ZA treated animals received molar ligation and 12 (12/23) did not. Four weeks later, in vivo μCT was performed and the following day the first and second maxillary molars were extracted. Thus, our study included groups veh-H and veh-EP with extraction of healthy teeth or teeth with EP in veh treated animals, and ZA-H and ZA-EP groups with extraction of healthy teeth or teeth with EP in ZA treated animals. Four weeks after tooth extraction, without discontinuation of veh and ZA treatment, rats were euthanized utilizing CO_2.

Specimen scanning

Deidentified maxillae were imaged, as described. [26]

Radiographic assessment of socket healing

Details of qualitative and quantitative radiographic assessment are provided in the supplemental material. Examples of normal, partial and limited socket healing are seen in Supplemental Figure 1.

Histology and TRAP staining

Details about histology and TRAP are provided in the supplemental material. All specimens were stained with picrosirius red (PSR) stain kit (Polysciences Inc, Warminster, PA, USA) and visualized under bright field and polarized light.

Immunohistochemistry

Anti-Collagen I (ab34710), anti-Collagen III (ab7778), anti-MMP-9 (ab38898), anti-MMP-13 (ab39012), and anti-α–SMA (ab5694) antibodies (ABCAM, Cambridge, MA, USA) were used.

Human specimens

Anonymous unstained slides and associated non-identifiable clinical information from two cases with histological diagnosis of ONJ were received from the UCLA School of Dentistry records. The first patient was a 70 yo female with a history of Fosamax treatment and recent extractions, and pain and drainage of the upper left maxilla. The second patient was a 68 yo female with IV ZA history and chronic bone exposure in the right posterior mandible. H&E and immunohistochemistry staining were performed, as above, for both patients.

Statistics

Experimental unit was a single animal. Data were analyzed using GraphPad Prism (GraphPad Software, Inc. La Jolla, CA). Descriptive statistics (mean and SEM), a two-way ANOVA for multiple comparisons, and Fischer's exact test for socket healing were used.

Results

Radiographic findings

In vivo μCT scanning revealed similar bone appearance around the 2nd molar of veh or ZA animals without ligature. In veh rats, ligature caused periodontal bone loss (Supplemental Figure 2A, white arrows). In ZA rats, bone loss around molars with ligature, was statistically significantly greater compared to non-ligated molars, but attenuated compared to veh animals (Supplemental Figure 2A, white arrows, B)

To assess the ZA effect on jaw bone morphology, BV/TV of the mandibular trabecular alveolar bone was measured, and showed a statistically significant increase in ZA animals (Supplemental Figure 3A). In the maxillae of these animals, woven bone filled the sockets of veh-H and veh-EP animals (Figure 6A, white arrows). In ZA-H animals, woven bone occupied the socket, while the socket outline was clearly visualized. In ZA-EP animals, impaired socket healing was noted (Figure 6A, white arrowheads). Qualitative (Figure 6B) and quantitative (Figure 6C) assessment demonstrated statistically significantly compromised socket healing of ZA-EP animals. These animals also demonstrated decreased BV/TV in the area of the extracted second molar (Supplemental Figure 3B).

Histologic findings

Histologically, veh-H and veh-EP animals showed socket filling with woven bone (Figure 6D, blue arrows), presence of prominent reversal lines and a pronounced periosteum at the alveolar crest (Figure 6D, green arrows). The mucosa consisted of keratinized epithelium, a lamina propria with dense connective tissue, and lack of marked inflammatory infiltrate (Figure 6D, yellow arrows). ZA-H animals demonstrated filling with woven bone (Figure 6E, blue arrows) and prominent reversal lines. The original socket borders were easily discernible (Figure 6E, white arrows). The mucosa consisted of keratinized epithelium and a lamina propria with a dense connective tissue lacking a marked inflammatory infiltrate (Figure 6E). In contrast, ZA-EP animals

showed impaired bone healing, epithelial invagination, and osteonecrotic areas with empty osteocyte lacunae (Figure 6E, black arrows). A marked inflammatory infiltrate was noted in the non-healing socket adjacent to osteonecrotic areas, extending into the submucosa and the basal epithelial layer (Figure 6E, aqua arrows). The % empty osteocyte lacunae (Figure 6F) and the absolute number of empty osteocyte lacunae in the alveolar bone (Supplemental Figure 3C), and the area of osteonecrosis (Figure 6G) were statistically significantly increased.

Osteoclast number was statistically significantly increased in the EP versus H groups, in both veh and ZA rats. As previously reported [8], the number of osteoclasts normalized to bone area (Figure 6H) and the absolute osteoclast number in the alveolar ridge (Supplemental Figure 3D) was statistically significantly elevated in the ZA vs. veh groups. However, the osteoclasts in the ZA groups demonstrated an altered morphology, appearing round, detached from the bone surface, and with pyknotic nuclei [101].

PSR staining revealed differences in collagen network organization among the groups. In veh-H and veh-EP animals, collagen fibers extended from the lamina propria, just below the epithelium into the alveolar bone, forming a dense, well-organized network (Figure 7A, 7A1, A2, B, B1, B2, aqua arrows). Collagen fiber birefringence had a yellow signal, suggestive of collagen type I prevalence [102]. In ZA-H animals, collagen fibers were markedly dense, maintained their ability to insert in the alveolar bone and demonstrated a yellow signal (Figure 7C, C1, C2, aqua arrows). In contrast, ZA-EP animals revealed collagen fibers with an overall green birefringence suggesting collagen type III predominance [102] (Figure 2D, D1, D2, green arrows). These collagen bundles did not extend into the alveolar bone (Figure 7D2, magenta arrows). Regions of signal absence (Figure 7D2, yellow arrows) were noted bordering the areas of osteonecrosis.

Immunohistochemical findings in rats

41

Collagen type I immunostaining was evident in all groups. As expected, no staining was present in regions of marked inflammatory infiltrate adjacent to areas of osteonecrosis (Supplemental Figure 4).

For veh-H, veh-EP and ZA-H animals, collagen type III immunoreactivity was more noticeable just underneath the epithelium (Figure 7E, F, and G, white arrows) and faint and diffuse in the remaining submucosal to the bone level (Figure 7E1, F1, G1). However, in the ZA-EP animals, a pronounced collagen type III signal was noted (Figure 7H, H1). The signal was especially prominent below the epithelium (Figure 7H, white arrow) adjacent to osteonecrotic bone (Figure 7H1, blue arrow), and adjacent to inflammation (Figure 7H1, green arrows) and epithelial invagination (Figure 7H1, red arrows).

MMP-8, MMP-9 and MMP-13 are molecules that can modify the matrix structure. No expression of MMP-8 was detected (not shown). MMP-9 positive cells were mostly observed in ZA-EP rats (Figure 8D, D1a, D1b, D2a, D2b arrows, I). Statistically significantly more positively immunoreactive cells were noted within the epithelium at areas of epithelial invagination (Figure 8D1a and D2a, magenta arrows), and around areas of osteonecrosis (Figure 8D1b and D2b, green arrows).

Few weakly immunostained MMP-13 cells were seen in the periosteum at the extraction site, but not in the submucosal area of veh-H, veh-EP and ZA- animals (Figure 8E, E1, E2, F, F1, F2, G, G1, G2). In socket healing areas, MMP-13 immunoreactivity was noted along the reversal lines and the bone- bone marrow interface (Figure 8E, F, G blue arrows). However, in ZA-EP rats MMP-13 immunostain was statistically significantly increased (Figure 8J). Positive cells were localized within and around epithelium in areas of epithelial invagination (Figure 8H, H1a and H2a, magenta arrows). Exuberant MMP-13 staining was noted at areas of inflammation and

peripheral to the necrotic alveolar ridge (Figure 8H, H1b, H2b, green arrows). Select MMP-13 positive osteocytes were seen adjacent to osteonecrotic areas (Figure 8H1b, black arrows).

We finally tested α-SMA, a cytoskeletal scaffold protein expressed in myofibroblasts [103]. Veh animals demonstrated low α-SMA signal, mainly confined to blood vessel walls (Figure 9A, A1, A2, B, B1, B2, white arrows). In ZA-H animals, α-SMA signal was also present on vessel walls (Figure 9C, C1 and C2, white arrows). Few, scattered positive cells were dispersed in the submucosa (Figure 9C1 and C2, yellow arrows), or in marrow spaces. However, no statistical difference from the veh treated groups was detected (Figure 9E). Interestingly, statistically significantly increased numbers of α-SMA positive cells were noted in the submucosa of ZA-EP animals localized not only around blood vessels but also adjacent to necrotic bone (Figure 9D, D1 and D2, green arrows, E).

Immunohistochemical findings in patient specimens

To investigate whether the same markers were relevant in a patient setting, we explored collagen type III, MMP-13 and α-SMA presence in specimens from ONJ patients (Figure 10). Adjacent to osteonecrotic areas (Figure 10, blue arrows) high levels of collagen type III in the extracellular matrix (Figure 10, red arrows), as well as cells positive for expression of MMP-13 (Figure 10, yellow arrows) and α-SMA were noted (Figure 10, magenta arrows). Blood vessel walls also demonstrated α-SMA immunoreactivity (Figure 10, white arrows).

Discussion

In rodents treated with antiresorptives, dental disease can induce radiographic and histologic ONJ-like lesions [24-26], while subsequent extraction of diseased, but not healthy teeth, results in clinically exposed bone in mice [101]. Here, we investigated healing of the alveolar ridge

43

in veh or ZA treated animals after extraction of healthy or EP teeth in a larger animal, the rat. First, we established that ligature placement induced experimental periodontal bone loss, by in vivo μCT. This important step confirmed the effectiveness of the ligature placement to induce periodontal bone loss. Radiographic assessment revealed that extraction of teeth with EP in ZA animals, but not in other groups resulted in impaired osseous healing of extraction sockets after four weeks. Histology confirmed these findings, and established extensive alveolar bone osteonecrosis and presence of inflammatory infiltrate adjacent to necrotic areas pointing to a temporal association between the inflammatory environment and osteocyte death.

Consequently, the main focus of our studies was to investigate potential changes in socket and wound healing markers among the four treatment groups. We explored extracellular matrix changes that might be associated with the observed structural differences around necrotic areas. Collagen, the major extracellular matrix component [104], acts as a structural scaffold in tissues, while during wound healing modulates cell proliferation and migration [105]. Type III collagen is an important ECM component, and the predominant collagen during the early repair phase of wound healing, synthesized by fibroblasts in the granulation tissue [99]. With the maturation and wound closure, type III collagen undergoes degradation, while type I collagen synthesis increases [99]. Chronic inflammatory processes, like dermatitis or myocardial inflammation, are associated with increased type III expression [106, 107]. Persistence of type III collagen paralleled presence of inflammation and osteonecrosis in the ZA-EP animals. Interestingly, areas where type I collagen immunostaining decreased and type III collagen increased coincided with weak birefringence in PSR staining.

During wound remodeling and maturation, extracellular matrix undergoes continuous modifications. MMPs have the ability of degrading ECM components, growth factors and

cytokines [108]. MMP-9 and MMP-13 in particular play key roles in the homeostasis of the periodontium and alveolar bone during health and disease [109, 110]. MMP-9 and MMP-13 positive cells were abundantly present in ZA-EP rats at inflamed sites adjacent to necrotic bone and within the epithelium. Importantly, select MMP-13 positive osteocytes were noted adjacent to osteonecrotic areas, probably as a result of osteocyte activation.

Progressive wound healing depends on the co-ordinated function of several cell populations. Among them, myofibroblasts, characterized by the presence of α-SMA-positive stress fibers play a central role in wound tissue closure, through their capacity to produce a strong contractile force in later wound healing stages [103]. As healing progresses, the myofibroblastic population decreases [111]. Persistent presence of myofibroblasts is associated with pathologic conditions, like hypertrophic scarring and cardiac or lung fibrosis [112-114]. In our studies, the marked increase of α-SMA positive cells in close proximity to the inflammatory infiltrate and to the necrotic bone in ZA-EP animals suggests prolonged presence of the myofibroblastic population.

In these experiments, we did not observe consistent exposure of necrotic bone. Although there were many animals with clinically apparent mucosal defects in the ZA-EP group, an epithelial layer was present. Presence of epithelial invagination towards the necrotic area was noted, suggesting that a longer time period might have allowed for epithelial migration to the bone surface. Alternatively, other parameters such as infection by specific microbes, genetic predisposition, systemic disease or concomitant treatment interventions that might compromise soft tissue responses might be necessary. Our findings resemble Stage 0 ONJ in patients, where the necrotic bone is not clinically exposed [1]. Interestingly, in our previous study of extraction of teeth with periradicular disease in mice we did observe bone exposure in ZA animals [101].

Differences of animal species (mice vs. rats), duration of ZA treatment (12 v. 8 weeks), spontaneous periradicular vs. EP lesions might account for this discrepancy.

The tissue formation phase of wound healing, follows the inflammatory phase, and is characterized by the development of granulation tissue. Subsequently, at the maturation phase, granulation tissue develops into fibrotic tissue, marked by replacement of the provisional matrix with collagen [115]. Our findings suggest excessive retention of granulation tissue in the ZA-EP animals, while resolution of granulation tissue and healing occurred in all other groups. Failure of granulation tissue resolution reflects a defective wound healing process. In the ZA-EP animals presence of inflammatory infiltrate around large areas of osteonecrosis, lack of an organized collagen network without fiber insertion in the necrotic bone, and epithelial invagination suggest a compromise of socket healing beyond granulation tissue retention. Whether the composition of the granulation tissue around the osteonecrotic areas is unique to the ZA animals or similar to the granulation tissue during normal socket healing warrants further investigation.

Some limitations need to be considered in translating our findings towards the human disease. We only used male rats to parallel our previous observations [24]. However, gender differences might affect socket healing. Although rodents provide useful animal models to study bone diseases, including ONJ, they demonstrate differences in their skeletal homeostasis compared to humans [116]. In our studies, we used a ZA dose of 200 µg/kg, which is three times greater than the dose for a patient with bone malignancy [1]. We elected to utilize this higher dose to increase the prevalence of the disease and generate more prominent tissue responses. It should be noted, that ONJ incidence in cancer patients appears to plateau between 2-3 years of treatment [1] or 24-36 ZA infusions. The animals in our study received 18 ZA injections, which is within the clinically relevant treatment regimen. Finally, our studies included a single observational time point. It

would be important to expand these studies for multiple points and longer periods, such that sockets healing in ZA animals could be characterized in more detail.

Importantly, our observations in rats were replicated in biopsy specimens from patients with clinically, radiographically and histologically diagnosed ONJ, thus supporting the potential significance of our findings. Clinical studies with larger numbers of human samples focusing on markers of socket healing could begin delineating the process of ONJ pathogenesis in patients.

Collectively, our data point to the disruption of the physiologic process of wound healing during the extraction of teeth with periodontitis in the presence of BPs. The prolonged presence of inflammatory cells in the healing alveolar ridge, predominance of a type III collagen rich matrix, increased MMP-9 and MMP-13 expression in resident and inflammatory cells, and persistence of a prominent myofibroblastic population were key observations that could underlie ONJ pathophysiology.

Supplemental material

https://journals.sagepub.com/doi/suppl/10.1177/0022034517732770/suppl_file/DS_10.1177_002

2034517732770.pdf

Figure 6. Radiographic and histologic assessment of extraction sockets

49

Figure 6. (A, B) *In vivo* assessment of periodontal bone loss *and in vitro* assessment of the edentulous maxillary alveolar ridge (C, D). Sagittal sections of sockets after extraction of healthy teeth in vehicle or ZA treatment groups. White arrows point to complete socket healing and white arrowheads point to impaired socket healing. Representative H&E-stained images from maxillae of all groups. Alveolar ridges of vehicle (E) or ZA treated (F) animals after extraction of healthy or diseased teeth, viewed at 4x and 20x magnification. Yellow arrows point to absence of inflammation in the connective tissue, green arrows point to the periosteum, blue arrows to the healing of the original extraction socket, white arrows to the original socket outline, aqua arrows to inflammatory infiltrate and black arrows to osteonecrotic areas. (G, H, I) Quantification of osteonecrotic area, empty osteocyte lacunae and number of TRAP$^+$ cells per bone area respectively. For all statistical comparisons ** statistically significantly different, $p<0.01$, *** statistically significantly different, $p<0.001$, **** statistically significantly different, $p<0.0001$. Differences among groups were calculated by two-way ANOVA for multiple comparisons. Data represent the mean value +- SEM. For qualitative socket healing, differences among groups were calculated by Fischer's exact test.

Figure 7. Picrosirius red staining and Type III collagen immunostain
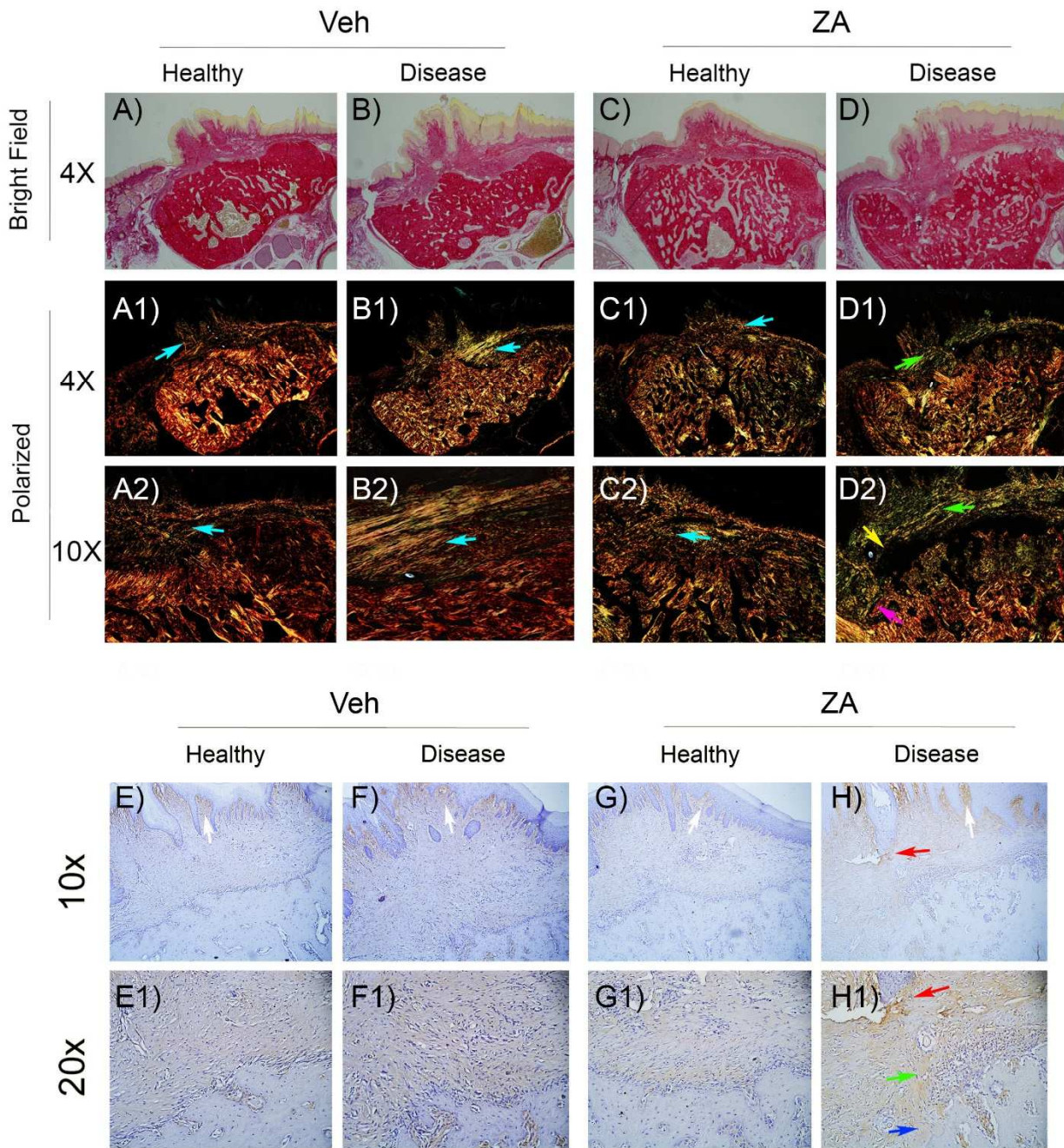
Figure 7. Picrosirius red staining of maxillary sockets of vehicle (A-A2, B-B2) or ZA (C-C2, D-D2) treated animals after extraction of healthy (A-A2, C-C2) or diseased (B-B2, D-D2) teeth,

visualized under bright field (A, B, C, D) or polarized light filter (A1, A2, B, B2, C1, C2, D1, D2), viewed at 4x (A, B, C, D, A1, B1, C1, D1), 10x (A2, B2, C2, D2) magnification. Aqua arrows point to yellow birefringence signal, green arrows to green birefringence signal, yellow arrows to absence of signal, magenta arrows to lack of signal extension into the alveolar bone. Collagen type III immunohistochemistry of maxillary sockets in vehicle (E, E1, F, F1) or ZA (G, G1, H, H1) treated animals after extraction of healthy (E, E1, G, G1) or diseased (F, F1, H, H1) teeth, viewed in 10x (E, F, G, H) or 20x (E1, F1, G1, H1). White arrows point to positive signal underneath the epithelum, blue arrows to signal adjacent to osteonecrotic bone, green arrows positive signal near inflammation, red arrows to positive signal adjacent to epithelial invagination.

Figure 8. MMP-9 and MMP-13 immunohistochemistry
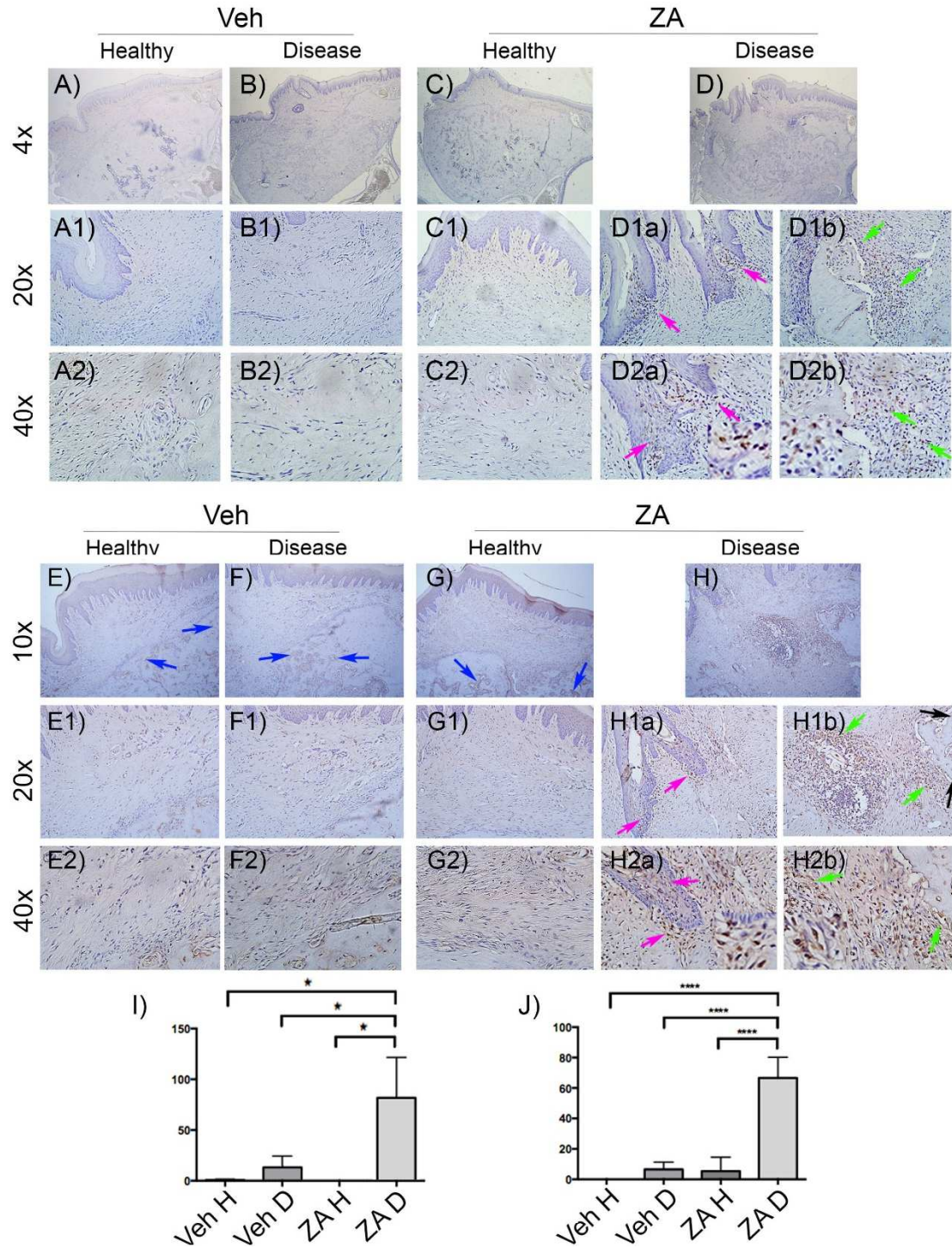
Figure 8. MMP-9 immunohistochemistry of edentulous alveoli in vehicle (A-A2, B-B2) or ZA (C-

C2, D, D1a, D1b, D2a, D2b) treated animals after extraction of healthy (A, A1, A2, C, C1, C2) or

53

diseased (B, B1, B2, D, D1a, D1b, D2a, D2b) teeth, viewed at 4x (A, B, C, D), 20x (A1, B1, C1, D1a, D1b) and 40x (A2, B2, C2, D2a, D2b) magnification. Magenta arrows point to positive cells around epithelial invagination and green arrows to positive cells at inflammatory areas and adjacent to necrotic bone. MMP-13 immunohistochemistry of maxillary alveolar sockets in vehicle (E-E2, F-F2) or ZA (G-G2, H, H1a, H1b, H2a, H2b) treated animals after extraction of healthy (E, E1, E2, G, G1, G2) or diseased (F, F1, F2, H, H1a, H1b, H2a, H2b) teeth, viewed at 10x (E, F, G, H), 20x (E1, F1, G1, H1a, H1b) or 40x (E2, F2, G2, H2a, H2b) magnification. Blue arrows point to positive signal in areas of reversal lines, magenta arrows to positive cells around epithelial invagination, green arrows to positive cells at inflammatory areas and adjacent to necrotic bone. (I) Quantification of MMP-9 and (J) MMP-13 positively immunostained cells. * statistically significantly different, $p < 0.05$, **** statistically significantly different, $p < 0.0001$. Differences among groups were calculated by two-way ANOVA for multiple comparisons. Data represent the mean value +- SEM.

Figure 9. a-SMA immunohistochemistry
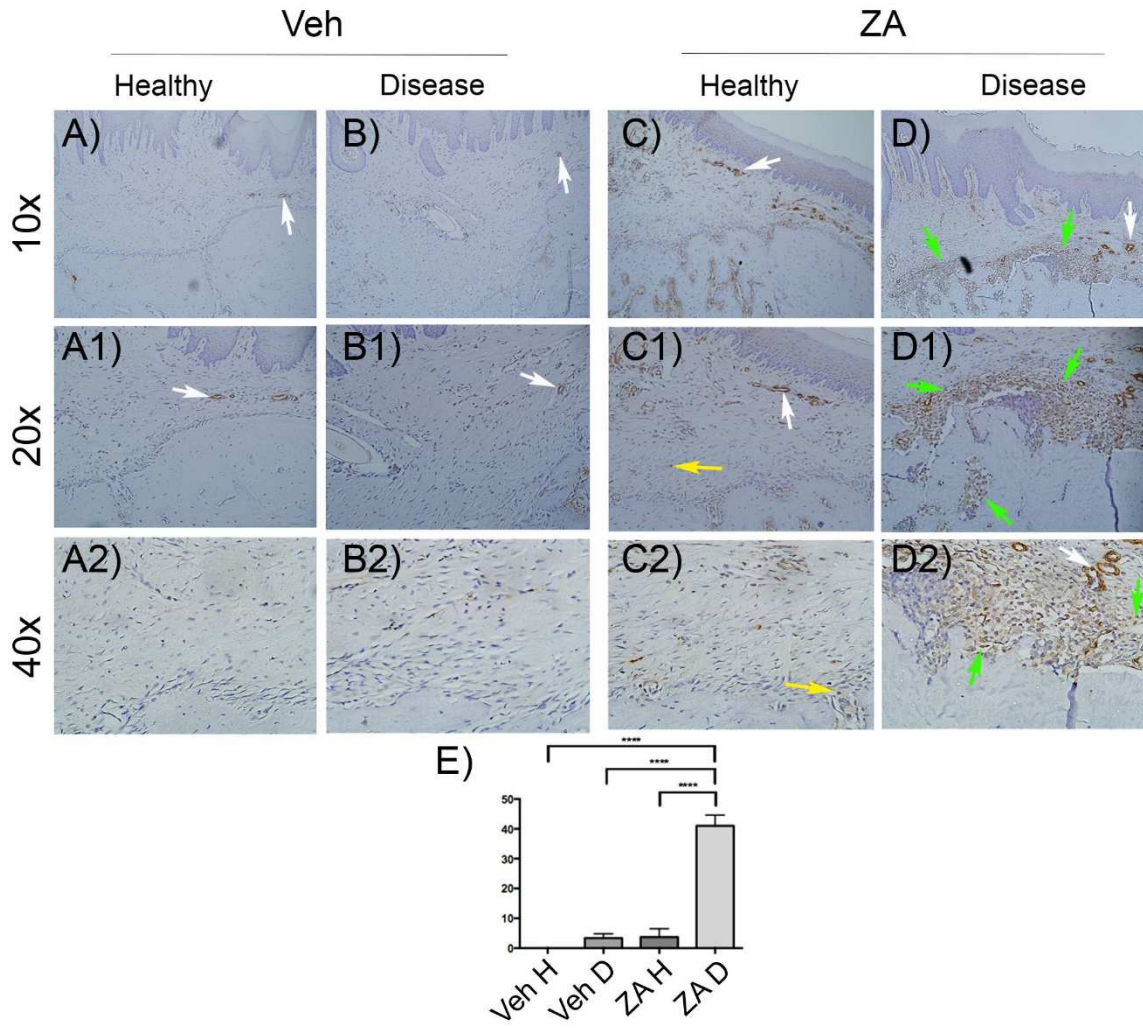
Figure 9. α-SMA immunohistochemistry of maxillary edentulous alveoli in vehicle (A-A2, B-B2) or ZA (C-C2, D-D2) treated animals after extraction of healthy (A, A1, A2, C, C1, C2) or diseased (B, B1, B2, D, D1, D2) teeth, viewed in 10x (A, B, C, D), 20x (A1, B1, C1, D1) or 40x (A2, B2, C2, D2) magnification. White arrows point to positive signal at the walls of blood vessels, yellow arrows to positive cells in the connective tissue, green arrows to positive cells around necrotic bone. (E) Quantification of α-SMA positively immunostained cells. **** statistically significantly

different, p<0.0001. Differences among groups were calculated by two-way ANOVA for multiple comparisons. Data represent the mean value +- SEM.

Figure 10. Human biopsies stained for Type III collagen, MMP-13 and α-SMA
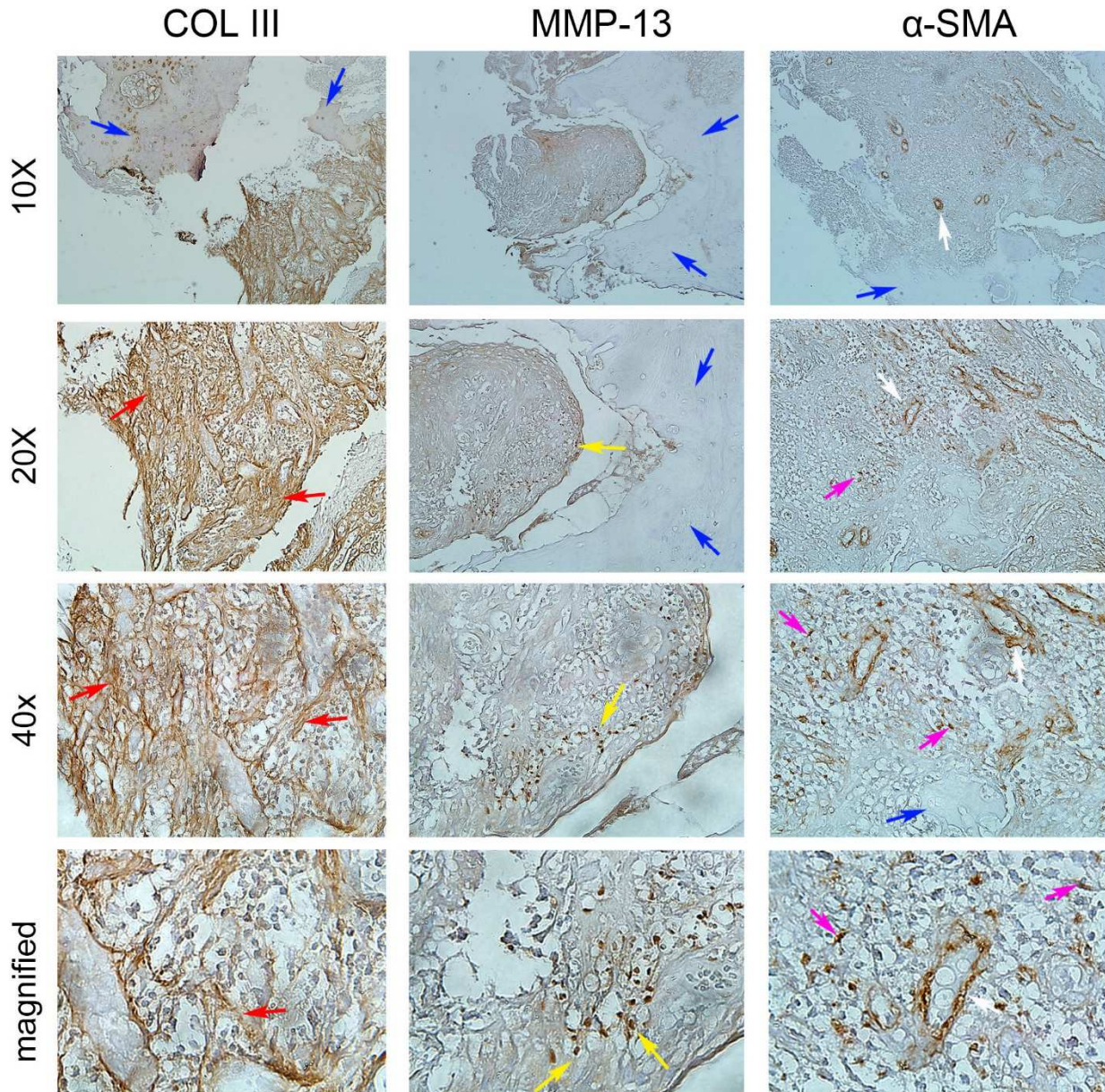
Figure 10.

Representative Collagen type III, MMP-13 and α-SMA immunohistochemistry of human biopsies in two female patients (68 and 70 years old) with history of ONJ after Fosamax or IV Zoledronic Acid treatment. Blue arrows point to necrotic bone, red arrows to positive collagen type III signal in the matrix around the areas of osteonecrosis, yellow arrows to cells with positive signal for MMP-13 immunostain adjacent to osteonecrotic areas, magenta arrows to cells with positive signal for α-SMA immunostain in the proximity of necrotic bone and white arrows to positive signal at the walls of blood vessels.

CHAPTER 4

RADIOGRAPHIC PREDICTORS OF BONE EXPOSURE IN STAGE 0 MRONJ

PATIENTS

Abstract

Objective: To explore the radiographic appearance of stage 0 MRONJ and examine 5 radiographic parameters (trabecular sclerosis, cortical erosion, periosteal reaction, sequestration, crater-like defect) as predictors of progression to bone exposure.

Study design: 23 patients with history of antiresorptive therapy, no bone exposure and non-specific signs and symptoms were included. Intraoral photographs, panoramic and CBCT images at initial visit and follow-up intraoral photographs were reviewed. 3 patients had dental disease (D.D.), 10 stage 0 MRONJ patients did not progress to bone exposure (N.B.E.), and 10 patients progressed to bone exposure (B.E.). Radiographic parameters were scored as absent (0), localized (1) or extensive (2), and their sum formed the composite radiographic index (CRI).

Results: D.D. patients demonstrated minimal radiographic findings and their CRI was significantly lower than that of N.B.E. and B.E. patients. Additionally, B.E. patients demonstrated a higher radiographic index than N.B.E. patients. Intriguingly, sequestration was observed in the initial CBCT of 90% (9/10) of B.E. patients. Contrary, 80% of N.B.E. patients showed absence of sequestration at initial CBCT examination.

Conclusion: CBCT imaging can aid stage 0 vs dental disease diagnosis. Radiographic sequestration at initial presentation can serve as a predictor of future bone exposure in stage 0 MRONJ patients.

Introduction

Medication-related osteonecrosis of the jaws (MRONJ) is a significant adverse effect of antiresorptive and antiangiogenic medications prescribed to patients with osteoporosis or bone malignancies [2, 61]. Various pharmacological agents, such as bisphosphonates, denosumab (a RANKL inhibitor) or bevacizumab (a monoclonal antibody to VEGF) have been associated with the development of the disease [27, 69, 117, 118]

MRONJ is defined as exposed bone in the oral cavity or bone that can be probed through an intraoral or extraoral fistula which does not heal for 8 weeks in a patient with a history of antiresorptive/antiangiogenic medication and no history of radiation therapy in the head and neck area. The most recent position paper by the American Association of Oral and Maxillofacial Surgeons (AAOMS) describes 4 stages of MRONJ (0-3), with stage 0 representing a non-exposed variant of the disease. Specifically, stage 0 refers to patients with no clinical evidence of exposed bone, but with presence of non-specific symptoms or clinical and radiographic abnormal findings [1]. Indeed, stage 0 MRONJ patients present with an intact mucosa and variable symptoms and signs, which poses a critical diagnostic dilemma.

A stage 0 MRONJ diagnosis may be reached after all other possible conditions that could account for the patient's symptoms have been ruled out. This diagnosis by exclusion approach increases the risk for over-diagnosis or under-diagnosis of patients with MRONJ [119-121]. Interestingly, 50% of patients with stage 0 MRONJ proceed to clinical bone exposure within 4-5 months after initial diagnosis [4]. However, prognostic markers to allow identification of patients that will progress to bone exposure vs. patients that can be maintained with subclinical disease have not been established. Correct and early diagnosis of patients with stage 0 MRONJ and

identification of parameters associated with development of bone exposure are of paramount importance in the management of these patients.

Given the absence of characteristic clinical features, thorough radiographic assessment can play a pivotal role in prompt diagnosis and correct clinical management. Cone beam computed tomography is a valuable tool, which can provide precise evaluation of osseous abnormalities [66, 122-125]. However, a detailed assessment of the radiographic appearance of stage 0 patients has not been reported. Additionally, radiographic markers of stage 0 MRONJ cases that can serve as predictors for future progression to clinical bone exposure are currently absent.

In this study, we have retrospectively assessed the CBCT scans of 23 patients with an initial clinical diagnosis of stage 0 MRONJ and have correlated their radiographic parameters with subsequent bone exposure.

Materials and Methods

Twenty-three patients with a history of exposure to bisphosphonates (BP), denosumab (Dmab) or both were included in the study. Antiresorptive therapy had been administered to the patients to treat osteoporosis or several types of bone malignancy including multiple myeloma, metastatic breast, lung or prostate cancer (Table 1). All patients had been referred to the Oral and Maxillofacial Surgery Clinic at the UCLA School of Dentistry from general dentists. Approval of the study by the UCLA Institutional Review Board (IRB) was obtained. All procedures followed the guidelines of the WMA Declaration of Helsinki - Ethical Principles for Medical Research Involving Human Subjects.

None of the patients presented with bone exposure or fistula formation probing to bone at initial visit. Patient signs and symptomatology were non-specific including dull bone pain, altered neurosensory function, mucosal erythema or edema.

All cases included intraoral photographs, panoramic radiographs and CBCT scans at initial presentation and at least one follow-up clinical examination including intraoral photographs. Several patients had multiple follow-up visits, which included intraoral photographs. Follow-up periods ranged from 1 month to three years with an average of 10 months. All cases meeting the inclusion criteria were included in the study. For all patients, the 3D Accuitomo 170 scanner (J Morita USA, Irvine, CA) was used. The exposure factors were 90 kVp and 6 mA with a 17.5-sec exposure time, during 360º rotation (standard exposure settings). The field of view (FOV) was 6x6 cm with a 0.125 mm isometric voxel or 10x14 cm with a 0.25 mm isometric voxel.

Clinical examination was performed by an Oral and Maxillofacial Surgeon (TA) with experience in MRONJ cases. CBCT scans were evaluated by a senior Oral and Maxillofacial

Radiology resident (AS) and a Board Certified Oral and Maxillofacial Radiologist with experience in MRONJ cases (ST). When consensus on the radiographic assessment was not reached, the opinion of ST was used.

Five radiographic parameters in the area of interest were evaluated in all cases at initial presentation: trabecular sclerosis, cortical erosion, periosteal reaction, sequestration, crater-like defect. The radiographic findings were classified as absent (value of 0) localized (involving the area of one tooth, value of 1) or extensive (exceeding the area of one tooth, value of 2). A composite radiographic index (CRI), which was the sum of the values for each of the five radiographic parameters was also used.

All patients were managed conservatively and were given emphasis on oral hygiene measures. No surgical intervention was performed in the oral region. Upon clinical follow-up, cases were evaluated for progression to clinical bone exposure (stage 1-3 MRONJ). All cases in which patients reported no symptomatology after dental retreatment were attributed to dental disease (D.D.). Cases in which patients reported persistent pain but no bone exposure were classified as stage 0 (N.B.E.). Cases with bone exposure (B.E.) were classified as stage 1, 2 or 3.

Statistics were performed with GraphPad Prism Software, (Inc. La Jolla, CA). Fischer's exact test was used for qualitative data comparison. One-way ANOVA was used for quantitative data comparison. P values <0.05 were considered statistically significant.

Results

The majority of the patients included in our study were female (18/23). Antiresorptive therapy duration varied, with osteoporosis patients having the most prolonged treatment (mean of 6 years). Details about patient systemic disease, sex, age, type of antiresorptive medication and treatment duration are shown in Table 1.

Radiographic evaluation (Figure 11A, B) revealed extensive trabecular sclerosis in 57% (13/23) of the patients and localized in 30% of the patients (7/23). Extensive cortical erosion was noted in 13% (3/23) and localized was seen in 57% (13/23) of patients. Periosteal reaction was visualized in 5 patients, with 9% (2/23) demonstrating extensive periosteal reaction and 13% (3/23) localized. 35% (8/23) and 13% (3/23) of scans demonstrated extensive or localized sequestrum formation respectively. Lastly, an extensive crater-like defect was visualized in 13% (3/23) CBCT scans, whereas a localized crater was noted in 57% (13/23).

We then explored how many of these patients progressed to stage 1-3 MRONJ consulting our follow-up database. In 3/23 cases, patient symptomatology and clinical abnormalities ceased after dental treatment and were therefore, attributed to common dental disease (D.D.) instead of stage 0 MRONJ. Indeed, after endodontic retreatment and caries removal, erythema and swelling subsided and pain symptomatology was significantly reduced. (Table 2, Figure 12A, A1, A2).

In 10/23 cases, patients presented with persistent pain, abnormal clinical findings and no evidence of bone exposure on their follow-up sessions (Table 2, Figure 12B, B1, B2). These patients were classified as stage 0 MRONJ with no bone exposure (N.B.E.) and continued to be followed-up.

In 10/23 cases, patients presented with clinical bone exposure (B.E.) and various degrees of inflammation/infection of the surrounding soft tissue upon first revisit. Three patients

progressed to stage 1 MRONJ, 5 patients to stage 2 MRONJ, whereas 2 patients demonstrated extra-oral fistula formation and were classified as stage 3 (Table 2, Figure 12C, C1, C2). Three of these patients had been treated for osteoporosis and 7 had been treated for bone malignancies (3 male and 7 female). The time interval between first presentation and progression to bone exposure was on average 3.9 months with a standard deviation of 2.6 months. The individual time interval between initial visit and bone exposure for all patients is reported in Supplemental Table 1.

Patients who were categorized as dental disease (D.D.) cases, demonstrated minimal radiographic findings upon initial presentation and their CRI was strongly statistically significantly lower than N.B.E. and B. E. patients ($p<0.05$ and $p<0.001$ respectively). Additionally, B.E. patients had a statistically significantly higher composite radiographic index in comparison to N.B.E. patients ($p<0.05$, Table 2).

Next, we tested whether any of the radiographic parameters could serve as predictors for future progression to bone exposure in stage 0 patients. Trabecular sclerosis was seen in all B.E. and N.B.E. patients and the extent of sclerotic changes was very similar between the two groups. No statistical significance of the presence of cortical erosion, periosteal reaction or crater-like defect was noted between the two groups (Figure 13).

Of note, 90% (9/10) of patients who progressed to bone exposure presented with radiographic signs of sequestration (6/10 extensive and 3/10 localized) in their initial CBCT scan. Only one patient who progressed to clinical bone exposure did not present with radiographic sequestration in the initial CBCT scan. In the stage 0 MRONJ group with N.B.E, 80% (8/10) showed absence of sequestrum formation in their initial radiographic examination. The incidence of radiographic sequestration between the B.E. and N.B.E. groups was statistically significant ($p<0.01$, Figure 3).

Discussion

Stage 0 is characterized as a non-exposed variant of MRONJ and presents with non-specific clinical signs, symptoms and radiographic features. The absence of specific clinical traits often creates a diagnostic challenge for clinicians [67]. In these cases, radiographic evaluation is a valuable tool towards a correct diagnosis as well as the estimation of the extent of osseous changes.

In a recent study, which included a few patients from the population of the current manuscript, we reported that CBCT offers a more thorough diagnostic assessment in comparison to panoramic radiographs in cases of suspected stage 0 MRONJ and alters the diagnostic thinking efficacy and management of patients with suspected stage 0 MRONJ [67]. Indeed, diagnosticians can more readily appreciate cortical and trabecular variations as well as osseous changes in the buccolingual dimension utilizing a three-dimensional scan [126-129]. In our current study, we only included patients that underwent both panoramic and CBCT scanning at the time of the initial visit.

Even though the importance of radiographic assessment in the diagnosis of stage 0 MRONJ has been emphasized [1], the radiographic findings that might be present in these patients have not been described in detail. For example, periosteal reaction and sequestrum formation are not reported as abnormal findings in stage 0 MRONJ patients in the AAOMS position paper [1]. Here, we assessed the radiographic appearance of stage 0 patients by assessing the presence and the extent of 5 radiographic parameters (trabecular sclerosis, cortical erosion, periosteal reaction, sequestration, crater-like defect). These radiographic parameters have previously been described in MRONJ patients with clinical bone exposure. Lamina dura thickening is another radiographic feature reported in MRONJ cases [85, 130]. In our experience, thickened lamina dura is not a common radiographic finding and can affect areas of the dentition not associated with symptomatology or

bone exposure. Importantly, in the current study, a considerable proportion of our patients were edentulous at the site of interest, making it impossible to discern lamina dura boundaries.

A strong female predilection was noted among the patients. This is mainly attributed to the all-female osteoporotic patients, who comprised almost half of the patient population (11/23). Nearly all patients included were in the 6th to 8th decade of age with an average of 70 years. This was due to the manifestation of systemic diseases treated with antiresorptives (osteoporosis, metastatic cancer, multiple myeloma) in a later stage of life [131-134]. An exception was a 30-year old male patient with sacrum sarcoma that was treated with denosumab. No patients were under antiangiogenic medication, probably due to the lower incidence of MRONJ in this group of patients when compared to bisphosphonate and denosumab-treated patients and the small number of patients in our study [1, 57, 135].

Over- or under-diagnosis of stage 0 MRONJ may have severe adverse effects on the patients' oral and skeletal health. Indeed, over-diagnosis of MRONJ may lead to detrimental outcomes, if discontinuation of antiresorptive treatment is elected [2, 136, 137]. Alternatively, under-diagnosing a patient with stage 0 MRONJ, as having common dental disease or other conditions, such as referred neuropathic pain, might lead to inappropriate and delayed treatment and might increase the possibility of developing clinical bone exposure. Proper diagnosis of stage 0 MRONJ can allow for management of local instigating factors, possible antibiotic treatment and more frequent follow-up visits [1].

Interestingly, 3 of 23 (13%) patients were initially diagnosed with stage 0 MRONJ but were subsequently classified as having common dental disease. The relatively low percentage of over-diagnosis in our study could be attributed to the accumulated considerable clinical expertise in managing MRONJ by the Oral and Maxillofacial Surgeons in our institution, as well as to the

comprehensive radiographic assessment of all MRONJ patients that includes panoramic and CBCT imaging. The presence of these three patients, however, allowed us to explore whether radiographic findings could assist in further distinguishing patients with common dental disease from patients with stage 0 MRONJ. We observed that an overall absence of trabecular sclerosis, cortical erosion, periosteal reaction, sequestration and crater-like defect disfavors the diagnosis of stage 0 MRONJ and supports the diagnosis of dental disease in dentate patients. Since CBCT examination can aid in the diagnosis of challenging cases of dental disease, where identifying the source of symptomatology can often be ambiguous [138, 139], a detailed radiographic assessment utilizing CBCT technology should be considered in symptomatic patients on antiresorptives [67].

Half (10/20) of the stage 0 MRONJ patients progressed to frank bone exposure within 1-7 months. The percentage of progression to clinical bone exposure and time interval from initial diagnosis are in agreement with the report by Fedele et al investigating bone exposure progression in patients initially presenting with stage 0 MRONJ [4].

Patients who subsequently developed bone exposure had a higher composite radiographic index in comparison to the patients who remained in stage 0. This suggests that a detailed radiographic evaluation not only aids in the differential diagnosis of conditions that present with similar symptomatology, but could assist in the identification of patients with stage 0 MRONJ that might progress to clinical bone exposure. To further investigate whether a specific radiographic parameter(s) had a bigger contribution in the differentiation between B.E. vs. N.B.E. patients, we compared the presence of each radiographic parameter in these two groups. We observed that the discrepancy in the composite radiographic index was mostly attributed to the different incidence of sequestration. In fact, presence of sequestration in the initial CBCT scan was a strong predictor for bone exposure in 9 out of 10 patients. In contrast, sequestration was seen only in 2 out of 10

patients who did not develop clinical exposure. These findings indicate that radiographic sequestration may serve as a reliable predictor of future bone exposure in stage 0 MRONJ patients.

Sequestration is characterized by devitalized bone separated from the surrounding bony tissue with inflamed granulation tissue. With time, epithelial rimming occurs around the detached necrotic bone, which subsequently exfoliates through the soft tissue or may lead to the formation of a sinus tract [24, 140]. This process of necrotic bone rejection could underlie the subsequent bone exposure observed in stage 0 MRONJ patients who present with radiographic sequestration. It is likely that the bony areas which undergo sequestration as part of necrotic bone rejection represent the bone exposure sites later observed in these patients. Furthermore, the high incidence of bone exposure development in patients with radiographic sequestration (9/11 or 82%) suggests that surgical removal of the sequestered bone should be considered in the management of these patients in an effort to decrease transition to clinical exposure.

We should recognize some limitations to our study. First, a relatively small number of patients were included, due to the rare incidence of stage 0 MRONJ. In particular, there were only a few patients originally diagnosed as stage 0 MRONJ that subsequently were classified as having common dental disease. This low number could be due to the increased experience with MRONJ patients in our institution and might not reflect the true incidence of patients over-diagnosed with stage 0 disease. Furthermore, our study did not allow for the assessment of the incidence of under-diagnosis of stage 0 MRONJ, since all patients were referred to our institution with suspected disease. A prospective study focusing on patients on antiresorptive medication would be needed to address potential under-diagnosis. A final limitation is that the period from the development of the clinical symptomatology to the visit to our institution was not known.

In summary, we present a retrospective study exploring the radiographic profile of patients diagnosed with stage 0 MRONJ, based on clinical examination. We conclude that the extent of radiographic changes was an important determinant in the differentiation between patients with dental disease vs. patients with MRONJ. Furthermore, sequestrum formation was an important radiographic predictor of patients with stage 0 MRONJ that subsequently developed clinical bone exposure.

We propose that patients with a history of antiresorptive/antiangiogenic medications receive a CBCT exam when they present with abnormal signs or symptoms. Presence of sclerosis, cortical erosion, periosteal reaction, sequestration, crate-like defect should guide the clinician towards the diagnosis of stage 0 MRONJ as opposed to common dental disease. Presence of sequestration, in particular, favors the diagnosis of stage 0 MRONJ with a higher risk for development of frank bone exposure.

Acknowledgments

Table 1. Patient demographics

Disease	No. of patients	Sex	Mean Age (+/- SD)	AR treatment	AR duration
Osteoporosis	11	F (11)	78 (+/- 5)	BP (10)	6 y (+/- 7.5y)
				Dmab (1)	
Multiple myeloma	3	F (3)	69 (+/- 2)	BP (3)	22 mo (+/- 3 mo)
Breast cancer	3	F (3)	59 (+/- 14)	BP+Dmab (3)	38mo (+/- 8 mo)
Prostate cancer	2	M (2)	80 (+/- 3)	BP (1)	60 mo (16 mo)
				BP +Dmab (1)	
Lung cancer	1	M (1)	58	Dmab	36 mo
Chondrosarcoma	1	M (1)	74	Dmab	36 mo
Sacrum sarcoma	1	M (1)	30	BP+Dmab	24 mo
Giant cell tumor	1	F (1)	63	Dmab	6 mo
Total	**23**	**F(18)**	**70**	**BP(15)**	**52 mo (+/-64mo)**
		M(5)		**Dmab(4)**	
				BP+Dmab (4)	

Table 1: Patient demographics and antiresorptive treatment information. AR= antiresorptive, y=years, mo=months, BP=bisphosphonates, Dmab=denosumab, SD= standard deviation

Figure 11. Radiographic assessment of all patients
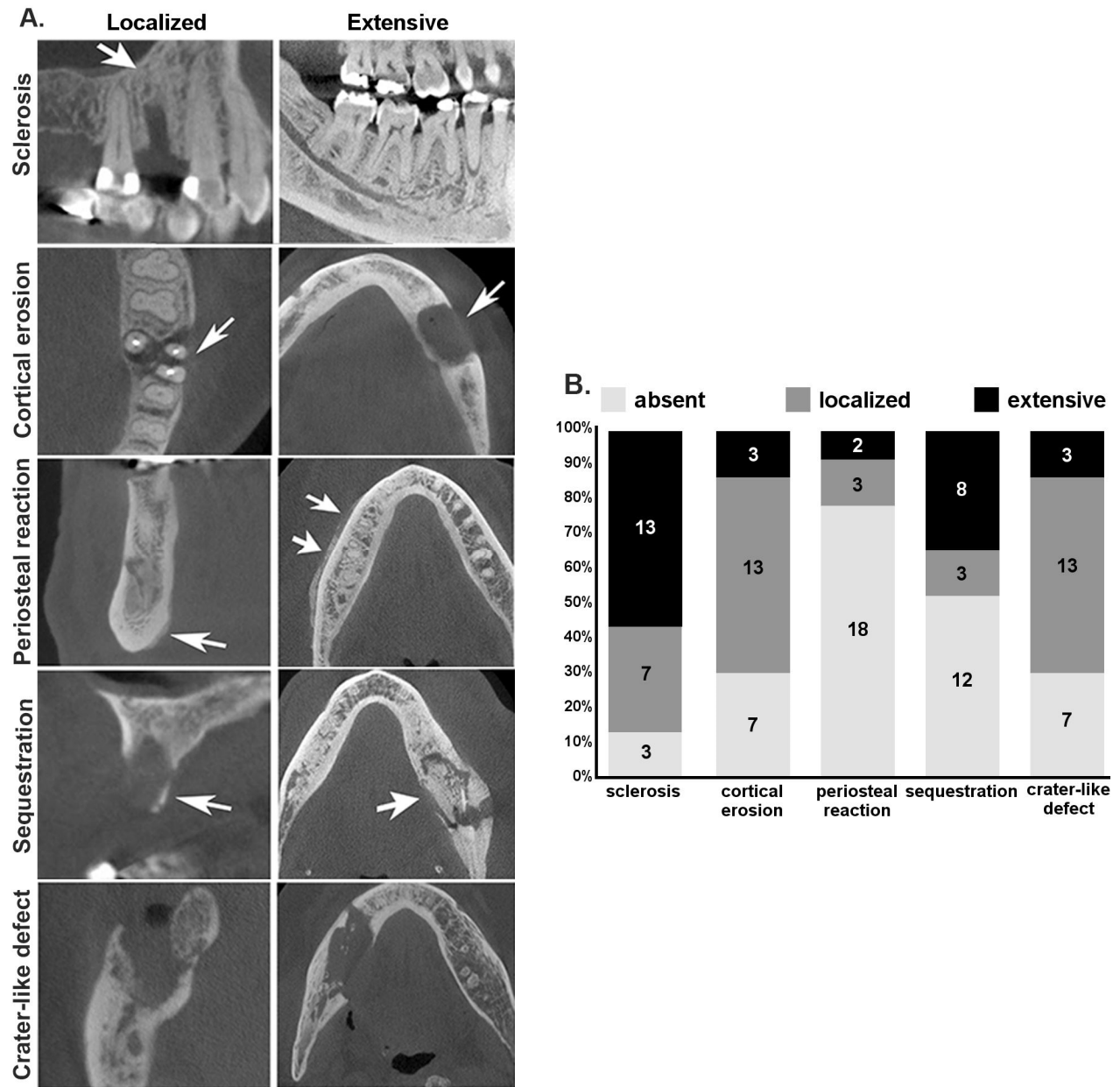
Figure 11: Radiographic assessment. Representative examples of localized or extensive Trabecular Sclerosis, Cortical erosion, Periosteal reaction, Sequestration, Crater-like defect (A). Incidence and extent of these radiographic parameters in all patients (B)

Table 2. Follow-up data and composite radiographic index (CRI)

Patient categories	No. of Patients	Mean Composite Radiographic Index (+/- SD)
Dental disease (D.D.)	3	0.33 +/- 0.57[#,&]
No bone exposure (N.B.E.)	10	4+/-0.51[+]
Bone exposure (B.E.)	10	5.8 +/-1.68
Total	23	

Table 2: Follow-up data and composite radiographic index (CRI) of dental disease patients (D.D.), patients who did not progress to bone exposure (N.B.E.) and patients who progressed to bone exposure (B.E). #: statistically significant to N.B.E. $p<0.05$, &: statistically significant to B.E. $p<0.001$, +: statistically significant to B.E. $p<0.05$, SD= standard deviation

Figure 12. Clinical and radiographic evaluation at initial presentation and clinical follow-up
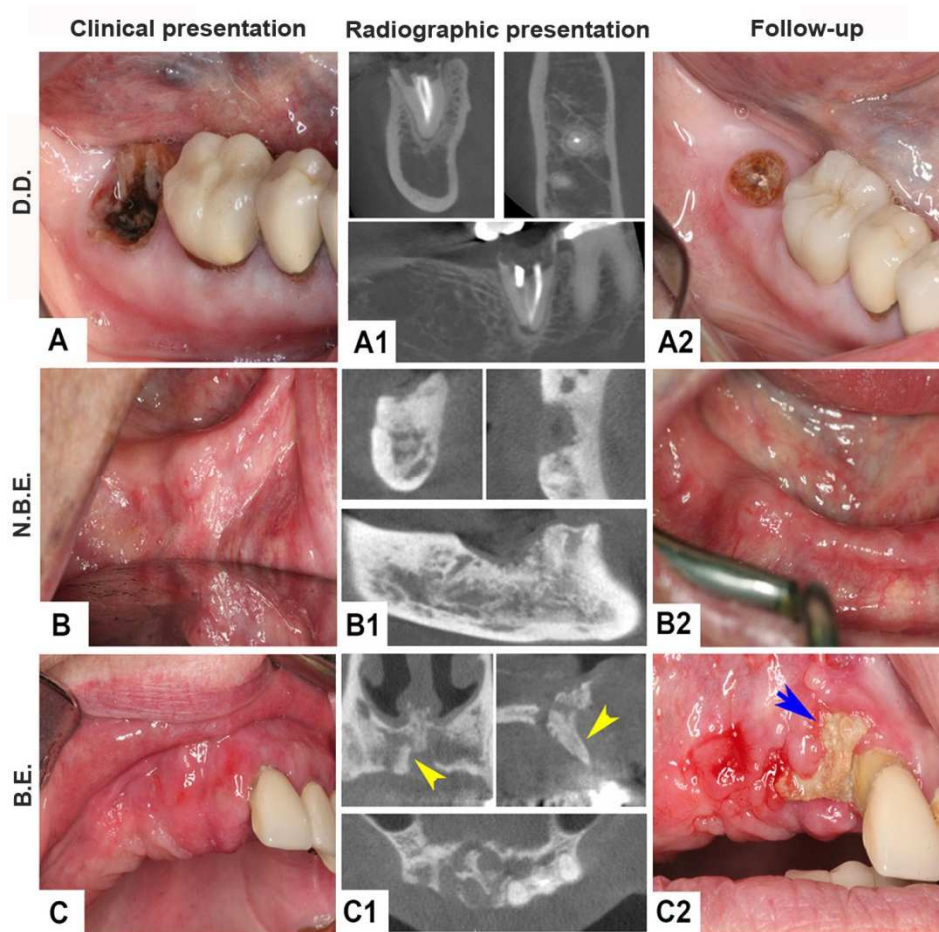
Figure 12: Clinical and radiographic evaluation at initial presentation and clinical follow-up. Initial clinical and radiographic presentation and clinical follow-up of a patient who was classified as a dental disease (D.D.) case (A, A1, A2), a patient with stage 0 MRONJ and no progression to bone exposure (N.B.E., B, B1, B2) and a patient with progression to bone exposure (B.E., C, C1, C2). Yellow arrowheads point to areas of sequestration. Blue arrow points to bone exposure.

Figure 13. Incidence and extent of radiographic markers in stage 0 patients
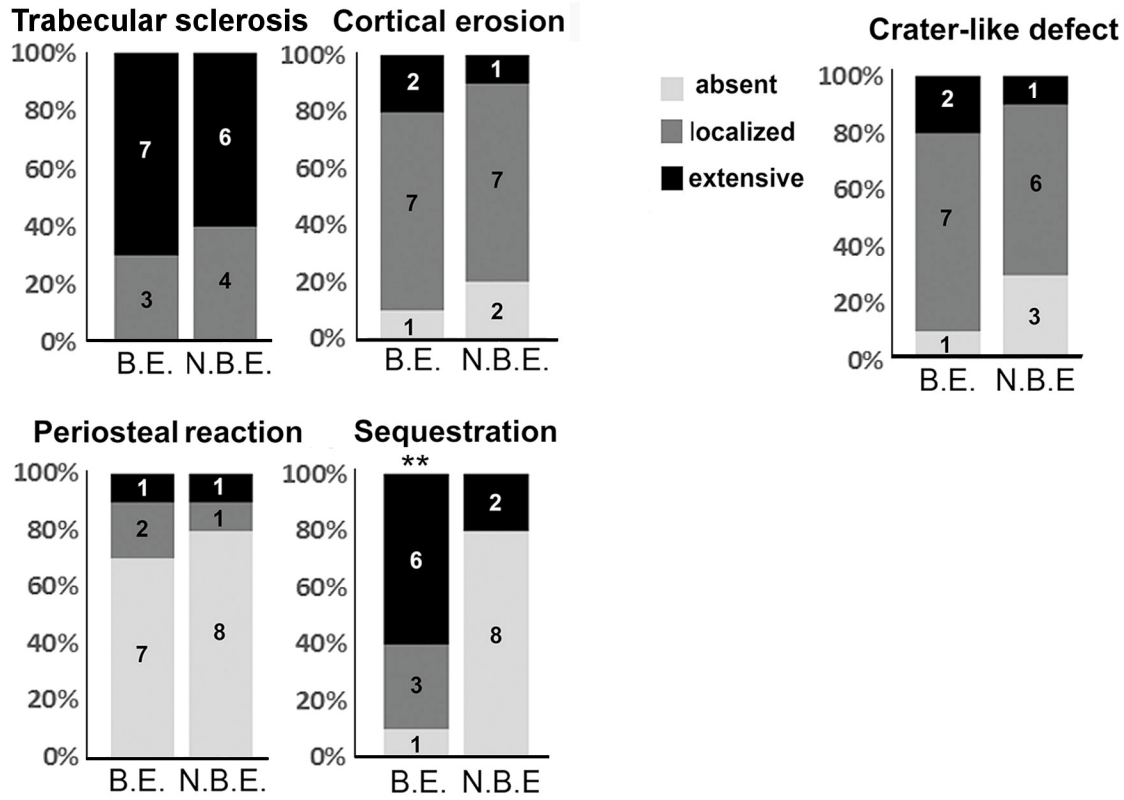
Figure 13: Incidence and extent of Trabecular Sclerosis, Cortical erosion, Periosteal reaction, Sequestration and Crater-like defect in patients who progressed to bone exposure (B.E.) or showed no bone exposure (N.B.E.). **: statistically significant with p<0.01

CHAPTER 5

LOCAL RANKL DELIVERY IMPROVES SOCKET HEALING IN BISPHOSPHONATE TREATED RATS

Abstract

Medication related osteonecrosis of the Jaws (MRONJ) is a severe complication of antiresorptive and anti-angiogenic medications prescribed to patients with osteoporosis or bone malignancies. Osteoclast inhibition is central in MRONJ pathogenesis. Here, we investigated if local delivery of RANKL (a key molecule in osteoclast activation) could enhance local osteoclast generation and improve MRONJ burden. Thirty Wistar-Hun rats were i.p. treated with saline or 66 μg/kg zoledronic acid (ZA) for a week. Then, mandibular molars were extracted bilaterally. Collagen tapes infused with water or RANKL were placed in the extraction sockets of 60 hemimandibles of veh (veh/RANKL-, veh/RANKL+) or ZA treated rats (ZA/RANKL-, ZA/RANKL+). ZA delivery continued for 3 or 12 days after surgery, rats were euthanized, and clinical, radiographic and histologic assessments were performed.

RANKL immunostain showed increased signal in the RANKL treated sites of veh or ZA rats compared to the non-RANKL treated sites. Visually, at the 3-day timepoint, no sockets demonstrated complete healing. At the 12-day timepoint, sockets of veh/RANKL- and veh/RANKL+ rats showed intact mucosa, while mucosal defects were noted in ZA/RANKL- rats. Interestingly, ZA/RANKL+ sockets showed absence of bone exposure. Histologically, at the 3-day timepoint, ZA/RANKL- sockets demonstrated extensive bone exposure and osteonecrosis. In contrast, ZA/RANKL+ rats showed soft tissue coverage and significantly reduced osteonecrosis,

similar to the veh groups. Importantly, in the ZA/RANKL+ group, osteoclasts attached to the bone surface and osteoclast numbers were higher compared to ZA/RANKL- sites. At the 12-day timepoint, persistent osteonecrosis and bone exposure were detected in the sockets of ZA/RANKL- animals. Contrary, ZA/RANKL+ rats demonstrated socket epithelialization and reduced osteonecrosis. Significantly more total and bony attached osteoclasts persisted in the ZA/RANKL+ vs the ZA/RANKL- group. A disruption was noted in the connective tissue-bone interface and the epithelium of the ZA/RANKL- group. In contrast, an intact collagen network and epithelium were seen in ZA/RANKL+ sites, resembling the veh groups. We present a novel approach towards improving socket healing, in the presence of ZA, by enhancing osteoclastic activity through local RANKL delivery. Our approach is clinically applicable and could improve treatment outcomes of patients on high-dose ZA therapy.

Introduction

Medication related osteonecrosis of the Jaw (MRONJ) is a rare but serious side effect of antiresorptive medications and can cause significant morbidity to patients. MRONJ is characterized by areas of exposed bone in the oral cavity for a period of more than 8 weeks[1, 2, 61]. The most common instigating local factor of MRONJ is tooth extraction or other dental surgical procedures, such as implant placement. A classic presentation of the disease is when a tooth is extracted and the extraction socket does not heal. However, tooth extraction in patients undergoing antiresorptive treatment often is unavoidable[1, 63, 141].

The main class of medications associated with MRONJ are antiresorptive agents that function as inhibitors of osteoclastic function or differentiation [1, 2, 61]. Antiresorptive medications are mainly used for the management of osteoporosis, and less frequently but at higher doses in patients with bone malignancy[137, 142-144]. Indeed, the fear of MRONJ is a main contributor for osteoporotic patients to not be compliant with their antiresorptive medications [145]. Osteoporosis is the most common metabolic bone disease with 43.4 million people affected by osteoporosis or osteopenia in the USA, representing 44% of the people aged 50 and older[146]. Indeed, reports in the scientific and public literature express serious concern about not treating osteoporosis more aggressively[145, 147-149]. A successful intervention to minimize the MRONJ risk would be beneficial for millions of osteoporotic patients that need to undergo a dental surgical procedure, such as a tooth extraction.

Receptor Activator of Nuclear Factor Kappa-B Ligand (RANKL) is a key molecule for the production of osteoclasts[71, 72, 150]. It is a homotrimer that binds to the RANK receptor of pre-osteoclastic cells, mediates the fusion of neighboring osteoclast precursors causing them to become multinucleated under the influence of other genes, such as DC-STAMP. RANKL also mediates

the transcription of several osteoclast-specific genes such as TRAP, cathepsin K and calcitonin receptor committing the cells to an osteoclastic phenotype. Indeed, certain antiresorptive treatments target RANKL as a way to inhibit osteoclast formation, and thus bone resorption[33, 151].

Given the central role of RANKL in osteoclastic differentiation and function, we hypothesized that RANKL could be delivered locally within the extraction socket in rats undergoing BP treatment to enhance the local generation of osteoclasts, mitigate the local BP effect on resorption and improve socket healing without discontinuing the systemic antiresorptive treatment.

Materials and methods

Animal care

Thirty Wistar-Hun 7-week-old rats were randomly assigned to receive saline or 66 μg/kg of zoledronic acid (ZA), (LKT laboratories, St. Paul, MN). Rats were injected intraperitoneally once a week in morning hours. Animals were kept and treated according to guidelines of the UCLA Chancellor's Animal Research Committee[8, 24, 101, 152].

After a week of pretreatment with saline or ZA, the first and second mandibular molars of both sides were extracted in all rats. After extraction, resorbable collagen tapes (ACE Surgical Supply, Brockton, MA) containing water or recombinant rat RANKL (Peprotech, Rocky Hill, NJ) were placed in the extraction sockets. 4 ul of water or aqueous RANKL solution (0.1mg/ml) were placed in each collagen tape. Water or RANKL loaded collagen tapes were placed in the extraction sockets of 30 hemi-mandibles of veh-treated rats and 30 hemimandibles of ZA-treated rats (a total of 60 hemimandibles were used). Each rat received a veh infused tape on one side of the mandible and a RANKL infused tape on the other. Sides were alternated to account for possible discrepancies in surgical technique.

ZA treatment was continued and rats were euthanized 3 or 12 days after tooth extraction utilizing CO_2. Twelve rats were euthanized 3 days after surgery (6 veh treated and 6 ZA treated) and 18 rats were euthanized 12 days after surgery (9 veh treated and 9 ZA treated). Mandibles were dissected and photographs of the specimens were obtained utilizing a digital optical microscope (Keyence VHX-1000, Osaka, Japan). Areas of unhealed mucosa were measured with Image J (NIH, imagej.nih.gov).

Micro CT

Micro CT scanning was performed, as described. Bone volume-total volume ratio measurements were performed in the distal root of the first molar starting from the apex and including 50 axial slices towards the coronal third, as we have previously described. [24].

Histology

Mandibles were fixed for 48 h in 4% paraformaldehyde and then decalcified in 14% EDTA for 4 weeks. Samples were paraffin embedded and 5 μm-thick cross sections were made perpendicular to the long axis of the alveolar ridge at the area of the mucosal defect. If the mucosa was completely healed, sections were made at the area between the first and second molars, approximately 2mm mesial to the mesial cusp of the third molar. H&E stained slides were digitally scanned image analysis was performed using the Aperio Image Scope software (Aperio Technologies, Inc., Vista, CA, USA). The osteonecrotic area(s) and empty osteocytes over total bone area (s) were quantified. [25, 26]

TRAP assay, Picrosirius red staining, immunohistochemistry

For enumeration of osteoclasts, tartrate-resistant acid phosphatase (TRAP) staining was performed (387A-IKT Sigma Aldrich, St. Louis, MO, USA). Osteoclast numbers were normalized over bone length. Acid phosphatase assay (ab83370, Abcam) was used to measure serum TRAP levels 3 days before and 3 days after surgery. Picrosirius red (Pc red) stain was used to study collagen organization [101]. Anti-RANKL (sc-7628, Santa Cruz) and Anti-Cytokeratin 14 (ab51054, Abcam) were used for immunohistochemistry [38].

Statistics

     Raw data were analyzed using the GraphPad Prism Software (GraphPad Software, Inc.

La Jolla, CA). Descriptive statistics were used to calculate the mean and the standard error of the

mean (SEM). Data were analyzed by a two-way ANOVA and post-hoc Tukey's test for multiple

comparisons among the various groups and t-test for a single comparison with a statistical

significance of $p<0.05$.

Results

Specimen photographs 3 and 12 days after surgery

Specimen photographs 3 days after tooth extraction showed mucosal defects with granulation tissue in all groups and ongoing mucosal healing (Figure 14A-E). Specimen photographs 12 days after tooth extraction revealed an intact alveolar mucosa in the mandibles of veh/RANKL- and veh/RANKL+ rats (Figure 14F, G). Alveolar mucosal defects, granulation tissue and exposed bone were noted in the alveoli of ZA/RANKL- (Figure 14H). Interestingly, intact mucosa was noted in most of the ZA/RANKL+ hemi-mandibles (Figure 14I). Areas of unhealed mucosa were significantly smaller in ZA/RANKL+ rats compared to ZA/RANKL- rats (Figure 14J).

Radiographic assessment 3 and 12 days after surgery

BV/TV values were less than 10% in all specimens from all groups 3 days after surgery (data not shown). Significant healing with woven bone was observed in the veh/RANKL- and veh/RANKL+ sites 12 days after surgery (Figure 15A). Significantly decreased BV/TV was seen in the extraction sockets of the ZA/RANKL- and ZA/RANKL+ groups compared to the veh treated groups. Interestingly, ZA/RANKL+ sites showed increased bone healing compared to the ZA/RANKL- sites 12 days after surgery. (Figure 15, A, B).

RANKL immunohistochemistry

Three days after surgery, RANKL immunohistochemistry revealed increased signal in the sockets of veh/RANKL+ and ZA/RANKL+ rats compared to the non RANKL treated groups.

RANKL signal was noted in the soft tissue of the sockets (Figure 16A, B, C, D, E, and Figure 16B, D, onsets, yellow arrows) 3 days after surgery. No significant differences were seen in the RANKL signal in the soft tissue of the mandibles 12 days after surgery (data not shown).

Serum TRAP assay

Serum TRAP assay was performed to ensure absence of off-target effects in rats. TRAP levels 3 days before and 3 days after surgery were compared in veh and ZA treated animals. TRAP levels before and after extraction and local RANKL delivery did not show a statistically significant increase neither in the vehn or in the ZA treated groups (Figure 16F).

Histologic assessment of extraction sockets 3 days after surgery

Histologic evaluation 3 days after surgery showed inflammatory infiltrate and sparse collagen fibers overlying the sockets of veh/RANKL- or veh/RANKL+ rats (Figure 17A, B, white arrows). Absence of complete epithelialization of the wound was noted in both groups. In the ZA/RANKL- group, extensive bone exposure was revealed (Figure 17C, black arrows). There was absence of soft tissue overlying the alveolar bone and prominent areas of bone exposure were revealed. Approximately 20% of bone in the extraction sockets of this group was necrotic (Figure 17C, C1, E). Contrary, ZA/RANKL+ sockets showed thin epithelium and soft tissue covering the sockets. (Figure 17D, E, white arrows). Importantly, osteonecrosis and empty osteocytes over bone area were significantly reduced compared to the ZA/RANKL- group (Figure 17D, D1, E).

TRAP staining in extraction sockets 3 days after surgery

TRAP staining revealed higher numbers of osteoclasts in the sockets of veh/RANKL+ vs veh/RANKL- groups (Figure 17A2, B2, G). Of note, statistically significantly more osteoclasts were also seen in the extraction sockets of ZA/RANKL+ compared to the ZA/RANKL- group (Figure 17C2, D2, G). As we have previously described, many osteoclasts in ZA treated rats showed an altered, round morphology with pyknotic nuclei and were not in contact with the bone surface. Interestingly, higher numbers of osteoclasts attached to the bone surface were seen in the extraction sockets of ZA/RANKL+ vs ZA/RANKL- sites. (Figure 17H).

Histologic assessment of extraction sockets 12 days after surgery

Intact epithelium with rete peg formation was detected in the alveoli of veh/RANKL- and veh/RANKL+ rats. Connective tissue showed interval resolution of the inflammatory infiltrate observed in the 3 days timepoint (18A, B, orange arrows). Significant amount of woven bone was seen occupying the extraction sockets in both groups of veh-treated animals. Osteonecrosis and empty osteocytes were minimal in the mandibles of both veh treated groups. (Figure 18A, A1, B, B1, E, F). Histologic evaluation of ZA/RANKL- sockets showed areas of epithelial disruption, bone exposure (18C, black arrow) and bony sequestration (18C1, blue arrow). Significant amount of persistent osteonecrosis and empty osteocytes were also detected (Figure 18C, C1, E). In contrast, the extraction sockets of ZA/RANKL+ treatment demonstrated continuous keratinized epithelium with no evidence of bone exposure. Of note, statistically significantly less osteonecrosis and empty osteocytes were seen in the alveoli of these animals the ZA/RANKL- group (Figure 18D, D1, E).

TRAP staining in extraction sockets 12 days after surgery

Twelve days after tooth extraction, comparable numbers of osteoclasts were seen in the sockets of veh/RANKL- and veh/RANKL+ groups (Figure 18A2, B2, G). Importantly, abundance of osteoclasts was noted in the alveoli of ZA/RANKL+ rats. Statistically significant increase in total osteoclast numbers was detected in this group compared to the ZA/RANKL- group. Of note, significantly higher numbers of osteoclasts attached to the bone surface were seen in the alveoli of ZA-treated rats with RANKL vs ZA treated rats without RANKL treatment (Figure 18F).

Picrosirius red and cytokeratin 14

Pc red revealed an organized collagen network in the veh treated groups with strongly birefringent collagen fibers extending from the submucosal soft tissue and inserting within the vital bone (Figure 19A, B, A1, B1, blue arrows). Contrary, in ZA/RANKL- rats disruption of the bone-soft tissue interface was noted with absence of collagen fiber insertion in the alveolar bone (Figure 19C, C1, white arrow). In the ZA/RANKL+ group, however, intact collagen network with strong collagen birefringence and collagen fiber insertion in the bone were noted. (Figure 19D, D1, blue arrows).

Cytokeratin 14 showed intact epithelium in veh groups (Figure 19E, F). Contrary, epithelial disruption (19G, black arrow) adjacent to the necrotic bone (19G, red arrow) were noted in ZA/RANKL- mandibles (Fig 19G). The ZA/RANKL+ sockets showed intact, continuous epithelium covering the extraction socket, akin the veh treated rats (Figure 19H).

Discussion

Medication related osteonecrosis of the jaws is a severe complication of antiresorptive and antiangiogenic medications that can considerably deteriorate the quality of life of already compromised patients. Although progress in animal and clinical research has increased our understanding on MRONJ development, treatment for the disease remains largely empirical. [2, 61].

Several hypotheses regarding MRONJ development exist and include bone remodeling inhibition, angiogenesis inhibition, local infection/inflammation, soft tissue toxicity, or immunity disruption[1, 42]. Interestingly, MRONJ has been reported with a similar prevalence and severity in patients with a history of bisphosphonates and denosumab (a monoclonal antibody to RANKL[27, 69, 153]. Even though these two groups of drugs act by entirely distinct pharmacologic mechanisms, they both target osteoclasts and result in reduced bone resorption and suppressed bone turnover [13]. Our data indicate that local restoration of osteoclastic function in a setting of BP treatment can reduce osteonecrosis and improve mucosal healing after tooth extraction. This present study, therefore, provides evidence in support of the bone remodeling inhibition hypothesis.

Our study showed that RANKL treatment enhanced bone healing in ZA treated rats compared to the ZA/RANKL- group 12 days after surgery. Osteoclastic resorption plays an essential role in socket remodeling after tooth extraction. In fact, 2 months after tooth extraction the alveolar crest demonstrates an abundance of osteoclasts in human biopsy specimens[100]. A longer duration of bisphosphonate treatment (more than 5 years vs less than 5 years) has also been associated with a prolonged wound healing period in extraction sockets of patients[154]. This is likely due to the disruption of the steps of oral wound healing, which include clot formation, formation of granulated tissue, establishment of connective tissue and preosseous tissue, filling of the extraction socket with trabecular woven bone, and remodeling of the socket to produce lamellar

bone[155]. Our study revealed that ZA/RANKL+ sites demonstrated increased socket healing compared to the ZA/RANKL- sites, likely due to an improvement in bone remodeling through activation of osteoclast-mediated bone resorption.

Our data showed no difference in TRAP serum levels before and after surgery, suggesting RANKL activity was mainly local and osteoclastogenesis was not stimulated in distant skeletal sites. Interestingly, serum TRAP levels were similar between the veh and ZA treated groups. This has been described before in the literature by Kuroshima et al [156]. In this study, ZA was administered to mice in a similar regimen to ours for 13 months. Similar to our results, this paper reports no significant changes in serum TRAP levels between veh and ZA treated groups. Additionally, Kuroshima et al reported an increased number of non-attached osteoclasts around mucosal wounds in the hard palate away from the alveolar ridge. Our data show that non-attached osteoclasts can also be found in the alveolar ridge and are present in significantly earlier timepoints (3 and 12 days).

Our study included two different time-points. We elected a timepoint of three days in order to capture the initial stages of wound healing (inflammatory phase) and a later timepoint of 12 days to investigate a more mature socket healing stage (proliferative phase). Three days after extraction, a considerable amount of osteonecrosis was noted in the mandibles of veh-treated rats with or without RANKL treatment. This is likely due to the early time-point elected after tooth extraction, which causes significant trauma to the soft and bony tissues. As expected, osteonecrosis in veh treated rats was minimal 12 days after tooth extraction, likely because of osteoclast activation and resorption of necrotic bone.

In ZA/RANKL- rats, mucosal defects, bone exposure and extensive bone necrosis were noted. Prominent osteonecrotic areas were seen 3 days after tooth extraction and persisted in the 12-day time-point. Contrary, ZA treated animals with RANKL treatment consistently demonstrated smaller osteonecrotic areas which coincided with an increase in osteoclastic activity. Our data suggest that local enhancement of osteoclastic activity resulting in resorption of necrotic bone can improve wound healing after tooth extraction despite the presence of systemic antiresorptive treatment.

As we and others have described before, bisphosphonate treatment does not result in complete osteoclast elimination but rather in a change in their morphology which eventually results in apoptosis[8, 156]. Bisphosphonates alter the mevalonate pathway by inhibiting and enzyme called farnesyl pyrophosphate synthase. This results in the impairment of small GTPases, such as Ras and Rho which are essential in maintaining osteoclast morphology, migration and cell survival. [157] Histologically, osteoclasts demonstrate a round shape contrary to the oval shape of non-bisphosphonate treated osteoclasts. Often, they are larger in size and hypernucleated. An increased DC-STAMP signal has been described in osteoclasts from MRONJ patients compared to healthy controls or samples from osteomyelitis or osteoradionecrosis patients. Bisphosphonate treated osteoclasts present with pyknotic nuclei and are seen at a distance from the bone, suggesting bone resorption is impaired. Interestingly, in ZA/RANKL+ rats, we appreciated more osteoclasts that were attached to the bony surface, suggesting they maintained their resorptive ability. RANKL has been shown to decrease apoptosis in osteoclasts treated with bisphosphonates in vitro[158]. It is possible that the decreased osteonecrosis we observed in ZA/RANKL+ sites was due to both an increase in osteoclast numbers and an increased survival of the osteoclasts already exposed to zoledronic acid.

In both veh groups and in ZA/RANKL+ rats, we were able to appreciate collagen fiber insertion within the alveolar bone, while in ZA/RANKL- animals the collagen network was discontinuous around the necrotic bone areas. The disruption in the interface between soft tissue and bone may play an important role in the initiation of epithelial migration which can result in sequestration and bone exposure. In a previous study, we have described altered socket healing after extraction of periodontally compromised teeth in rats treated with bisphosphonates. In particular, we noticed a disorganized collagen network with weak collagen bundle birefringence and lack of insertion of collagen fibers in the necrotic bone. [65]. Epithelial migration approaching the osteonecrotic areas had also been observed and was rimmed by immune cells expressing MMP-9 and MMP-13. It is possible that the restoration of bone resorption and the ongoing remodeling of vital bone seen in ZA/RANKL+ sites might have prevented epithelial migration and helped accommodate the insertion of the periodontium fibers after tooth extraction.

Importantly, our study showed improvement of MRONJ lesions without the need for antiresorptive treatment discontinuation. The bisphosphonate dose (66 ug/kg) we utilized parallels the dose of zoledronic acid prescribed to oncologic patients. Nonetheless, the therapeutic approach we describe may also be efficient in osteoporotic patients, given that the cumulative bisphosphonate dose they receive is generally lower compared to cancer patients due to the utilization of less severe regimens. In fact, zoledronic acid (Reclast) is prescribed to osteoporotic patients in 5mg once every 12 months whereas 4mg of zoledronic acid (Zometa) is used every 3-4 weeks in oncologic patients. [159-161] We believe that achieving improved socket healing without discontinuing bisphosphonate treatment is crucial because 'a drug holiday', may potentially compromise the patient's skeletal health[2, 136].

We recognize some limitations to our study. We elected RANKL delivery through a collagen substrate due to its wide clinical application. This form of delivery allows for a relatively short contact time between RANKL and the tissues. However, this experimental duration was sufficient to show the differential socket healing between the ZA/RANKL- and the ZA/RANKL+ sites. In future studies, we aim to improve our delivery method utilizing engineered hydrogels that allow a slower molecule release. Moreover, we intent to expand our study to include longer timepoints (6-8 weeks) to better replicate the clinical scenario of MRONJ.

Here, we present a clinically relevant application of local RANKL delivery as it is plausible that a collagen sponge (a very commonly used substrate during extractions) could be infused with RANKL and inserted within the extraction socket of patients on antiresorptives, in an effort to accelerate wound healing and minimize the incidence of MRONJ. The intervention we describe would have beneficial effects, not only for minimizing MRONJ occurrence, but also to alleviate the fear of osteoporotic patients and thus improve compliance with antiresorptive medications. Additionally, it would allow clinicians to more easily elect extraction of hopeless teeth in patients at risk of MRONJ and therefore, minimize complications from persistent dental infection.

Figure 14. Clinical images of mandibles 3 and 12 days after surgery

Figure 14: Clinical images of mandibles 3 and 12 days after surgery. Images of the mandibular mucosa of veh or ZA treated rats with or without RANKL treatment 3 days after surgery. Mucosal defects and ongoing mucosal healing is seen. (14A-D, red circles). Quantification of unhealed mucosal area over total mucosal area 3 days after surgery. Image of the mandibular mucosa of veh or ZA treated rats with or without RANKL treatment 12 days after surgery. Image of the mandibular mucosa of a veh-treated rat without RANKL treatment (14F). Complete mucosal healing is seen (blue circle). Image of the mandibular mucosa of a veh-treated rat with RANKL treatment (14G). Complete mucosal healing is seen (blue circle). Image of the mandibular mucosa of a ZA treated rats without RANKL treatment (14H). A large mucosal defect and bone exposure are noted (red circle). Image of the mandibular mucosa of a ZA-treated rat with RANKL treatment (14I). Complete mucosal healing is seen (blue circle). Quantification of unhealed mucosal area over total mucosal area 12 days after surgery (14J). *=statistically significant with a p value<0.05

Figure 15. MicroCT assessment of veh or ZA treated sites with or without RANKL treatment
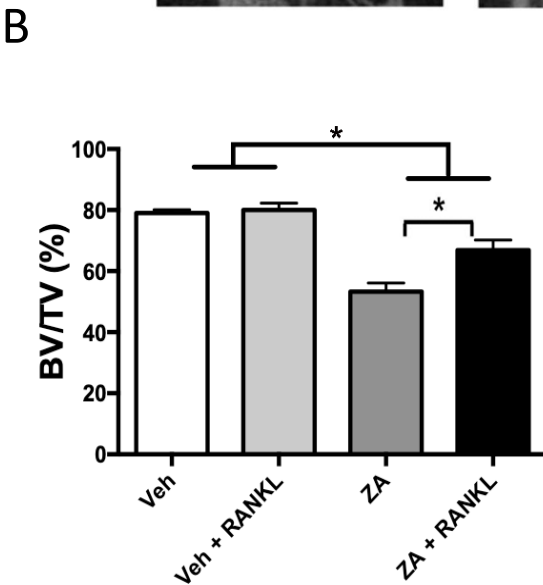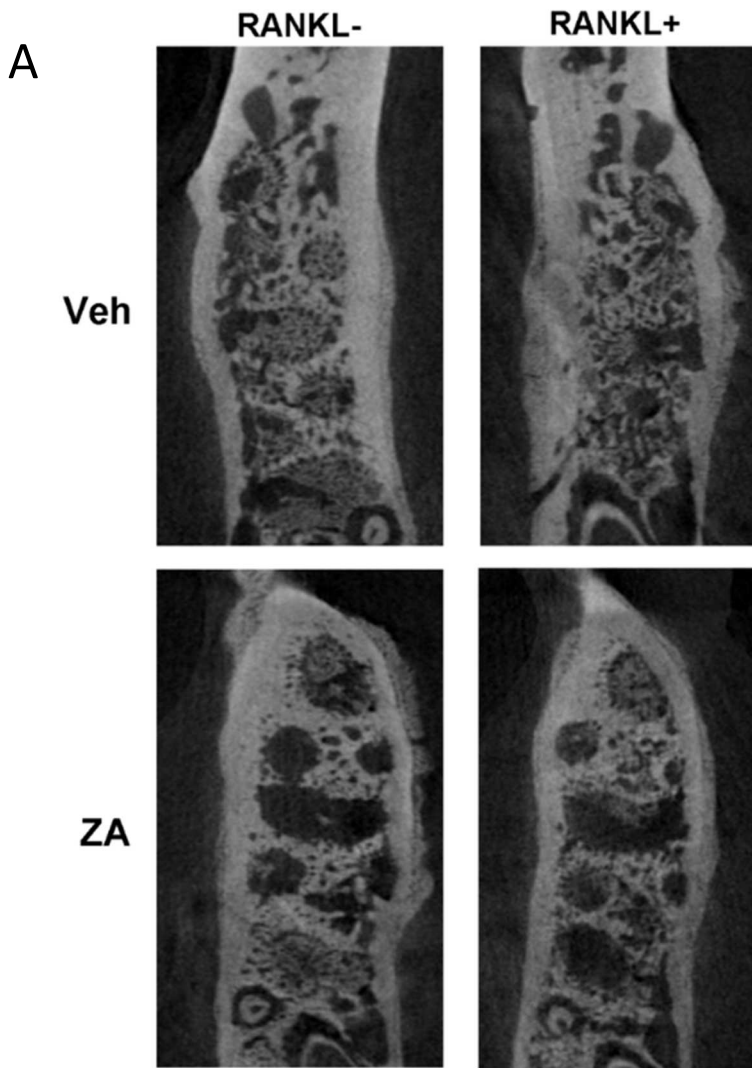
Figure 15: MicroCT assessment (axial view) of veh or ZA treated sites with or without RANKL treatment (Figure 15A). Quantification of bone volume over tissue volume in the distal root of the first molar (Figure 15, B). *= statistically significant with a p value <0.05

Figure 16: RANKL immunohistochemistry of veh or ZA treated rats with or without RANKL treatment. (16A-D). Yellow arrows in onsets point to RANKL stain on osteoclasts. Quantification of RANKL positive cells over soft tissue area (16E). Serum TRAP levels 3 days before and 3 days after surgery in veh and ZA treated rats. **= statistically significant with a p value <0.01 , *** = statistically significant with a p value <0.001

Figure 17. Histologic sections and TRAP staining 3 days after extraction
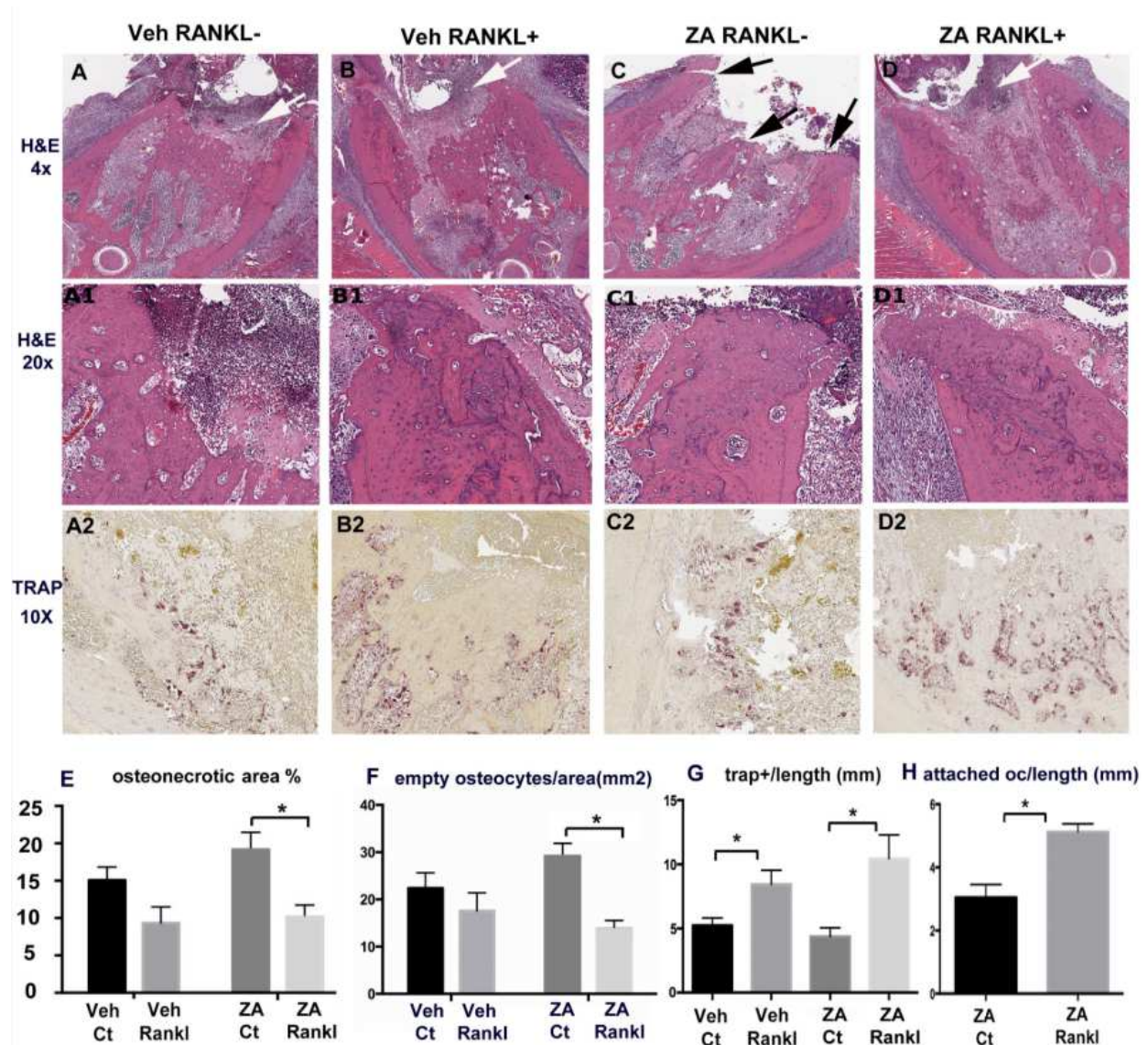
Figure 17. Histologic sections of extraction sockets of vehicle or ZA treated rats with or without local RANKL treatment 3 days after tooth extraction and RANKL delivery. Histologic section of the mandible of a veh-treated rat without RANKL treatment (17A, A1). Inflammatory cells and collagen fibers are seen overlying the alveolar bone (white arrow). Histologic section of the mandible of a veh-treated rat with RANKL treatment (17B, B1). Inflammatory cells, collagen fibers and epithelium are seen overlying the alveolar bone (white arrow). Histologic section of

the mandible of a ZA-treated rat without RANKL treatment (17C, C1). Absence of soft tissue overlying the alveolar bone is seen. Significant areas of bone exposure and osteonecrosis are noted (black arrow). Histologic section of the mandible of a ZA-treated rat with RANKL treatment. Inflammatory cells, collagen fibers and epithelium are seen overlying the alveolar bone (17D, D1, white arrow). Small areas of necrosis are noted. TRAP staining of veh or ZA treated sites with or without RANKL treatment (17A2-D2). Quantification of osteonecrotic area over total bone area (17E), empty osteocytes over bone area (17F), TRAP positive cells over bone length (17G) and attached osteoclasts over bone length (17H) *= statistically significant with a p value <0.05.

Figure 18. Histologic sections and TRAP staining 12 days after extraction
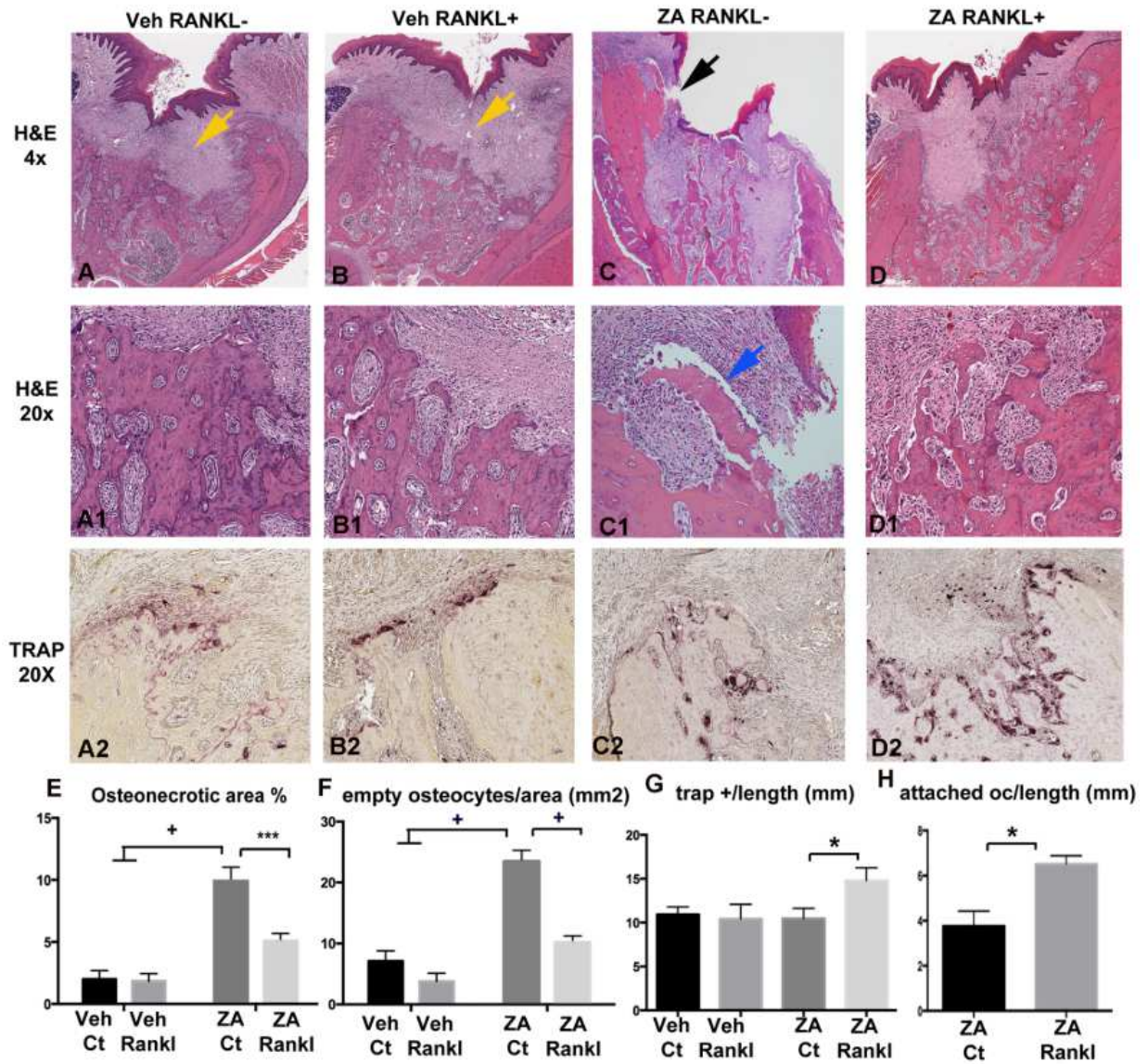
Figure 18: Histologic sections of extraction sockets of vehicle or ZA treated rats with or without local RANKL treatment 12 days after tooth extraction and RANKL delivery. Extraction socket of a veh-treated rat without RANKL treatment. Intact epithelium, absence of inflammatory infiltrate (orange arrow) and minimal osteonecrosis are noted (18A, A1). Extraction socket of a veh-treated rat with RANKL treatment (18B, B1). Intact epithelium, absence of inflammatory infiltrate (orange arrow) and minimal osteonecrosis are noted. Extraction socket of a ZA-treated

rat without RANKL treatment (18C, C1). Epithelial disruption and bone exposure (black arrow). Bony sequestration and osteonecrosis are noted (blue arrow). Extraction socket of a ZA-treated rat with RANKL treatment. Intact epithelium, absence of significant inflammation or bone exposure and reduced osteonecrosis are seen. (18D, D1). TRAP staining of veh or ZA treated rats with or without RANKL treatment (18A2-D2). Quantification of osteonecrotic area over total bone area (18E), empty osteocytes over bone area (18F), TRAP positive cells over bone length (18G) and attached osteoclasts over bone length (18H)   *** = statistically significant with a p value <0.001, + = statistically significant with a p value <0.0001

Figure 19. Picrosirius red and Cytokeratin 14 staining 12 days after extraction
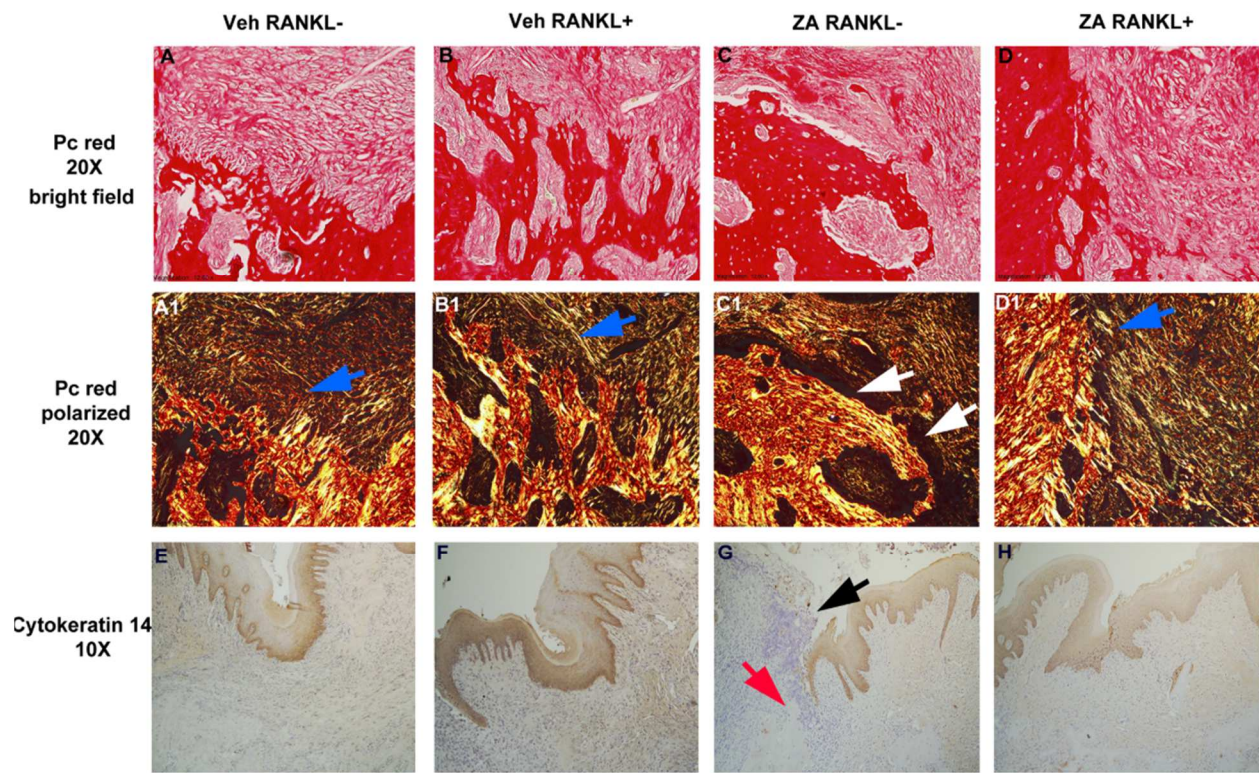
Figure 19. Picrosirius red stain of veh or ZA treated sites with or without RANKL treatment. (bright field-19A-D, polarized light-19A1-D1). Blue arrows point to insertion of collagen fibers in the bone. White arrows point to lack of collagen fiber insertion in the bone. Cytokeratin 14 stain of veh or ZA treated sites with or without RANKL treatment (19E-H). Black arrows points to epithelial disruption red arrow point to necrotic bone.

CHAPTER 6

M1 OVER M2 MACROPHAGES POLARIZATION IN ZOLEDRONATE TREATED MICE WITH PERIODONTAL DISEASE AND ROSIGLITAZONE TREATMENT AS THERAPY FOR MRONJ

Abstract

Macrophages are important regulators of bone remodeling and an M1 polarization has been implicated in the development of MRONJ. Here, we characterized the phenotype of macrophages in zoledronate treated mice with periodontal disease and explored the role of rosiglitazone, a drug that has been reported to invert M1/M2 macrophages ratio, in MRONJ amelioration. Sixty-six mice received ZA or saline treatment and a 6.0 ligature around their second molar. Mice were sacrificed 1, 2 or 4 weeks after ligature. Sixty-eight mice were treated with ZA or saline and half mice of each group received rosiglitazone for two weeks (veh/rosi-, veh/rosi+, ZA/rosi-, ZA/rosi+). 6.0 ligatures were placed around their second molars and 20 mice were sacrificed after 2 weeks. The remaining forty-eight mice were treated with ZA or saline and half mice from each group received rosiglitazone treatment. 6.0 ligatures were placed around their molars for 2 weeks and were replaced by 5.0 ligatures for 4 weeks. Micro-CT, histologic and immunohistochemical analyses were carried out.

An M1 predilection was noted in ZA treated mice with periodontitis 1, 2 or 4 weeks after ligature. M1 cells were found positive for MMP-13 and caused disruption of the surrounding collagen network in ZA mice. Rosiglitazone caused a reversal in the M1/M2 ratio in ZA mice and a further increase in M2 macrophages in veh mice. Bone loss attenuation was seen in the veh/rosi+ vs the veh/rosi- group in the 2-week timepoint. Increase of the epithelium to crest distance was

seen in the ZA/rosi+ compared to the ZA/rosi- group 2 weeks after ligature placement. Bone exposure incidence, epithelium to crest distance and osteonecrosis were similar in ZA/rosi- and ZA/rosi+ mice 6 weeks after ligature. Our data point to an important role of M1 macrophages polarization with an overexpression of MMP-13 in MRONJ development and provide insight on the utilization of rosiglitazone as a therapeutic means.

Introduction

MRONJ is a severe complication of antiresorptive and antiangiogenic medications which results in significant deterioration of the affected patients' quality of life. Although the pathophysiologic mechanisms underlying this disease are not clear, dental inflammation/infection and altered immune response are central in disease development[1, 25, 40, 42, 162].

Tooth extraction is the main inciting factor for MRONJ[1]. However, dental inflammation is by far the most common reason for tooth extraction in adults[64, 163]. In fact, animal studies have shown that extraction of diseased teeth combined with antiresorptive treatment is sufficient to induce MRONJ, whereas sockets undergo uneventful healing after extraction of healthy teeth[101].

Macrophages are a predominant population in periodontal disease lesions, are specialized in phagocytosis and can be grossly classified as pro-inflammatory (M1) or pro-resolving (M2) [73, 164]. Macrophages which are polarized towards the pro-inflammatory phenotype respond to cytokines, such as IL-1 or IL-6[165]. Exposure to cytokines such as IL-4 or IL-10 results to an M2 polarization[166]. Macrophages are closely associated with bone remodeling and bone resident macrophages have an emerging role in bone homeostasis. M1 macrophages are commonly

associated with bone loss whereas, M2 macrophages have been linked to an anabolic skeletal effect. [73, 167, 168]

An increased M1/M2 ratio has been previously reported around osteonecrotic lesions of mice with multiple myeloma[46]. Additionally, a TLR-4 increase resulting in M1 macrophage polarization has been described in osteonecrotic lesions of mice treated with zoledronic acid[45]. Rosiglitazone is an anti-diabetic drug which has been used in the past to reverse the M1/M2 ratio and reduce bone loss in periodontal disease[74]. Here, we hypothesized that an M1 over M2 predominance would be observed around osteonecrotic areas and that rosiglitazone treatment would reduce inflammation and improve MRONJ.

Materials and Methods

Animal care

Sixty-six mice were treated with saline or 200 μg/kg of zoledronic acid (ZA), (LKT laboratories, St. Paul, MN). Mice received a 6.0 ligature around their second molars and were sacrificed 1, 2 or 4 weeks after ligature placement.

Experiment with rosiglitazone treatment

Sixty-eight mice were randomly assigned to receive saline or 200 μg/kg of zoledronic acid (ZA), (LKT laboratories, St. Paul, MN). Mice were injected intraperitoneally twice a week in morning hours. Animals were kept and treated according to guidelines of the UCLA Chancellor's Animal Research Committee. Half animals from the saline or ZA treated mice received 50ug/kg of rosiglitazone (Selleckchem, Houston, Tx) dissolved in DMSO three times a week in morning hours. Non-rosiglitazone treated mice received DMSO injections.

After a week of pretreatment with saline or ZA, 6.0 sized ligatures were placed around the second molars on one side. 20 mice were sacrificed 2 weeks after ligature placement. The remaining 48 mice were received a 5.0 ligature after removal of the 6.0 ligature that was in place. Four weeks later, the 48 mice were sacrificed.

Micro CT

Dissected maxillae were imaged by high-resolution ex vivo μCT utilizing the SkyScan 1172 μCT scanner (SkyScan, Kontich, Belgium), as described. Volumetric image data were converted to DICOM format and imported in the Dolphin Imaging software to generate 3D and multiplanar reconstructed images. The distance from the cemento-enamel junction (CEJ) to the alveolar crest (AC) was measured at the mesial surface of the second molar.

Histology

Maxillae were fixed for 48 h in 4% paraformaldehyde and then decalcified in 14% EDTA for 4 weeks. Samples were paraffin embedded and 5 μm-thick cross sections were made perpendicular to the long axis of the alveolar ridge at the area of ligature. H&E stained slides were digitally scanned image analysis was performed using the Aperio Image Scope software (Aperio Technologies, Inc., Vista, CA, USA). The osteonecrotic area(s) and empty osteocytes over total bone area (s) were quantified.

Immunohistochemistry

Double staining of INOS (ab 15323, Abcam), F4/80 (ab 111101, Abcam), Arg1 (M01106-1, Boster), antibodies were performed in all combinations. MMP-13 (39012, Abcam) antibody was also used. Positive cells were measure on Image J (NIH) and were normalized by the soft tissue area that was measured per sample.

Statistics

Raw data were analyzed using the GraphPad Prism Software (GraphPad Software, Inc. La Jolla, CA). Descriptive statistics were used to calculate the mean and the standard error of the mean (SEM). Data were analyzed by a two-way ANOVA and post-hoc Tukey's test for multiple comparisons among the various groups and t-test for a single comparison with a statistical significance of $p < 0.05$.

Results

iNOS (M1 marker) and Arg1 (M2 marker) double staining showed a significant increase of M1 cells and a dramatic reduction in M2 cells in ZA treated animals in three timepoints (1, 2,

or 4 weeks) after ligature placement. iNOS and Arg1 were also combined with F4/80 staining to confirm their macrophage origin (Figure 20, A). The M1 macrophages were noted on the surface of the alveolar bone in the ZA treated animals whereas they were seen at a distance from the bone in the veh treated mice. Additionally, a layer of M2 macrophages was noted in proximity to the alveolar bone in veh treated mice (Figure 20, B).

Our picrosirius red data showed a disorganized collagen fiber network along the periodontal bone in ZA treated but not in veh treated mice. Indeed, the areas where the collagen network was discontinued were populated with iNOS positive cells. (Figure 21). We performed co-immunostain to test whether these iNOS positive M1 macs were also expressing MMP-13. An exuberant increase in MMP-13 signal was seen in the ZA treated animals and almost complete co-localization of MMP-13 and iNOS signal was detected in the same animals. The MMP-13 positive cells were seen rimming the alveolar bone. The co-localization of MMP-13 and iNOS signal was also observed in the maxillae of the veh treated mice. However, these cells were not in contact with the alveolar bone. (Figure 22, A). Statistically significant increase in the MMP-13 positive and the double positive iNOS and MMP-13 cells was seen in the ZA treated compared to the veh treated alveoli 1, 2 or 4 weeks after ligature placement (Figure 22, B).

Rosiglitazone treatment

In veh treated animals that had received rosiglitazone treatment (veh/rosi+), a significant increase in M2 macrophages and an M1 decrease was noted compared to the veh/rosi- animals 2 weeks after ligature placement. Interestingly, a reversal of M1/M2 ratio was observed in ZA/rosi+ alveoli with a predominance of M2 macs vs the M1 dominated alveoli of ZA/rosi- animals (Figure 23, A). Statistically significant increase in M2 numbers and decreased M1 numbers were noted in

the rosiglitazone treated groups of veh or ZA animals compared to the non-rosiglitazone groups. (Figure 23, B).

Radiographic assessment 2 weeks after ligature placement

Bone loss was statistically significantly attenuated in veh/rosi+ alveoli compared to the veh/rosi- group 2 weeks after ligature placement. In ZA treated mice, bone loss was significantly attenuated, as we have described before. No statistically significant differences were seen in the periodontal bone loss between ZA/rosi- and the ZA/rosi+ groups (Figure 24, A, B).

Histologic assessment 2 weeks after ligature placement

The epithelium to crest distance was increased in ZA/rosi+ vs the ZA/rosi- animals 2 weeks after ligature placement. A minimal amount of osteonecrosis was seen in the alveoli of ZA treated sites regardless of rosi treatment. No statistically significant differences were noted between ZA/rosi- and ZA/rosi+ sites. No frank bone exposure was seen in any of the ZA treated sites (Figure 25A, B, C).

Radiographic assessment 6 weeks after ligature placement

Micro CT revealed no statistical significant differences between the rosi treated vs the non-rosi treated sites in veh or ZA treated animals. The bone loss was increased compared to the 2-week timepoint in veh treated animals regardless of rosiglitazone treatments. ZA treated animals demonstrated attenuated bone loss compared to the veh treated animals at the 6-week timepoint. The bone loss levels in ZA treated animals were similar at the 2-week timepoint and the 6 weeks timepoint (Figure 26).

Histologic assessment 6 weeks after ligature placement

No veh treated sites showed bone exposure regardless of rosiglitazone treatment. 10/12 sites of the ZA/rosi- group showed histologic bone exposure whereas 10/11 sites of the ZA/rosi+ group demonstrated bone exposure 6 weeks after ligature placement. Osteonecrosis was increased in ZA/rosi- and ZA/rosi+ animals compared to veh treated mice. No statistical differences were detected in the levels of osteonecrosis between ZA/rosi- and ZA/rosi+ groups (Figure 27).

Discussion

Macrophages are important regulators of inflammatory response and bone homeostasis[169]. The role of macrophages has been characterized before in periodontal disease and other systemic conditions, such as rheumatoid arthritis and vascular calcifications[170, 171]. Lately, a new population called osteomacs (osteal macrophages) has been identified and further highlights the role of macrophages in bone remodeling. In fact, genetic macrophage depletion in the MAFIA mouse has been associated with delayed fracture healing, osteopenia, irresponsiveness to the anabolic effects of PTH and growth retardation in prenatal macrophage depletion[167, 172, 173].

A few studies have investigated the role of macrophages in MRONJ pathogenesis. In these studies, a clear predominance of M1 vs M2 polarization has been reported. In fact, in a study by Zhang et al, systemic infusion with M2 cells and blocking of IL-17 showed a reduction in MRONJ incidence in the extraction socket of mice burdened with multiple myeloma[46]. In a more recent publication by Zhu et al, M1 polarization in the extraction sockets of zoledronate treated mice was found to be TLR-4 mediated and TLR4-/- mice demonstrated ameliorated socket healing and a decrease in M1 population[45]. Our data corroborate an M1 polarization in zoledronate treated alveoli with periodontal disease. Interestingly, this M1 predominance was seen in the absence of tooth extraction suggesting that M1 macrophages may be important in initial steps of MRONJ development before dentoalveolar trauma has been induced.

A strong co-localization of iNOS and MMP-13 signal was observed in the alveoli of ZA treated mice rimming the periodontal bone. Importantly, these cells were found in the areas of collagen network disruption in ZA treated mice. In a previous study, we have described the lack of collagen fiber insertion in the alveolar bone in the extraction sockets of periodontally compromised teeth under bisphosphonate treatment[65]. Here, we confirmed the over-expression of

MMP-13 in zoledronate treated mice with periodontal disease even in the absence of tooth extraction. MMP-13 is a matrix metalloproteinase expressed mainly by osteoblasts and macrophages that has been implicated in osteoarthritis, inflammatory bowel disease and periodontitis. In periodontitis in particular, it has been reported to be increased in the crevicular fluid and in the tissues around active periodontal disease[174-176]. Our data collectively show an abundance in pro-inflammatory M1 macrophages which express MMP-13 causing degradation of the collagen fibers around the bone. It is possible that the weakened osteo-mucosal connection and the persistent inflammation are responsible for the initiation of epithelial migration and bone exposure noted in clinical MRONJ.

Rosiglitazone is a PPAR-g activator which has been used to increase insulin sensitivity in adipose tissue in patients with Type II diabetes. Rosiglitazone has been implicated in a reduction in osteoblast differentiation and bone mineral density in the skeleton of rodents and patients[177, 178]. However, it has been shown to exert a protective role against periodontal bone loss in the jaws of rodents[179]. The mechanisms through which rosiglitazone exerts its beneficial effects in periodontal lesions were elucidated by a study by Viniegra et al[74]. In this study, rosiglitazone increased the pro-resolving M2 population in the periodontal lesions enhancing the regeneration of alveolar bone and combating the osteolysis induced by a ligature model of periodontitis. Our data confirmed an M2 polarization in the rosiglitazone treated mice both in the veh and the ZA groups. Additionally, attenuated periodontal bone loss was visualized in veh treated animals receiving rosiglitazone treatment compared to the veh/rosi- group 2 weeks after ligature placement. A further reduction in periodontal bone loss was not seen in the ZA/rosi+ group compared to the ZA/rosi- group likely due to the robust inhibition of periodontal bone loss that zoledronic acid mediated.

Interestingly, we were able to detect an increase in the epithelium to alveolar crest distance in ZA/rosi+ alveoli compared to the ZA/rosi- group. Given that the levels of the periodontal bone were similar between the groups it is likely that epithelial migration was attenuated in the presence of rosiglitazone treatment. Epithelial migration has been reported to be mediated by matrix metalloproteinases which are overexpressed in inflamed periodontal pockets[180]. The anti-inflammatory effects of rosiglitazone and the reduction of M1 macrophages replaced by the pro-resolution M2 macrophages might have helped attenuate epithelial migration.

Periodontal bone loss was significantly increased 6 weeks after ligature placement, as expected, in veh treated animals. Intriguingly, the protective role of rosiglitazone against radiographic periodontal bone loss was not observed in this timepoint. This is possibly due to the aggressive periodontitis model we employed which involved replacement of the 6.0 ligature after 2 weeks with a thicker 5.0 ligature that stayed in place for another 4 weeks. ZA inhibition of periodontal bone loss was also noted in the 6 weeks timepoint, as expected.

ZA/rosi- and ZA/rosi+ groups showed histologic bone exposure in the vast majority (10/12 and 10/11 respectively) of the sites investigated 6 weeks after ligature placement. We attribute this event to the aggressive periodontitis model we elected and the high amounts of potent bisphosphonate treatment. We used this model in an effort to increase bone exposure incidence and facilitate the characterization of the disease as it appears in human patients. However, it is possible that this drastic periodontitis model which resulted in a significant obliteration of the periodontal soft tissues did not allow rosiglitazone treatment to reduce bone exposure incidence and improve MRONJ burden. Similarly, the levels of osteonecrosis did not improve in the ZA/rosi+ group compared to the ZA/rosi- group.

MRONJ is a severe disease which can have serious sequalae in already compromised patients[1]. Improving MRONJ burden with a drug that also has anti-diabetic effects is an attractive hypothesis. However, further studies need to be performed to determine the efficacy of rosiglitazone in MRONJ amelioration. In future studies, we intend to utilize a milder periodontitis stimulus (6.0 ligature for 6 weeks) to better study our hypothesis. Our data confirm an M1 macrophage predilection in ZA treated animals with periodontal disease and prove that rosiglitazone can negate the M1/M2 ratio. Although a reduction in epithelium to alveolar crest distance was seen in ZA/rosi+ sites 2 weeks after ligature placement, more studies with longer experimental timepoints are needed to better replicate the clinical scenario and to investigate disease amelioration under rosiglitazone treatment.

Figure 20. iNOS and Arg1 immunohistochemistry
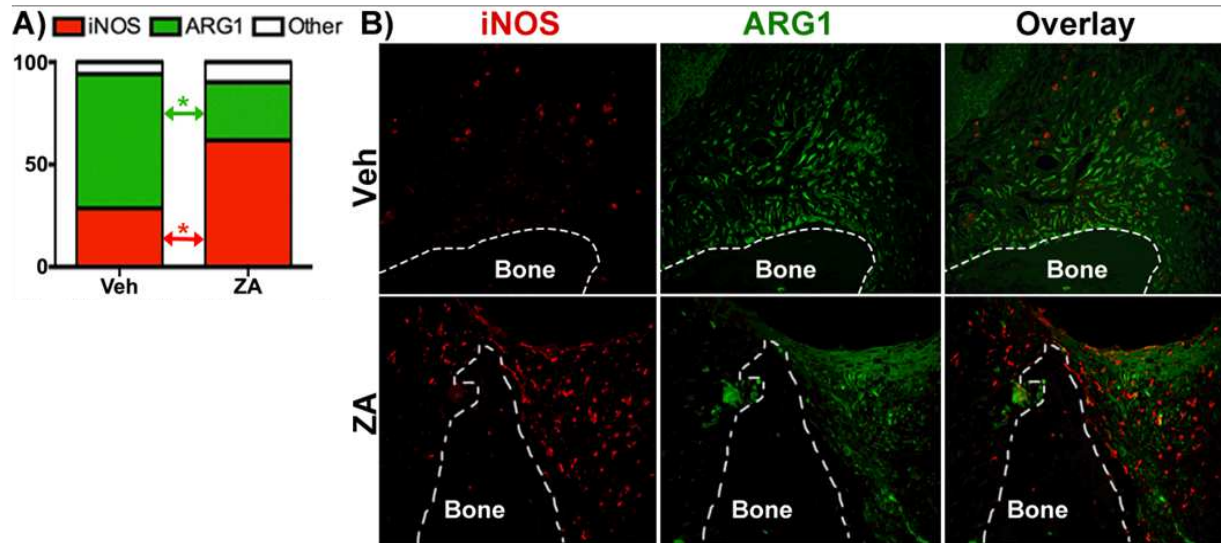
Figure 20: Percentage of f4/80 positive cells stained for M1 (iNOS) or M2 (Arg1) in veh or ZA treated sites (Figure 20,A). iNOS and Arg1 double staining in veh or ZA treated mice. M1 predominance in the ZA treated mice compared veh treated mice where an M2 polarization was noted. * statistically significant $p < 0.05$

Figure 21. Picrosirius red and iNOS staining
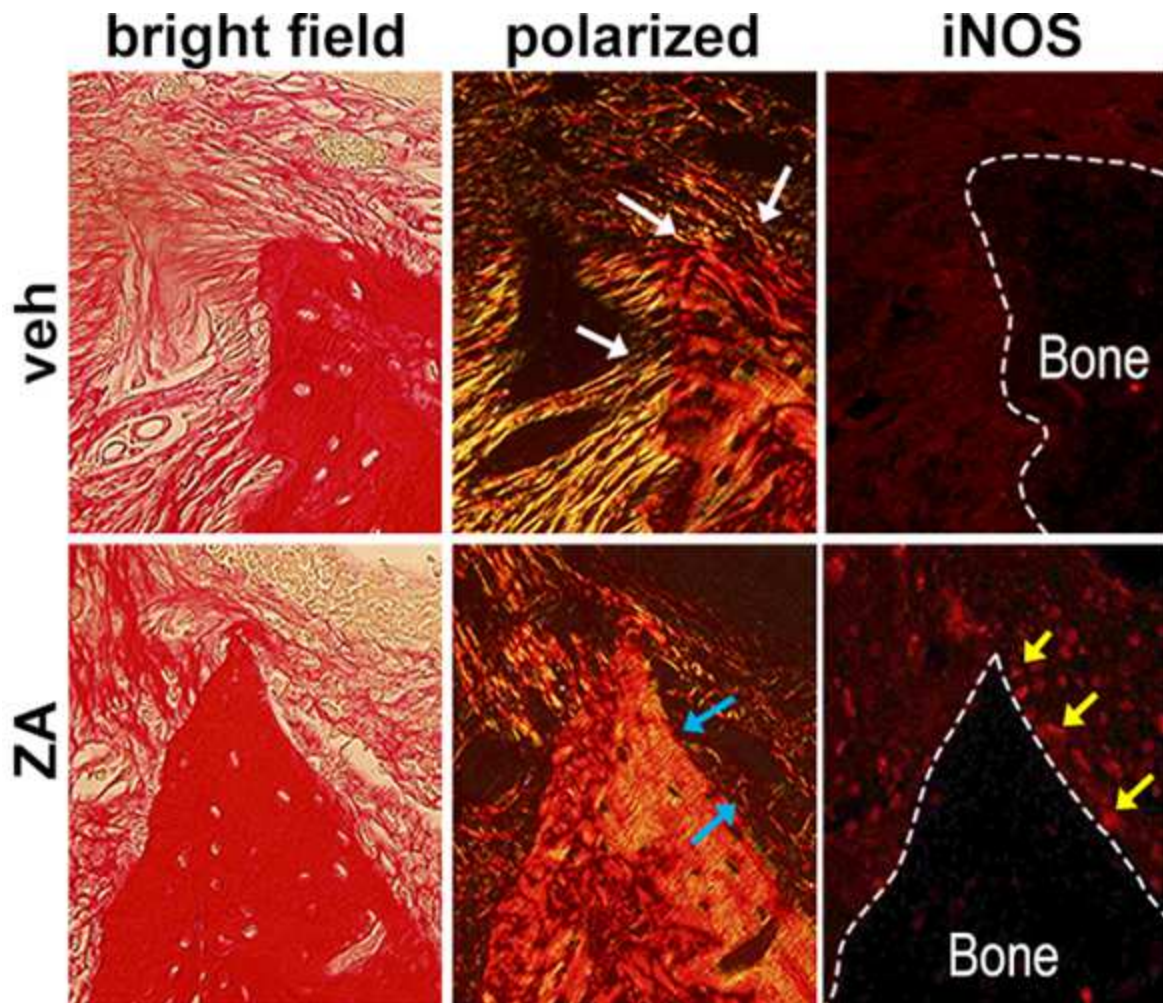
Figure 21: Picrosirius red and iNOS staining. White arrows point to collagen fiber insertion into the alveolar bone. Blue arrows show collagen network disruption. Yellow arrows point to iNOS positive cells

Figure 22. iNOS and MMP-13 staining
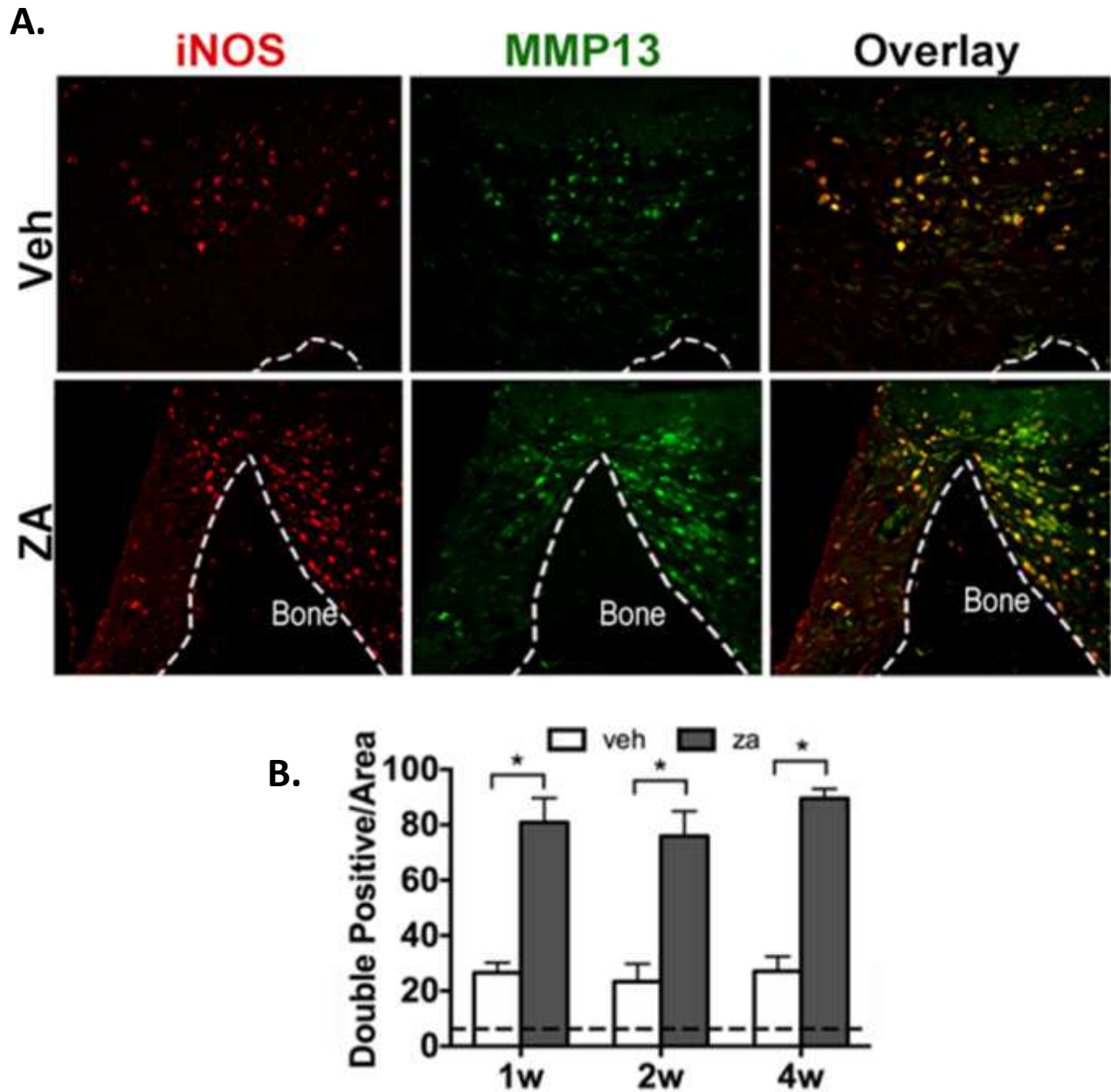
Figure 22: iNOS and MMP-13 double staining in veh or ZA treated animals 2 weeks after

ligature placement (Figure 22, A). Double positive cells normalized for soft tissue area in mm^2 in

veh or ZA treated mice 1, 2, 4 weeks after ligature placement (Figure 22, B). *statistically

significant p<0.05

Figure 23. iNOS and Arg1 staining after rosiglitazone treatment
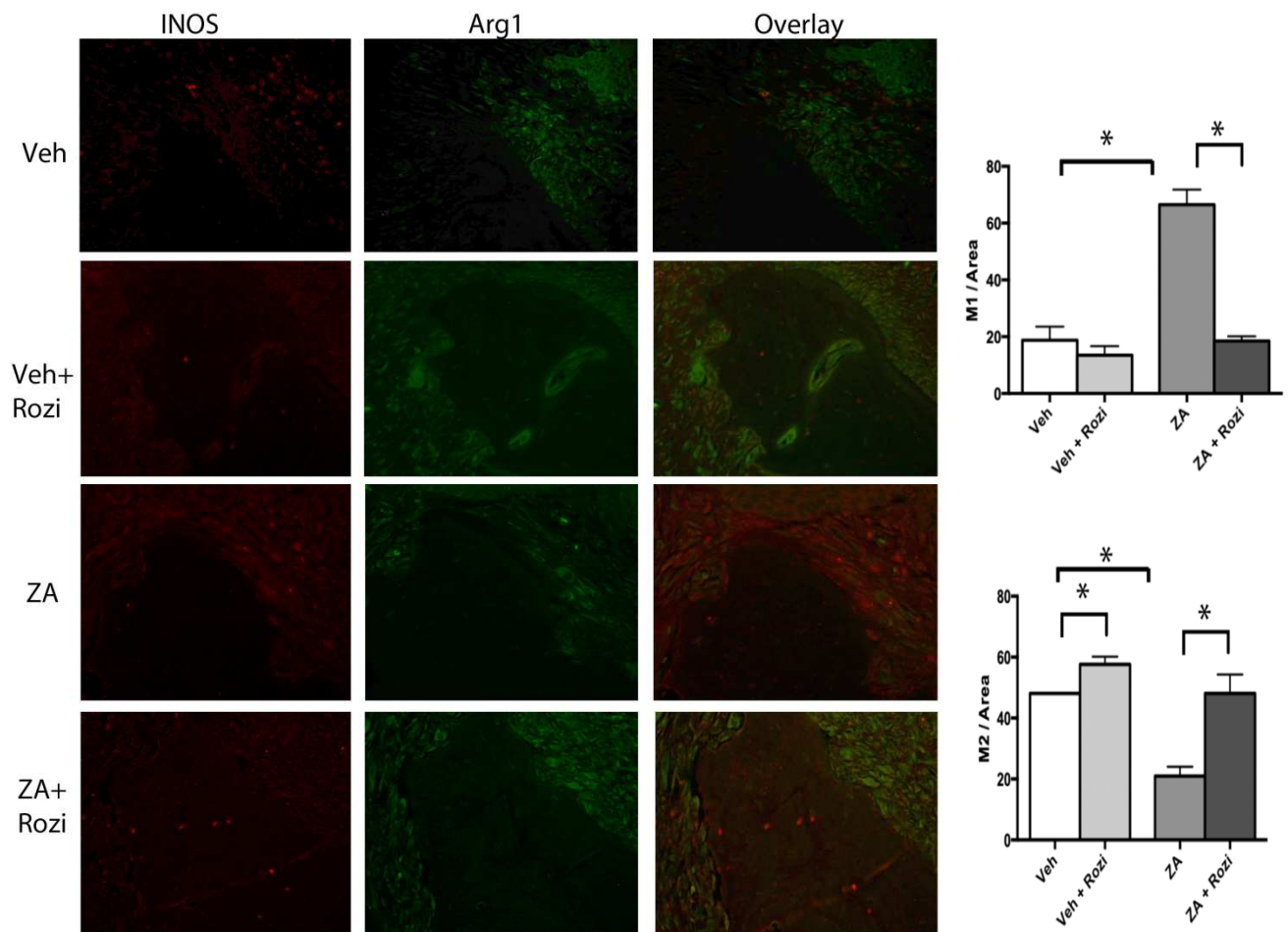
Figure 23: iNOS and Arg1 staining in veh or ZA treated animals with or without rosiglitazone treatment. (Figure 23). M1 or M2 cells normalized over soft tissue area in mm^2, *statistically significant $p<0.05$

Figure 24. Radiographic assessment 2 weeks after rosiglitazone treatment onset
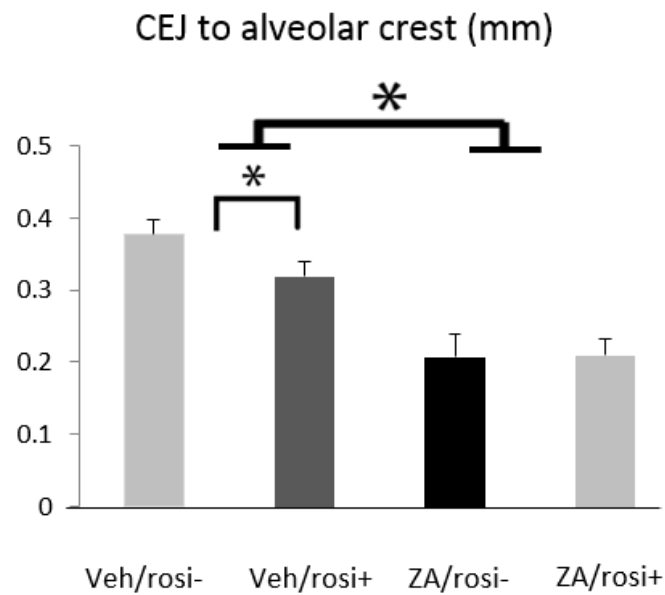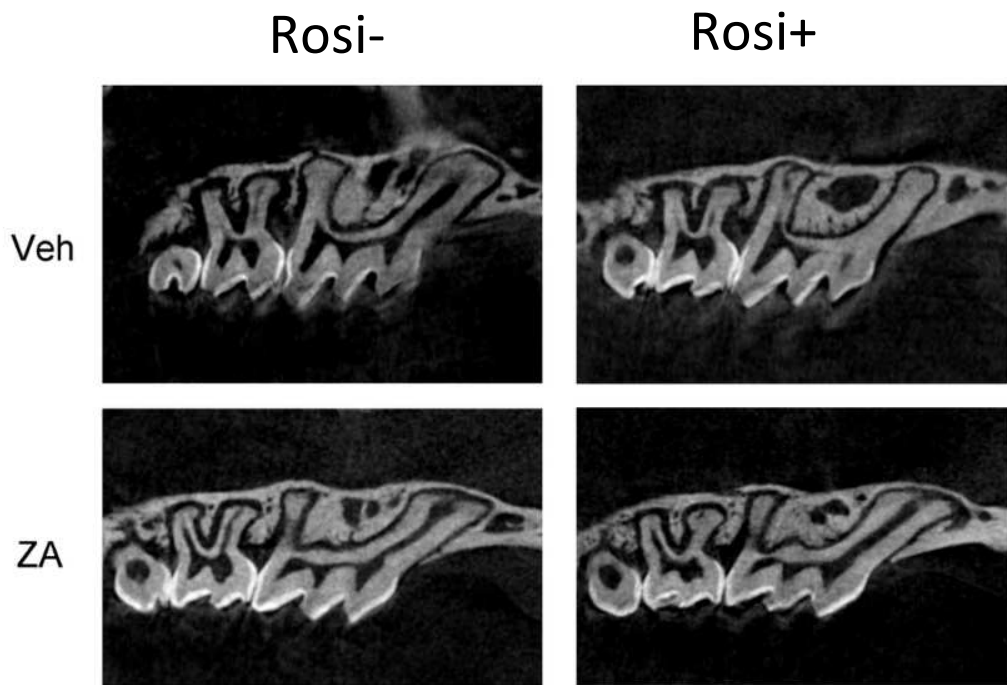
Figure 24: Sagittal images of the alveoli of veh or ZA treated animals with or without rosi treatment

(Figure 24). CEJ to crest distance in mm, * statistically significant p<0.05

Figure 25. Histologic sections 2 weeks after rosiglitazone treatment
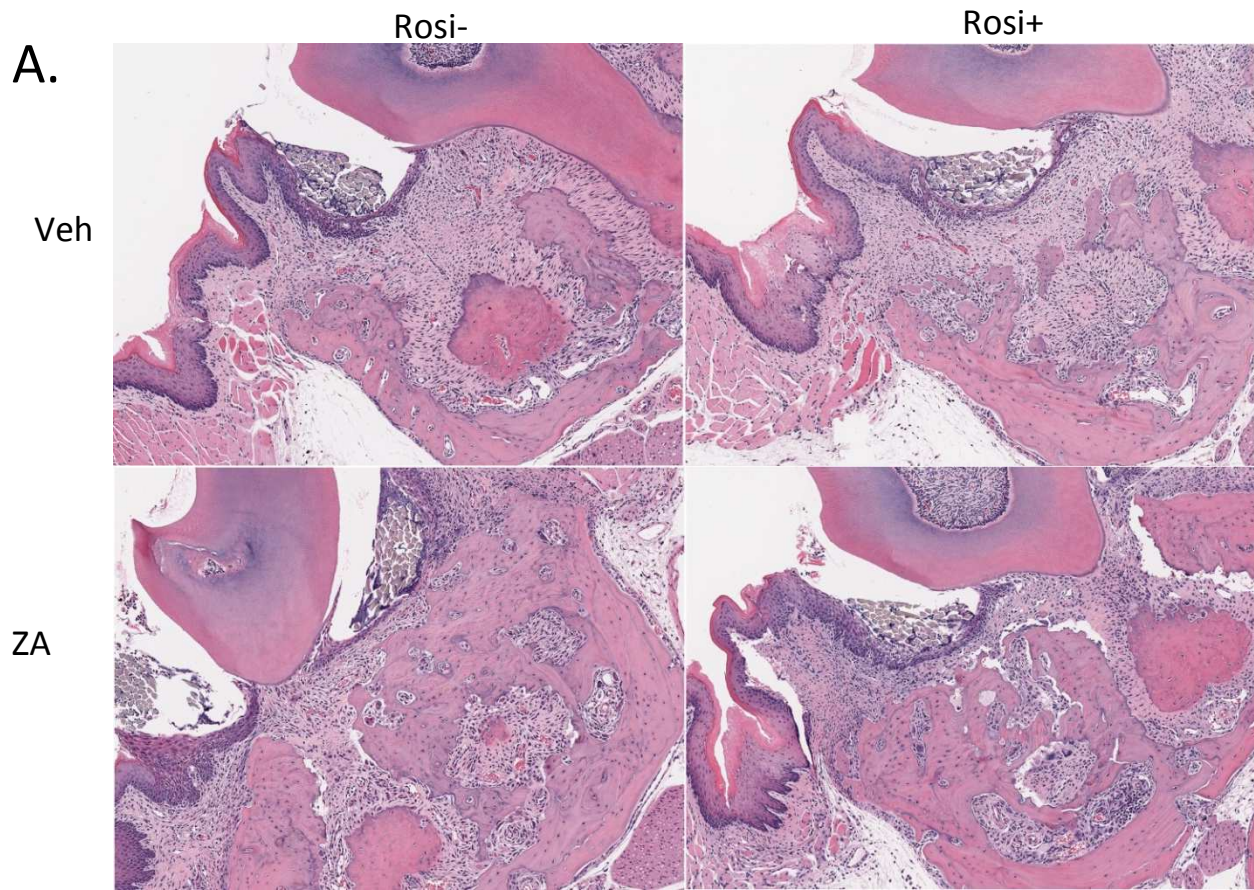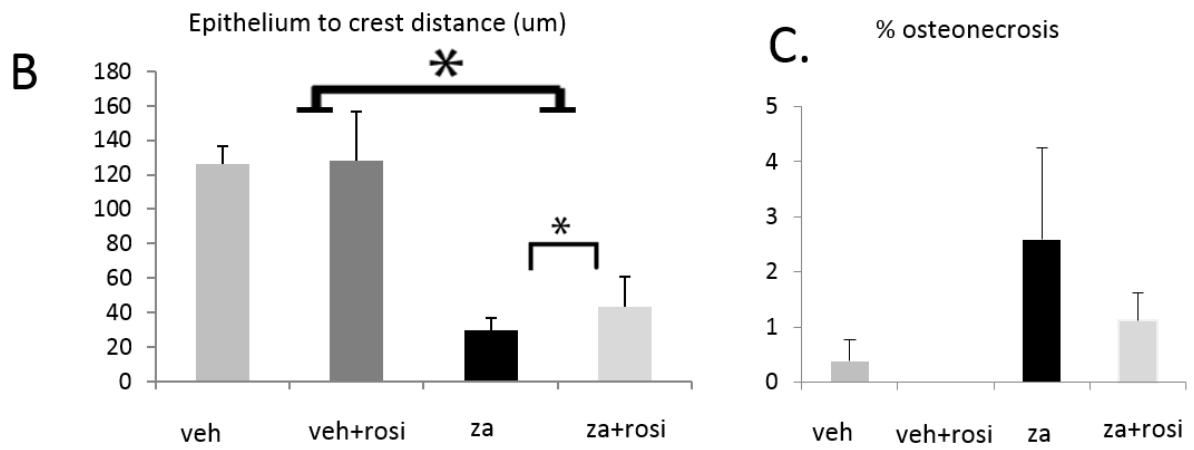
A.

	Rosi-	Rosi+
Veh		
ZA		

Figure 25: Histologic sections of veh or ZA treated animals with or without rosiglitazone treatment (Figure 25, A). Epithelium to alveolar crest distance in um (B), Percent osteonecrotic areas (C), *p<0.05

Figure 26. Radiographic assessment 6 weeks after rosiglitazone treatment onset
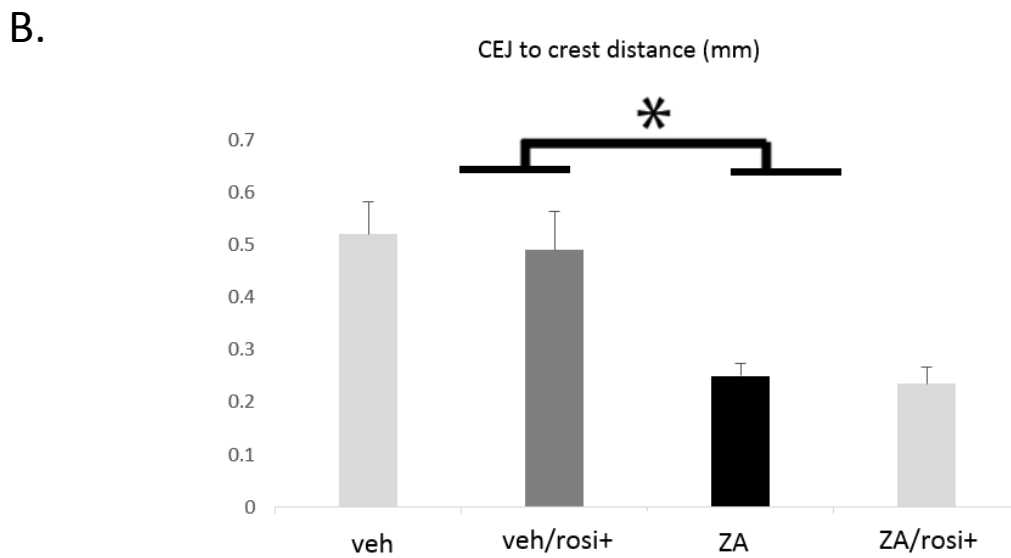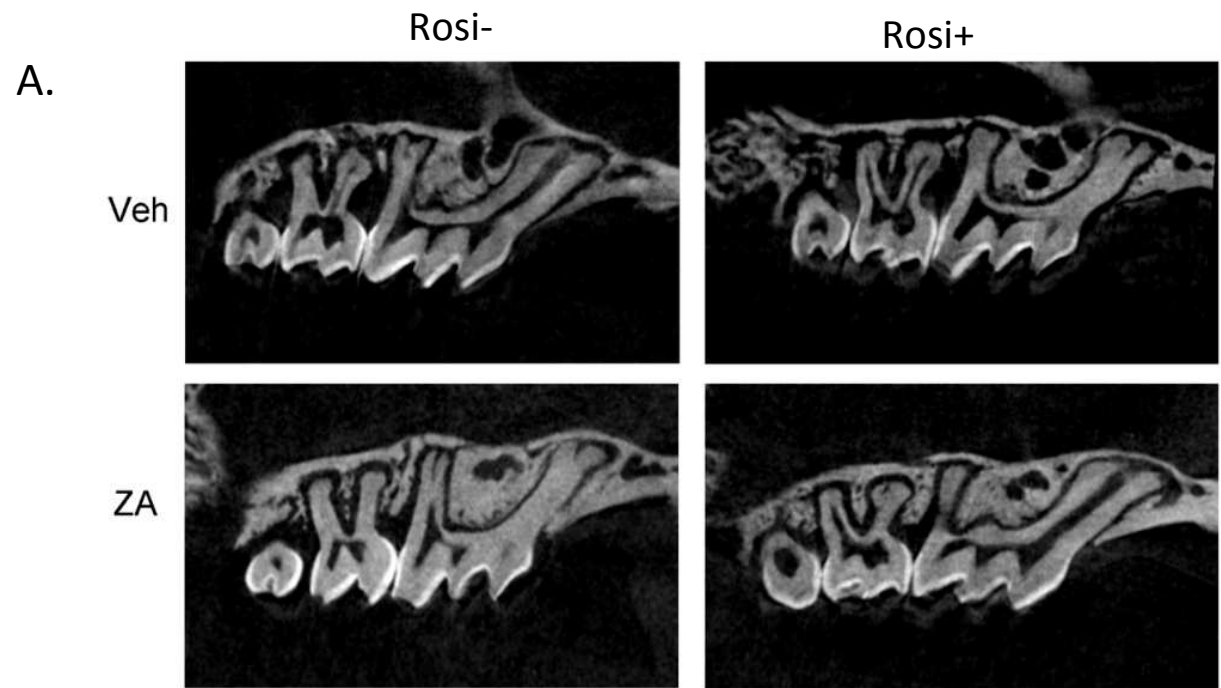
Figure 26: Radiographic assessment of veh or ZA treated mice with or without rosiglitazone

treatment 6 weeks after ligature placement (Figure 26, A). CEJ to crest distance in mm (B).

*P<0.05

Figure 27. Histologic sections 6 weeks after rosiglitazone treatment onset
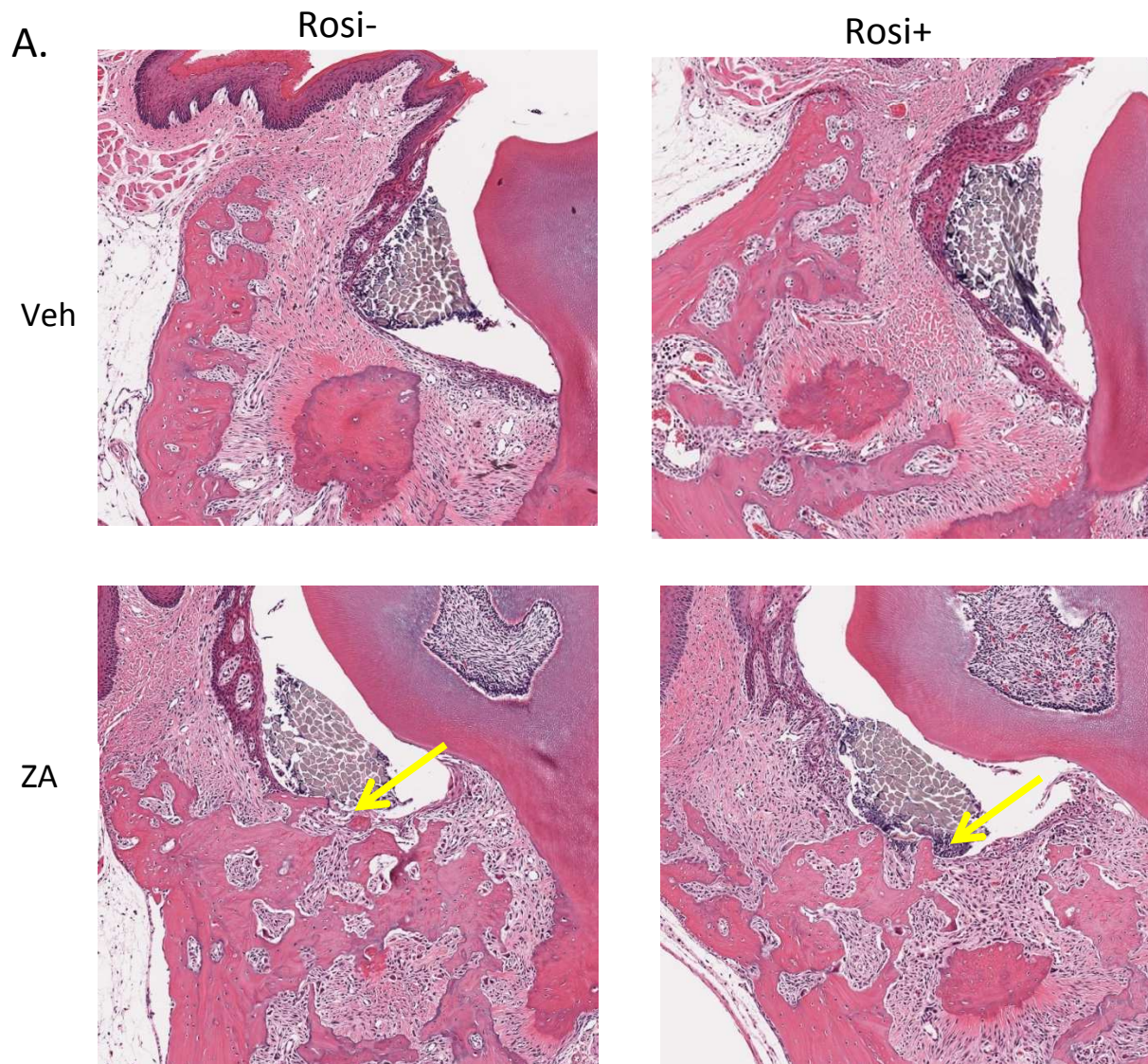
A.

Rosi-

Rosi+

Veh

ZA

B.

# of exposed sites

C.

Epithelium to crest distance (um)

D.

% osteonecrotic area

Figure 27: Histologic sections of veh or ZA treated mice with or without rosiglitazone treatment. Yellow arrows point to bone exposure (Figure 27, A), number of exposed sites in za animals (B), epithelium to crest distance in um (C), percent osteonecrotic area, *p<0.05

CHAPTER 7

SUMMARY AND FUTURE DIRECTIONS

MRONJ is a severe disease which affects osteoporotic and bone cancer patients. Although MRONJ incidence is reportedly low, it is likely that it will continue to increase as new pharmacologic agents are being associated with its development and antiresorptive medications continue to be vastly prescribed. Significant progress has been made towards the elucidation of its pathogenetic mechanisms and its treatment. Our data show that MRONJ is a multifactorial disease largely affected by changes in vascularity, local inflammation and inhibition of bone remodeling.

In our studies, we showed that extraction of healthy teeth is not sufficient to induce MRONJ in antiresorptive treated rodents. Extraction of diseased teeth, in contrast, leads to significant radiographic and histologic changes which closely parallel the disease in humans. Radiographic changes include periosteal bone formation, lack of socket healing and sequestration. Histologic changes involve osteonecrosis, sequestration, persistent inflammation and bone exposure.

We also observed the overexpression of several markers via immunohistochemistry in the extraction sockets of inflamed teeth in the presence of antiresorptive treatment. We observed a delayed wound healing stage in these sockets with an increase in the immature Type III collagen vs Type I collagen. A disruption was seen in the bone-soft tissue interface in the rodents presenting with osteonecrosis. Additionally, MMP-9 was increased in these animals and MMP-9 positive cells were seen in the area of the epithelium, around the inflammatory areas of the soft tissue and rimming the osteonecrotic bone. An exuberant increase of MMP-13 was also noted in these sockets with MMP-13 positive cells extending from the epithelium to the surface of the osteonecrotic bone. In the same study, we observed an over-expression of α-SMA signal in contact with the necrotic

121

bone. It is possible that the cells expressing these matrix metallo-proteinases and α-SMA are key in the process of epithelial migration and initiation of bone exposure. Our data were confirmed with human biopsies which demonstrate increased MMP-13, COL III and α-SMA. The perseverance of inflammatory cells around necrotic bone demonstrates an impaired stage of socket healing and provides an important insight to the mechanisms of MRONJ development in patients.

In our studies involving the role of macrophages in the development of MRONJ we noticed a clear predominance of M1 vs M2 macs around osteonecrotic lesions. The M1 macrophages were in contact with the necrotic bone and interfered with the insertion of collagen fibers in the underlying trabecular bone. Additionally, these M1 macrophages expressed MMP-13. Our data confirm a predilection in M1 macrophage polarization in an antiresorptive environment. The lack of pro-resolution M2 macrophages and the persistence of M1 macrophages secreting pro-inflammatory cytokines may explain the compromised wound healing observed in MRONJ lesions. Although we were successful in reversing the M1/M2 ratio with our studies that employed rosiglitazone treatment, we were not able to detect significant difference in the incidence of bone exposure or the amount of osteonecrosis in the jaws of zoledronate treated mice with rosiglitazone treatment vs without rosiglitazone treatment 6 weeks after periodontal disease was induced.

In our patient studies, we concluded that CBCT is instrumental in distinguishing between common dental disease patients and stage 0 MRONJ patients. It is important to properly diagnose these patients presenting with vague symptoms and signs in order to avoid patients in need of simple dental procedures, such as root canals, receiving excessive treatment including severe antibiotic regimens, surgical procedures or discontinuation of their systemic antiresorptive treatment. Interestingly, we found that patients with sequestration at initial presentation are highly likely to progress to frank bone exposure within 6 months. These patients are more likely to benefit

from close follow-ups and more aggressive treatment than patients presenting without sequestra in their initial radiographic examination.

Lastly, we explored RANKL delivery as a therapeutic approach for MRONJ in an extraction model in rats under zoledronate treatment. We appreciated a significant improvement in mucosal healing, bone healing and a reduction in bone exposure and osteonecrosis. This approach is clinically relevant and could be used to minimize MRONJ incidence and help uneventful healing after tooth extraction in patients treated with antiresorptives.

Future studies

Rosiglitazone treatment

We believe that the reason why we could not detect an improvement in MRONJ burden 6 weeks after rosiglitazone treatment onset was the aggressive periodontitis model we employed. In this model, a 6.0 silk ligature is tied around the second molars of the mice and is left in place for two weeks. Then, the 6.0 silk ligature is removed and a larger, 5.0 size silk ligature is tied around the same tooth and is left in place for 4 weeks. We utilized this model in an effort to increase bone exposure incidence in order to better replicate the human disease. MRONJ occurs in approximately 1% of patients receiving oncologic doses of bisphosphonates or denosumab. In osteoporotic patients, the incidence in even lower (approximately 1:10,000). Therefore, a strong inflammatory stimulus is needed in combination with high doses of potent antiresorptives to achieve a significant incidence of MRONJ. However, utilizing this really aggressive model resulted in considerable elimination of the connective tissue. The lack of MRONJ improvement in rosiglitazone treated mice was largely attributed to the obliteration of the soft tissues in the presence of a 5.0 ligature. In future studies, we aim to repeat this experiment utilizing the milder 6.0 ligature model to allow for a relative restoration of the macrophage environment around the alveolar bone.

MMP-13 inhibition

Throughout our studies, we have observed a substantial increase in MMP-13 signal in the soft tissues, on the bone surface and in osteocytes of the alveolar bone in rodents with MRONJ. This finding has been consistent in both mouse and rat studies. MMP-13 is mostly expressed by osteoblasts and immune cells, mainly macrophages. Our data suggest that MMP-13 is a key molecule in MRONJ development. In future studies, we intend to explore the effects of MMP-13 inhibition. MMP-13 knockout mice are not lethal and are readily available. Monoclonal antibodies against MMP-13 have also been used mainly in osteoarthritis studies. We hypothesize that MMP-13 elimination may have a protective effect against MRONJ development and may decrease submucosal inflammation in rodent jaws.

RANKL delivery method improvement

Our RANKL therapy data were proof that local increase of osteoclastic function is beneficial in the socket healing of zoledronate treated rats. We utilized a collagen tape due to its wide clinical application in extraction socket healing in clinical practice. However, we were not able to characterize the RANKL release in a time dependent manner. An engineered hydrogel with a more precise release over time would be a better method for the delivery of RANKL to the tissues. Such a delivery method would also allow a longer contact between the therapeutic molecule and the extraction socket tissues. A longer lasting treatment would also allow a longer experimental duration (6-8 weeks) which would more faithfully replicate the clinical scenario of MRONJ.

REFERENCES

1.   Ruggiero SL, Dodson TB, Fantasia J, et al. American Association of Oral and Maxillofacial Surgeons position paper on medication-related osteonecrosis of the jaw--2014 update. *J Oral Maxillofac Surg.* 2014;72:1938-1956.

2.   Khan AA, Morrison A, Hanley DA, et al. Diagnosis and management of osteonecrosis of the jaw: a systematic review and international consensus. *J Bone Miner Res.* 2015;30:3-23.

3.   Schiodt M, Reibel J, Oturai P, Kofod T. Comparison of nonexposed and exposed bisphosphonate-induced osteonecrosis of the jaws: a retrospective analysis from the Copenhagen cohort and a proposal for an updated classification system. *Oral Surg Oral Med Oral Pathol Oral Radiol.* 2014;117:204-213.

4.   Fedele S, Porter SR, D'Aiuto F, et al. Nonexposed variant of bisphosphonate-associated osteonecrosis of the jaw: a case series. *Am J Med.* 2010;123:1060-1064.

5.   Walton K, Grogan TR, Eshaghzadeh E, et al. Medication related osteonecrosis of the jaw in osteoporotic vs oncologic patients-quantifying radiographic appearance and relationship to clinical findings. *Dentomaxillofac Radiol.* 2018:20180128.

6.   Dimopoulos MA, Kastritis E, Bamia C, et al. Reduction of osteonecrosis of the jaw (ONJ) after implementation of preventive measures in patients with multiple myeloma treated with zoledronic acid. *Ann Oncol.* 2009;20:117-120.

7.   de Souza Tolentino E, de Castro TF, Michellon FC, et al. Adjuvant therapies in the management of medication-related osteonecrosis of the jaws: Systematic review. *Head Neck.* 2019;41:4209-4228.

8.   de Molon RS, Shimamoto H, Bezouglaia O, et al. OPG-Fc but Not Zoledronic Acid Discontinuation Reverses Osteonecrosis of the Jaws (ONJ) in Mice. *J Bone Miner Res.* 2015;30:1627-1640.

9.   Kwon YD, Kim DY. Role of Teriparatide in Medication-Related Osteonecrosis of the Jaws (MRONJ). *Dent J (Basel).* 2016;4.

10.   Hadaya D, Soundia A, Freymiller E, et al. Nonsurgical Management of Medication-Related Osteonecrosis of the Jaws Using Local Wound Care. *J Oral Maxillofac Surg.* 2018;76:2332-2339.

11.   Kennel KA, Drake MT. Adverse effects of bisphosphonates: implications for osteoporosis management. *Mayo Clin Proc.* 2009;84:632-637; quiz 638.

12.   Gong L, Altman RB, Klein TE. Bisphosphonates pathway. *Pharmacogenet Genomics.* 2011;21:50-53.

13.   Baron R, Ferrari S, Russell RG. Denosumab and bisphosphonates: different mechanisms of action and effects. *Bone.* 2011;48:677-692.

14.   Gunawan F, George E, Kotowicz M. Denosumab-induced hypocalcaemia in metastatic castrate-resistant prostate cancer. *Endocrinol Diabetes Metab Case Rep.* 2019;2019.

15.   Florez H, Ramirez J, Monegal A, Guanabens N, Peris P. Spontaneous vertebral fractures after denosumab discontinuation: A case collection and review of the literature. *Semin Arthritis Rheum.* 2019;49:197-203.

16.   Lamy O, Stoll D, Aubry-Rozier B, Rodriguez EG. Stopping Denosumab. *Curr Osteoporos Rep.* 2019;17:8-15.

17.   Mucke T, Krestan CR, Mitchell DA, Kirschke JS, Wutzl A. Bisphosphonate and Medication-Related Osteonecrosis of the Jaw: A Review. *Semin Musculoskelet Radiol.* 2016;20:305-314.

18.   Messer JG, Castillo EJ, Abraham AM, et al. Anti-vascular endothelial growth factor antibody monotherapy causes destructive advanced periodontitis in rice rats (Oryzomys palustris). *Bone.* 2020;130:115141.

19.   Aghaloo TL, Tetradis S. Osteonecrosis of the Jaw in the Absence of Antiresorptive or Antiangiogenic Exposure: A Series of 6 Cases. *J Oral Maxillofac Surg.* 2017;75:129-142.

20.   Sung EC, Chan SM, Sakurai K, Chung E. Osteonecrosis of the maxilla as a complication to chemotherapy: a case report. *Spec Care Dentist.* 2002;22:142-146.

21. Horie N, Kawano R, Kaneko T, Shimoyama T. Methotrexate-related lymphoproliferative disorder arising in the gingiva of a patient with rheumatoid arthritis. *Aust Dent J.* 2015;60:408-411.

22. Bi Y, Gao Y, Ehirchiou D, et al. Bisphosphonates cause osteonecrosis of the jaw-like disease in mice. *Am J Pathol.* 2010;177:280-290.

23. Zhang Q, Yu W, Lee S, Xu Q, Naji A, Le AD. Bisphosphonate Induces Osteonecrosis of the Jaw in Diabetic Mice via NLRP3/Caspase-1-Dependent IL-1beta Mechanism. *J Bone Miner Res.* 2015;30:2300-2312.

24. Aghaloo TL, Kang B, Sung EC, et al. Periodontal disease and bisphosphonates induce osteonecrosis of the jaws in the rat. *J Bone Miner Res.* 2011;26:1871-1882.

25. Kang B, Cheong S, Chaichanasakul T, et al. Periapical disease and bisphosphonates induce osteonecrosis of the jaws in mice. *J Bone Miner Res.* 2013;28:1631-1640.

26. de Molon RS, Cheong S, Bezouglaia O, et al. Spontaneous osteonecrosis of the jaws in the maxilla of mice on antiresorptive treatment: a novel ONJ mouse model. *Bone.* 2014;68:11-19.

27. Ruggiero SL, Mehrotra B, Rosenberg TJ, Engroff SL. Osteonecrosis of the jaws associated with the use of bisphosphonates: a review of 63 cases. *J Oral Maxillofac Surg.* 2004;62:527-534.

28. Bedogni A, Fedele S, Bedogni G, et al. Staging of osteonecrosis of the jaw requires computed tomography for accurate definition of the extent of bony disease. *Br J Oral Maxillofac Surg.* 2014;52:603-608.

29. Allen MR. Bisphosphonates and osteonecrosis of the jaw: moving from the bedside to the bench. *Cells Tissues Organs.* 2009;189:289-294.

30. Huja SS, Fernandez SA, Hill KJ, Li Y. Remodeling dynamics in the alveolar process in skeletally mature dogs. *Anat Rec A Discov Mol Cell Evol Biol.* 2006;288:1243-1249.

31. Allen MR, Kubek DJ, Burr DB. Cancer treatment dosing regimens of zoledronic acid result in near-complete suppression of mandible intracortical bone remodeling in beagle dogs. *J Bone Miner Res.* 2010;25:98-105.

32. Cheong S, Sun S, Kang B, et al. Bisphosphonate uptake in areas of tooth extraction or periapical disease. *J Oral Maxillofac Surg.* 2014;72:2461-2468.

33. Kostenuik PJ, Nguyen HQ, McCabe J, et al. Denosumab, a fully human monoclonal antibody to RANKL, inhibits bone resorption and increases BMD in knock-in mice that express chimeric (murine/human) RANKL. *J Bone Miner Res.* 2009;24:182-195.

34. Aghaloo TL, Cheong S, Bezouglaia O, et al. RANKL inhibitors induce osteonecrosis of the jaw in mice with periapical disease. *J Bone Miner Res.* 2014;29:843-854.

35. Wood J, Bonjean K, Ruetz S, et al. Novel antiangiogenic effects of the bisphosphonate compound zoledronic acid. *J Pharmacol Exp Ther.* 2002;302:1055-1061.

36. Santini D, Vincenzi B, Tonini G, Scarpa S, Baldi A. Zoledronic acid exhibits inhibitory effects on osteoblastic and osteolytic metastases of prostate cancer. *Clin Cancer Res.* 2003;9:3215; author reply 3216.

37. Santini D, Vincenzi B, Dicuonzo G, et al. Zoledronic acid induces significant and long-lasting modifications of circulating angiogenic factors in cancer patients. *Clin Cancer Res.* 2003;9:2893-2897.

38. Gkouveris I, Hadaya D, Soundia A, et al. Vasculature submucosal changes at early stages of osteonecrosis of the jaw (ONJ). *Bone.* 2019;123:234-245.

39. de Molon RS, Hsu C, Bezouglaia O, et al. Rheumatoid Arthritis Exacerbates the Severity of Osteonecrosis of the Jaws (ONJ) in Mice. A Randomized, Prospective, Controlled Animal Study. *J Bone Miner Res.* 2016;31:1596-1607.

40. Kim T, Kim S, Song M, et al. Removal of Pre-Existing Periodontal Inflammatory Condition before Tooth Extraction Ameliorates Medication-Related Osteonecrosis of the Jaw-Like Lesion in Mice. *Am J Pathol.* 2018;188:2318-2327.

41. Lin JH. Bisphosphonates: a review of their pharmacokinetic properties. *Bone.* 1996;18:75-85.

42. Aghaloo T, Hazboun R, Tetradis S. Pathophysiology of Osteonecrosis of the Jaws. *Oral Maxillofac Surg Clin North Am.* 2015;27:489-496.

43. Filleul O, Crompot E, Saussez S. Bisphosphonate-induced osteonecrosis of the jaw: a review of 2,400 patient cases. *J Cancer Res Clin Oncol.* 2010;136:1117-1124.

44. Kikuiri T, Kim I, Yamaza T, et al. Cell-based immunotherapy with mesenchymal stem cells cures bisphosphonate-related osteonecrosis of the jaw-like disease in mice. *J Bone Miner Res.* 2010;25:1668-1679.

45. Zhu W, Xu R, Du J, et al. Zoledronic acid promotes TLR-4-mediated M1 macrophage polarization in bisphosphonate-related osteonecrosis of the jaw. *FASEB J.* 2019;33:5208-5219.

46. Zhang Q, Atsuta I, Liu S, et al. IL-17-mediated M1/M2 macrophage alteration contributes to pathogenesis of bisphosphonate-related osteonecrosis of the jaws. *Clin Cancer Res.* 2013;19:3176-3188.

47. Bamias A, Kastritis E, Bamia C, et al. Osteonecrosis of the jaw in cancer after treatment with bisphosphonates: incidence and risk factors. *J Clin Oncol.* 2005;23:8580-8587.

48. Saad F, Brown JE, Van Poznak C, et al. Incidence, risk factors, and outcomes of osteonecrosis of the jaw: integrated analysis from three blinded active-controlled phase III trials in cancer patients with bone metastases. *Ann Oncol.* 2012;23:1341-1347.

49. Kyrgidis A, Vahtsevanos K, Koloutsos G, et al. Bisphosphonate-related osteonecrosis of the jaws: a case-control study of risk factors in breast cancer patients. *J Clin Oncol.* 2008;26:4634-4638.

50. Fehm T, Beck V, Banys M, et al. Bisphosphonate-induced osteonecrosis of the jaw (ONJ): Incidence and risk factors in patients with breast cancer and gynecological malignancies. *Gynecol Oncol.* 2009;112:605-609.

51. Yamazaki T, Yamori M, Ishizaki T, et al. Increased incidence of osteonecrosis of the jaw after tooth extraction in patients treated with bisphosphonates: a cohort study. *Int J Oral Maxillofac Surg.* 2012;41:1397-1403.

52. Mozzati M, Arata V, Gallesio G. Tooth extraction in patients on zoledronic acid therapy. *Oral Oncol.* 2012;48:817-821.

53.   Mozzati M, Arata V, Gallesio G, Carossa S. Tooth extraction and oral bisphosphonates: comparison of different surgical protocols. *Joint Bone Spine.* 2011;78:647-648.

54.   Tsao C, Darby I, Ebeling PR, et al. Oral health risk factors for bisphosphonate-associated jaw osteonecrosis. *J Oral Maxillofac Surg.* 2013;71:1360-1366.

55.   Vahtsevanos K, Kyrgidis A, Verrou E, et al. Longitudinal cohort study of risk factors in cancer patients of bisphosphonate-related osteonecrosis of the jaw. *J Clin Oncol.* 2009;27:5356-5362.

56.   Nicolatou-Galitis O, Migkou M, Psyrri A, et al. Gingival bleeding and jaw bone necrosis in patients with metastatic renal cell carcinoma receiving sunitinib: report of 2 cases with clinical implications. *Oral Surg Oral Med Oral Pathol Oral Radiol.* 2012;113:234-238.

57.   Guarneri V, Miles D, Robert N, et al. Bevacizumab and osteonecrosis of the jaw: incidence and association with bisphosphonate therapy in three large prospective trials in advanced breast cancer. *Breast Cancer Res Treat.* 2010;122:181-188.

58.   Nicoletti P, Cartsos VM, Palaska PK, Shen Y, Floratos A, Zavras AI. Genomewide pharmacogenetics of bisphosphonate-induced osteonecrosis of the jaw: the role of RBMS3. *Oncologist.* 2012;17:279-287.

59.   Marini F, Tonelli P, Cavalli L, et al. Pharmacogenetics of bisphosphonate-associated osteonecrosis of the jaw. *Front Biosci (Elite Ed).* 2011;3:364-370.

60.   Yang G, Hamadeh IS, Katz J, et al. SIRT1/HERC4 Locus Associated With Bisphosphonate-Induced Osteonecrosis of the Jaw: An Exome-Wide Association Analysis. *J Bone Miner Res.* 2018;33:91-98.

61.   Allen MR. Medication-Related Osteonecrosis of the Jaw: Basic and Translational Science Updates. *Oral Maxillofac Surg Clin North Am.* 2015;27:497-508.

62.   Marx RE. Pamidronate (Aredia) and zoledronate (Zometa) induced avascular necrosis of the jaws: a growing epidemic. *J Oral Maxillofac Surg.* 2003;61:1115-1117.

63.   Chrysanthakopoulos NA. Reasons for extraction of permanent teeth in Greece: a five-year follow-up study. *Int Dent J.* 2011;61:19-24.

64.   Hull PS, Worthington HV, Clerehugh V, Tsirba R, Davies RM, Clarkson JE. The reasons for tooth extractions in adults and their validation. *J Dent.* 1997;25:233-237.

65.   Soundia A, Hadaya D, Esfandi N, et al. Zoledronate Impairs Socket Healing after Extraction of Teeth with Experimental Periodontitis. *J Dent Res.* 2018;97:312-320.

66.   Olutayo J, Agbaje JO, Jacobs R, Verhaeghe V, Velde FV, Vinckier F. Bisphosphonate-Related Osteonecrosis of the Jaw Bone: Radiological Pattern and the Potential Role of CBCT in Early Diagnosis. *J Oral Maxillofac Res.* 2010;1:e3.

67.   Shimamoto H, Grogan TR, Tsujimoto T, et al. Does CBCT alter the diagnostic thinking efficacy, management and prognosis of patients with suspected Stage 0 medication-related osteonecrosis of the jaws? *Dentomaxillofac Radiol.* 2017:20170290.

68.   Claire EJ, Aurelie G, Julia S, et al. Denosumab-related osteonecrosis of the jaw: a retrospective study. *J Oral Pathol Med.* 2017.

69.   Aghaloo TL, Felsenfeld AL, Tetradis S. Osteonecrosis of the jaw in a patient on Denosumab. *J Oral Maxillofac Surg.* 2010;68:959-963.

70.   Paulo S, Abrantes AM, Laranjo M, et al. Bisphosphonate-related osteonecrosis of the jaw: specificities. *Oncol Rev.* 2014;8:254.

71.   Liu   W,   Zhang   X.   Receptor   activator   of   nuclear   factor-kappaB   ligand (RANKL)/RANK/osteoprotegerin system in bone and other tissues (review). *Mol Med Rep.* 2015;11:3212-3218.

72.   Wada T, Nakashima T, Hiroshi N, Penninger JM. RANKL-RANK signaling in osteoclastogenesis and bone disease. *Trends Mol Med.* 2006;12:17-25.

73.   Michalski MN, McCauley LK. Macrophages and skeletal health. *Pharmacol Ther.* 2017;174:43-54.

74.   Viniegra A, Goldberg H, Cil C, et al. Resolving Macrophages Counter Osteolysis by Anabolic Actions on Bone Cells. *J Dent Res.* 2018;97:1160-1169.

75. Sonis ST, Watkins BA, Lyng GD, Lerman MA, Anderson KC. Bony changes in the jaws of rats treated with zoledronic acid and dexamethasone before dental extractions mimic bisphosphonate-related osteonecrosis in cancer patients. *Oral Oncol.* 2009;45:164-172.

76. Hokugo A, Christensen R, Chung EM, et al. Increased prevalence of bisphosphonate-related osteonecrosis of the jaw with vitamin D deficiency in rats. *J Bone Miner Res.* 2010;25:1337-1349.

77. Abtahi J, Agholme F, Sandberg O, Aspenberg P. Effect of local vs. systemic bisphosphonate delivery on dental implant fixation in a model of osteonecrosis of the jaw. *J Dent Res.* 2013;92:279-283.

78. Kuroshima S, Yamashita J. Chemotherapeutic and antiresorptive combination therapy suppressed lymphangiogenesis and induced osteonecrosis of the jaw-like lesions in mice. *Bone.* 2013;56:101-109.

79. Williams DW, Lee C, Kim T, et al. Impaired bone resorption and woven bone formation are associated with development of osteonecrosis of the jaw-like lesions by bisphosphonate and anti-receptor activator of NF-kappaB ligand antibody in mice. *Am J Pathol.* 2014;184:3084-3093.

80. Phipps KR, Stevens VJ. Relative contribution of caries and periodontal disease in adult tooth loss for an HMO dental population. *J Public Health Dent.* 1995;55:250-252.

81. Marx RE, Sawatari Y, Fortin M, Broumand V. Bisphosphonate-induced exposed bone (osteonecrosis/osteopetrosis) of the jaws: risk factors, recognition, prevention, and treatment. *J Oral Maxillofac Surg.* 2005;63:1567-1575.

82. Ripamonti CI, Maniezzo M, Campa T, et al. Decreased occurrence of osteonecrosis of the jaw after implementation of dental preventive measures in solid tumour patients with bone metastases treated with bisphosphonates. The experience of the National Cancer Institute of Milan. *Ann Oncol.* 2009;20:137-145.

83. Gotcher JE, Jee WS. The progress of the periodontal syndrome in the rice cat. II. The effects of a diphosphonate on the periodontium. *J Periodontal Res.* 1981;16:441-455.

84. Aguirre JI, Akhter MP, Kimmel DB, et al. Oncologic doses of zoledronic acid induce osteonecrosis of the jaw-like lesions in rice rats (Oryzomys palustris) with periodontitis. *J Bone Miner Res.* 2012;27:2130-2143.

85. Arce K, Assael LA, Weissman JL, Markiewicz MR. Imaging findings in bisphosphonate-related osteonecrosis of jaws. *J Oral Maxillofac Surg.* 2009;67:75-84.

86. Boonyapakorn T, Schirmer I, Reichart PA, Sturm I, Massenkeil G. Bisphosphonate-induced osteonecrosis of the jaws: prospective study of 80 patients with multiple myeloma and other malignancies. *Oral Oncol.* 2008;44:857-869.

87. Otto S, Schreyer C, Hafner S, et al. Bisphosphonate-related osteonecrosis of the jaws - characteristics, risk factors, clinical features, localization and impact on oncological treatment. *J Craniomaxillofac Surg.* 2012;40:303-309.

88. Vescovi P, Campisi G, Fusco V, et al. Surgery-triggered and non surgery-triggered Bisphosphonate-related Osteonecrosis of the Jaws (BRONJ): A retrospective analysis of 567 cases in an Italian multicenter study. *Oral Oncol.* 2011;47:191-194.

89. Yang H, Pan H, Yu F, Chen K, Shang G, Xu Y. A novel model of bisphosphonate-related osteonecrosis of the jaw in rats. *Int J Clin Exp Pathol.* 2015;8:5161-5167.

90. Tsurushima H, Kokuryo S, Sakaguchi O, Tanaka J, Tominaga K. Bacterial promotion of bisphosphonate-induced osteonecrosis in Wistar rats. *Int J Oral Maxillofac Surg.* 2013;42:1481-1487.

91. Kobayashi Y, Hiraga T, Ueda A, et al. Zoledronic acid delays wound healing of the tooth extraction socket, inhibits oral epithelial cell migration, and promotes proliferation and adhesion to hydroxyapatite of oral bacteria, without causing osteonecrosis of the jaw, in mice. *J Bone Miner Metab.* 2010;28:165-175.

92. Park S, Kanayama K, Kaur K, et al. Osteonecrosis of the Jaw Developed in Mice: DISEASE VARIANTS REGULATED BY gammadelta T CELLS IN ORAL MUCOSAL BARRIER IMMUNITY. *J Biol Chem.* 2015;290:17349-17366.

93. Barba-Recreo P, Del Castillo Pardo de Vera JL, Garcia-Arranz M, Yebenes L, Burgueno M. Zoledronic acid - related osteonecrosis of the jaws. Experimental model with dental extractions in rats. *J Craniomaxillofac Surg.* 2014;42:744-750.

94. Dayisoylu EH, Ungor C, Tosun E, et al. Does an alkaline environment prevent the development of bisphosphonate-related osteonecrosis of the jaw? An experimental study in rats. *Oral Surg Oral Med Oral Pathol Oral Radiol.* 2014;117:329-334.

95. Yamashita J, McCauley LK. Antiresorptives and osteonecrosis of the jaw. *J Evid Based Dent Pract.* 2012;12:233-247.

96. Manfredi M, Mergoni G, Goldoni M, et al. A 5-year retrospective longitudinal study on the incidence and the risk factors of osteonecrosis of the jaws in patients treated with zoledronic acid for bone metastases from solid tumors. *Med Oral Patol Oral Cir Bucal.* 2017;22:e342-e348.

97. Fung P, Bedogni G, Bedogni A, et al. Time to onset of bisphosphonate-related osteonecrosis of the jaws: a multicentre retrospective cohort study. *Oral Dis.* 2016.

98. Gosain A, DiPietro LA. Aging and wound healing. *World J Surg.* 2004;28:321-326.

99. Olczyk P, Mencner L, Komosinska-Vassev K. The role of the extracellular matrix components in cutaneous wound healing. *Biomed Res Int.* 2014;2014:747584.

100. Araujo MG, Silva CO, Misawa M, Sukekava F. Alveolar socket healing: what can we learn? *Periodontol 2000.* 2015;68:122-134.

101. Soundia A, Hadaya D, Esfandi N, et al. Osteonecrosis of the jaws (ONJ) in mice after extraction of teeth with periradicular disease. *Bone.* 2016;90:133-141.

102. Junqueira LC, Assis Figueiredo MT, Torloni H, Montes GS. Differential histologic diagnosis of osteoid. A study on human osteosarcoma collagen by the histochemical picrosirius-polarization method. *J Pathol.* 1986;148:189-196.

103. Hinz B, Celetta G, Tomasek JJ, Gabbiani G, Chaponnier C. Alpha-smooth muscle actin expression upregulates fibroblast contractile activity. *Mol Biol Cell.* 2001;12:2730-2741.

104. Cuttle L, Nataatmadja M, Fraser JF, Kempf M, Kimble RM, Hayes MT. Collagen in the scarless fetal skin wound: detection with picrosirius-polarization. *Wound Repair Regen.* 2005;13:198-204.

105. Tracy LE, Minasian RA, Caterson EJ. Extracellular Matrix and Dermal Fibroblast Function in the Healing Wound. *Adv Wound Care (New Rochelle).* 2016;5:119-136.

106. Hirota A, Ebihara T, Kusubata M, et al. Collagen of chronically inflamed skin is over-modified and upregulates secretion of matrix metalloproteinase 2 and matrix-degrading enzymes by endothelial cells and fibroblasts. *J Invest Dermatol.* 2003;121:1317-1325.

107. Pauschinger M, Doerner A, Remppis A, Tannhauser R, Kuhl U, Schultheiss HP. Differential myocardial abundance of collagen type I and type III mRNA in dilated cardiomyopathy: effects of myocardial inflammation. *Cardiovasc Res.* 1998;37:123-129.

108. Li W, Zhu Y, Singh P, Ajmera DH, Song J, Ji P. Association of Common Variants in MMPs with Periodontitis Risk. *Dis Markers.* 2016;2016:1545974.

109. Honibald EN, Mathew S, Padmanaban J, Sundaram E, Ramamoorthy RD. Perioceutics: Matrix metalloproteinase inhibitors as an adjunctive therapy for inflammatory periodontal disease. *J Pharm Bioallied Sci.* 2012;4:S417-421.

110. Hernandez Rios M, Sorsa T, Obregon F, et al. Proteolytic roles of matrix metalloproteinase (MMP)-13 during progression of chronic periodontitis: initial evidence for MMP-13/MMP-9 activation cascade. *J Clin Periodontol.* 2009;36:1011-1017.

111. Wynn TA, Ramalingam TR. Mechanisms of fibrosis: therapeutic translation for fibrotic disease. *Nat Med.* 2012;18:1028-1040.

112. Slemp AE, Kirschner RE. Keloids and scars: a review of keloids and scars, their pathogenesis, risk factors, and management. *Curr Opin Pediatr.* 2006;18:396-402.

113. Pardo A, Selman M. Lung Fibroblasts, Aging, and Idiopathic Pulmonary Fibrosis. *Ann Am Thorac Soc.* 2016;13:S417-S421.

114. Chistiakov DA, Orekhov AN, Bobryshev YV. The role of cardiac fibroblasts in post-myocardial heart tissue repair. *Exp Mol Pathol.* 2016;101:231-240.

115. Lucas T, Waisman A, Ranjan R, et al. Differential roles of macrophages in diverse phases of skin repair. *J Immunol.* 2010;184:3964-3977.

116. Frost HM, Jee WS. On the rat model of human osteopenias and osteoporoses. *Bone Miner.* 1992;18:227-236.

117. Fantasia JE. The Role of Antiangiogenic Therapy in the Development of Osteonecrosis of the Jaw. *Oral Maxillofac Surg Clin North Am.* 2015;27:547-553.

118. Estilo CL, Fornier M, Farooki A, Carlson D, Bohle G, 3rd, Huryn JM. Osteonecrosis of the jaw related to bevacizumab. *J Clin Oncol.* 2008;26:4037-4038.

119. Mawardi H, Treister N, Richardson P, et al. Sinus tracts--an early sign of bisphosphonate-associated osteonecrosis of the jaws? *J Oral Maxillofac Surg.* 2009;67:593-601.

120. Patel S, Choyee S, Uyanne J, et al. Non-exposed bisphosphonate-related osteonecrosis of the jaw: a critical assessment of current definition, staging, and treatment guidelines. *Oral Dis.* 2012;18:625-632.

121. Junquera L, Gallego L. Nonexposed bisphosphonate-related osteonecrosis of the jaws: another clinical variant? *J Oral Maxillofac Surg.* 2008;66:1516-1517.

122. Singer SR, Mupparapu M. Plain film and CBCT findings in a case of bisphosphonate-related osteonecrosis of the jaw. *Quintessence Int.* 2009;40:163-165.

123. Treister NS, Friedland B, Woo SB. Use of cone-beam computerized tomography for evaluation of bisphosphonate-associated osteonecrosis of the jaws. *Oral Surg Oral Med Oral Pathol Oral Radiol Endod.* 2010;109:753-764.

124. Barragan-Adjemian C, Lausten L, Ang DB, Johnson M, Katz J, Bonewald LF. Bisphosphonate-related osteonecrosis of the jaw: model and diagnosis with cone beam computerized tomography. *Cells Tissues Organs.* 2009;189:284-288.

125. Wilde F, Heufelder M, Lorenz K, et al. Prevalence of cone beam computed tomography imaging findings according to the clinical stage of bisphosphonate-related osteonecrosis of the jaw. *Oral Surg Oral Med Oral Pathol Oral Radiol.* 2012;114:804-811.

126. Torres SR, Chen CS, Leroux BG, et al. Mandibular cortical bone evaluation on cone beam computed tomography images of patients with bisphosphonate-related osteonecrosis of the jaw. *Oral Surg Oral Med Oral Pathol Oral Radiol.* 2012;113:695-703.

127. Suomalainen A, Pakbaznejad Esmaeili E, Robinson S. Dentomaxillofacial imaging with panoramic views and cone beam CT. *Insights Imaging.* 2015;6:1-16.

128. Fryback DG, Thornbury JR. The efficacy of diagnostic imaging. *Med Decis Making.* 1991;11:88-94.

129. Boeddinghaus R, Whyte A. Current concepts in maxillofacial imaging. *Eur J Radiol.* 2008;66:396-418.

130. Cardoso CL, Barros CA, Curra C, et al. Radiographic Findings in Patients with Medication-Related Osteonecrosis of the Jaw. *Int J Dent.* 2017;2017:3190301.

131. Lobbezoo DJ, van Kampen RJ, Voogd AC, et al. Prognosis of metastatic breast cancer: are there differences between patients with de novo and recurrent metastatic breast cancer? *Br J Cancer.* 2015;112:1445-1451.

132. Ferlay J, Shin HR, Bray F, Forman D, Mathers C, Parkin DM. Estimates of worldwide burden of cancer in 2008: GLOBOCAN 2008. *Int J Cancer.* 2010;127:2893-2917.

133. Ciolli S. Multiple myeloma. *Clin Cases Miner Bone Metab.* 2012;9:150-152.

134. Kanis JA, McCloskey EV, Johansson H, et al. European guidance for the diagnosis and management of osteoporosis in postmenopausal women. *Osteoporos Int.* 2013;24:23-57.

135. Dodson TB. The Frequency of Medication-related Osteonecrosis of the Jaw and its Associated Risk Factors. *Oral Maxillofac Surg Clin North Am.* 2015;27:509-516.

136. McClung M, Harris ST, Miller PD, et al. Bisphosphonate therapy for osteoporosis: benefits, risks, and drug holiday. *Am J Med.* 2013;126:13-20.

137. Dickinson M, Prince HM, Kirsa S, et al. Osteonecrosis of the jaw complicating bisphosphonate treatment for bone disease in multiple myeloma: an overview with recommendations for prevention and treatment. *Intern Med J.* 2009;39:304-316.

138. Mota de Almeida FJ, Knutsson K, Flygare L. The effect of cone beam CT (CBCT) on therapeutic decision-making in endodontics. *Dentomaxillofac Radiol.* 2014;43:20130137.

139. Tetradis S, Anstey P, Graff-Radford S. Cone beam computed tomography in the diagnosis of dental disease. *Tex Dent J.* 2011;128:620-628.

140. Jennin F, Bousson V, Parlier C, Jomaah N, Khanine V, Laredo JD. Bony sequestrum: a radiologic review. *Skeletal Radiol.* 2011;40:963-975.

141. Huang YF, Chang CT, Muo CH, Tsai CH, Shen YF, Wu CZ. Impact of bisphosphonate-related osteonecrosis of the jaw on osteoporotic patients after dental extraction: a population-based cohort study. *PLoS One.* 2015;10:e0120756.

142. Stafford RS, Drieling RL, Hersh AL. National trends in osteoporosis visits and osteoporosis treatment, 1988-2003. *Arch Intern Med.* 2004;164:1525-1530.

143. Walter C, Al-Nawas B, Grotz KA, et al. Prevalence and risk factors of bisphosphonate-associated osteonecrosis of the jaw in prostate cancer patients with advanced disease treated with zoledronate. *Eur Urol.* 2008;54:1066-1072.

144. Palmieri C, Fullarton JR, Brown J. Comparative efficacy of bisphosphonates in metastatic breast and prostate cancer and multiple myeloma: a mixed-treatment meta-analysis. *Clin Cancer Res.* 2013;19:6863-6872.

145. Jha S, Wang Z, Laucis N, Bhattacharyya T. Trends in Media Reports, Oral Bisphosphonate Prescriptions, and Hip Fractures 1996-2012: An Ecological Analysis. *J Bone Miner Res.* 2015;30:2179-2187.

146. Wright NC, Looker AC, Saag KG, et al. The recent prevalence of osteoporosis and low bone mass in the United States based on bone mineral density at the femoral neck or lumbar spine. *J Bone Miner Res.* 2014;29:2520-2526.

147. Foundation NO. Statement from American Society for Bone and Mineral Research, National Osteoporosis Foundation and National Bone Health Alliance Nation's Scientific and Medical Bone Health Experts Call for Action On Dangers of Not Treating Osteoporosis More Aggressively. 2016

148. Khosla S, Cauley JA, Compston J, et al. Addressing the Crisis in the Treatment of Osteoporosis: A Path Forward. *J Bone Miner Res.* 2016.

149. Khosla S, Shane E. A Crisis in the Treatment of Osteoporosis. *J Bone Miner Res.* 2016;31:1485-1487.

150. Boyce BF, Xing L. Functions of RANKL/RANK/OPG in bone modeling and remodeling. *Arch Biochem Biophys.* 2008;473:139-146.

151. Goessl C, Katz L, Dougall WC, et al. The development of denosumab for the treatment of diseases of bone loss and cancer-induced bone destruction. *Ann N Y Acad Sci.* 2012;1263:29-40.

152. Hadaya D, Gkouveris I, Soundia A, et al. Clinically Relevant Doses of Sclerostin Antibody Do Not Induce Osteonecrosis of the Jaw (ONJ) in Rats with Experimental Periodontitis. *J Bone Miner Res.* 2018.

153. Aghaloo TL, Dry SM, Mallya S, Tetradis S. Stage 0 osteonecrosis of the jaw in a patient on denosumab. *J Oral Maxillofac Surg.* 2014;72:702-716.

154. Shudo A, Kishimoto H, Takaoka K, Noguchi K. Long-term oral bisphosphonates delay healing after tooth extraction: a single institutional prospective study. *Osteoporos Int.* 2018;29:2315-2321.

155. Allen MR. The effects of bisphosphonates on jaw bone remodeling, tissue properties, and extraction healing. *Odontology.* 2011;99:8-17.

156. Kuroshima S, Go VA, Yamashita J. Increased numbers of nonattached osteoclasts after long-term zoledronic acid therapy in mice. *Endocrinology.* 2012;153:17-28.

157. Drake MT, Clarke BL, Khosla S. Bisphosphonates: mechanism of action and role in clinical practice. *Mayo Clin Proc.* 2008;83:1032-1045.

158. Sutherland KA, Rogers HL, Tosh D, Rogers MJ. RANKL increases the level of Mcl-1 in osteoclasts and reduces bisphosphonate-induced osteoclast apoptosis in vitro. *Arthritis Res Ther.* 2009;11:R58.

159.   Lambrinoudaki I, Vlachou S, Galapi F, Papadimitriou D, Papadias K. Once-yearly zoledronic acid in the prevention of osteoporotic bone fractures in postmenopausal women. *Clin Interv Aging.* 2008;3:445-451.

160.   Kohno N, Aogi K, Minami H, et al. Zoledronic acid significantly reduces skeletal complications compared with placebo in Japanese women with bone metastases from breast cancer: a randomized, placebo-controlled trial. *J Clin Oncol.* 2005;23:3314-3321.

161.   Saad F, Gleason DM, Murray R, et al. Long-term efficacy of zoledronic acid for the prevention of skeletal complications in patients with metastatic hormone-refractory prostate cancer. *J Natl Cancer Inst.* 2004;96:879-882.

162.   Kim S, Williams DW, Lee C, et al. IL-36 Induces Bisphosphonate-Related Osteonecrosis of the Jaw-Like Lesions in Mice by Inhibiting TGF-beta-Mediated Collagen Expression. *J Bone Miner Res.* 2017;32:309-318.

163.   Marx RE, Cillo JE, Jr., Ulloa JJ. Oral bisphosphonate-induced osteonecrosis: risk factors, prediction of risk using serum CTX testing, prevention, and treatment. *J Oral Maxillofac Surg.* 2007;65:2397-2410.

164.   Gordon S. Elie Metchnikoff: father of natural immunity. *Eur J Immunol.* 2008;38:3257-3264.

165.   Bystrom J, Evans I, Newson J, et al. Resolution-phase macrophages possess a unique inflammatory phenotype that is controlled by cAMP. *Blood.* 2008;112:4117-4127.

166.   Mantovani A, Sica A, Sozzani S, Allavena P, Vecchi A, Locati M. The chemokine system in diverse forms of macrophage activation and polarization. *Trends Immunol.* 2004;25:677-686.

167.   Cho SW, Soki FN, Koh AJ, et al. Osteal macrophages support physiologic skeletal remodeling and anabolic actions of parathyroid hormone in bone. *Proc Natl Acad Sci U S A.* 2014;111:1545-1550.

168.   Sinder BP, Pettit AR, McCauley LK. Macrophages: Their Emerging Roles in Bone. *J Bone Miner Res.* 2015;30:2140-2149.

169.   Cho SW. Role of osteal macrophages in bone metabolism. *J Pathol Transl Med.* 2015;49:102-104.

170.   Kaneko M, Tomita T, Nakase T, et al. Expression of proteinases and inflammatory cytokines in subchondral bone regions in the destructive joint of rheumatoid arthritis. *Rheumatology (Oxford).* 2001;40:247-255.

171.   Tintut Y, Patel J, Territo M, Saini T, Parhami F, Demer LL. Monocyte/macrophage regulation of vascular calcification in vitro. *Circulation.* 2002;105:650-655.

172.   Pettit AR, Chang MK, Hume DA, Raggatt LJ. Osteal macrophages: a new twist on coupling during bone dynamics. *Bone.* 2008;43:976-982.

173.   Vi L, Baht GS, Whetstone H, et al. Macrophages promote osteoblastic differentiation in-vivo: implications in fracture repair and bone homeostasis. *J Bone Miner Res.* 2015;30:1090-1102.

174.   Hernandez M, Valenzuela MA, Lopez-Otin C, et al. Matrix metalloproteinase-13 is highly expressed in destructive periodontal disease activity. *J Periodontol.* 2006;77:1863-1870.

175.   Wang M, Sampson ER, Jin H, et al. MMP-13 is a critical target gene during the progression of osteoarthritis. *Arthritis Res Ther.* 2013;15:R5.

176.   Vizoso FJ, Gonzalez LO, Corte MD, et al. Collagenase-3 (MMP-13) expression by inflamed mucosa in inflammatory bowel disease. *Scand J Gastroenterol.* 2006;41:1050-1055.

177.   Bilezikian JP, Josse RG, Eastell R, et al. Rosiglitazone decreases bone mineral density and increases bone turnover in postmenopausal women with type 2 diabetes mellitus. *J Clin Endocrinol Metab.* 2013;98:1519-1528.

178.   Ali AA, Weinstein RS, Stewart SA, Parfitt AM, Manolagas SC, Jilka RL. Rosiglitazone causes bone loss in mice by suppressing osteoblast differentiation and bone formation. *Endocrinology.* 2005;146:1226-1235.

179.   Di Paola R, Mazzon E, Maiere D, et al. Rosiglitazone reduces the evolution of experimental periodontitis in the rat. *J Dent Res.* 2006;85:156-161.

180.   Makela M, Larjava H, Pirila E, et al. Matrix metalloproteinase 2 (gelatinase A) is related to migration of keratinocytes. *Exp Cell Res.* 1999;251:67-78.